1997

Induced Acceleration of Phosphine Exchange in Metal Carbonyls by Pendant Groups of Coordinated Polyphosphines

Ping Ye
Eastern Illinois University

THESIS REPRODUCTION CERTIFICATE

TO: Graduate Degree Candidates (who have written formal theses)

SUBJECT: Permission to Reproduce Theses

The University Library is receiving a number of requests from other institutions asking permission to reproduce dissertations for inclusion in their library holdings. Although no copyright laws are involved, we feel that professional courtesy demands that permission be obtained from the author before we allow theses to be copied.

PLEASE SIGN ONE OF THE FOLLOWING STATEMENTS:

Booth Library of Eastern Illinois University has my permission to lend my thesis to a reputable college or university for the purpose of copying it for inclusion in that institution's library or research holdings.

_____ 9/29/97

Author Date

I respectfully request Booth Library of Eastern Illinois University not allow my thesis to be reproduced because:

_____

_____

_____

_____ _____

Author Date

Induced Acceleration of Phosphine Exchange in Metal Carbonyls

by Pendant Groups of Coordinated Polyphosphines

(TITLE)

BY

Ping Ye

1969 –

THESIS

SUBMITTED IN PARTIAL FULFILLMENT OF THE REQUIREMENTS
FOR THE DEGREE OF

Master of Science in Chemistry

IN THE GRADUATE SCHOOL, EASTERN ILLINOIS UNIVERSITY
CHARLESTON, ILLINOIS

1997
YEAR

I HEREBY RECOMMEND THIS THESIS BE ACCEPTED AS FULFILLING
THIS PART OF THE GRADUATE DEGREE CITED ABOVE

9/29/97
DATE

ADVISER

9/29/97
DATE

DEPARTMENT HEAD

Induced Acceleration of Phosphine Exchange in Metal Carbonyls by Pendant Groups of Coordinated Polyphosphines

By: Ping Ye

Advisor: Dr. Richard L. Keiter

Submitted date: Sept. 26, 1997

Approved by the thesis committee:

Dr. Ellen A. Keiter	9/29/97 Date
Dr. Richard L. Keiter	9/29/97 Date
Dr. Jerry W. Ellis	9-29-1997 Date
Dr. Daniel J. Sheeran	9/29/97 Date

Abstract

The kinetics and thermodynamics of isomerization of $(OC)_5CrPPh_2CH_2CH(PPh_2)_2$ to its linkage isomer, $(OC)_5CrPPh_2CH(PPh_2)CH_2PPh_2$, in chloroform-d have been studied with $^{31}P\{^1H\}$ NMR.

$$(OC)_5Cr[\eta^1\text{-}PPh_2CH_2CH(PPh_2)_2] \rightleftarrows (OC)_5Cr[\eta^1\text{-}PPh_2CH(PPh_2)CH_2PPh_2]$$

The equilibrium constants for the reaction are 3.60, 2.61, 2.04, and 1.67 at 10 °C, 25 °C, 40 °C, and 53 °C, respectively. The forward reaction becomes more favorable as the temperature is decreased. The values of ΔH, ΔS, and $\Delta G(25\ ^\circ C)$ were determined to be -13.6 kJ mol^{-1}, -37.6 J $mol^{-1}K^{-1}$, and -2.4 kJ mol^{-1}, respectively. The large decrease in entropy favors the reverse reaction while the decrease in enthalpy favors the forward reaction. Previous work has shown that for the analogous tungsten isomerization, values of ΔH, ΔS, and $\Delta G(25\ ^\circ C)$ are -12.2 kJ mol^{-1}, -28 J $mol^{-1}K^{-1}$, and -3.9 kJ mol^{-1}, respectively.[51] It can be concluded that the greater decrease in entropy for the chromium reaction accounts for its overall diminished favorableness as compared to the tungsten reaction.

Rate constants for the forward reaction in chloroform at 10 °C, 25 °C, 40 °C are 2.0 x 10^{-7} s^{-1}, 2.1 x 10^{-6} s^{-1}, and 1.7 x 10^{-5} s^{-1} with half-lives to equilibrium of 31 days, 3 days, and 8 hours, respectively. These reactions are about an order of magnitude slower than the analogous tungsten reaction, but about four orders of magnitude faster than isomerization of $(OC)_5CrPPh_2CH_2CH_2P(tol)_2$.[55c] The enthalpy of activation, $\Delta H^{\neq}$, for the forward and reverse reactions are 105 kJ mol^{-1} and 120 kJ mol^{-1}, respectively, larger by 12 kJ mol^{-1} and 15 kJ mol^{-1} than observed for tungsten. The entropy of activation, $\Delta S^{\neq}$, for the forward

and reverse reactions were found to be 1.4 J $mol^{-1}K^{-1}$ and 40 J $mol^{-1}K^{-1}$, respectively. These values are considerably more positive than those obtained previously for tungsten (-28 J $mol^{-1}K^{-1}$ and -1.0 J $mol^{-1}K^{-1}$).

It is concluded that abnormally fast isomerization rates for $(OC)_5MPPh_2CH_2CH(PPh_2)_2$ (M = Cr, W) result because the short phosphine arm interacts with the equatorial carbonyl groups in the transition state, lowering the activation energy, and leading to labilization of the coordinated phosphorus atom which results in its replacement by the second phosphine arm. The concept of interaction between the short phosphine arm and the equatorial carbonyl groups is supported by long-range phosphorus-carbon coupling ($^4J_{PC}$), believed to augmented by a through-space mechanism. The entropies of activation suggest that phosphorus exchange in chromium has a much more significant dissociative component than for the analogous tungsten system. It would be expected that the smaller chromium atom would be less likely to form a stable 7-coordinate complex because of steric crowding.

Complexes, $(OC)_5WPPh_2C(PPh_2)=CH_2$ and $[(OC)_5WPPh_2]_2C=CH_2$ have been synthesized for the first time. The crystal structure of the former compound has been determined. Unlike the similar $(OC)5WPPh_2CH_2PPh_2$ complex, the dangling phosphorus atom is not directed toward the equatorial carbonyl groups and no long-range phosphorus-carbon coupling ($^4J_{PC}$) is observed.

Acknowledgements

I would like to thank Dr. Richard L. Keiter for his knowledge, guidance and encouragement.

I would like to thank Dr. Ellen A. Keiter for the training of operating the QE-300 NMR spectrometer.

I would also like to thank Dr. Ilia Guzei and Dr. Arnold Rheingold of the University of Delaware for doing the crystal structure analysis. Thank Dr. Giles L. Henderson for FTIR instruction, Dr. Jerry W. Ellis, Mr. Ken Osborne, and Mr. Jeremy Wheeler, for their helpful assistance, both within and outside the field of chemistry. I also extend my thanks to other faculty and staff of the Chemistry Department for all of their help.

The National Science Foundation is acknowledged for financial support.

Finally, I thank my husband for the help, understanding, and support he has given since long before this work was begun.

Table of Contents

Abstract.....i

Acknowledgements.....iii

Table of contents.....iv

List of figures.....v

Chapter I. Kinetics and thermodynamics study of phosphine exchange in $(OC)_5Cr[\eta^1\text{-}PPh_2CH_2CH(PPh_2)_2]$

A. Introduction..... 1

B. Results and discussion.....18

C. Experimental section.....36

Chapter II. Synthesis of $[(OC)_5WPPh_2]_2C{=}CH_2$ and crystal structure of $(CO)_5WPPh_2C(PPh_2){=}CH_2$

A. Introduction.....42

B. Results and discussion.....45

C. Experimental section.....53

Figures.....56

References.....109

Appendix.....115

List of Figures

1. ^{1}H NMR spectrum of $(Ph_2P)_2C=CH_2$.....56
2. $^{13}C\{^{1}H\}$ NMR spectrum of $(Ph_2P)_2C=CH_2$.....57
3. $^{31}P\{^{1}H\}$ NMR spectrum of $(Ph_2P)_2C=CH_2$.....58
4. ^{1}H NMR spectrum of $(OC)_5CrPPh_2H$.....59
5. $^{13}C\ \{^{1}H\}$ NMR spectrum of $(OC)_5CrPPh_2H$.....60
6. $^{31}P\ \{^{1}H\}$ NMR spectrum of $(OC)_5CrPPh_2H$.....63
7. IR spectrum of $(OC)_5CrPPh_2H$ in the carbonyl region.....64
8. $^{31}P\{^{1}H\}$ NMR spectrum of $Cl_2Pd(PPh_2)_2C=CH_2$.....65
9. ^{1}H NMR spectrum of $Cl_2Pd(PPh_2)_2C=CH_2$.....66
10. $^{31}P\{^{1}H\}$ NMR spectrum of $Cl_2Pd(PPh_2)_2CHCH_2PPh_2Cr(CO)_5$.....67
11. IR spectrum of $Cl_2Pd(PPh_2)_2CHCH_2PPh_2Cr(CO)_5$ in the carbonyl region.....68
12. $^{31}P\{^{1}H\}$ NMR spectrum of isomers $(OC)_5Cr[\eta^1\text{-}PPh_2CH_2CH(PPh_2)_2]$ (**6**) and $(OC)_5Cr[\eta^1\text{-}(PPh_2)_2CHCH_2PPh_2]$ (**7**), showing that the compound **6** is first formed from the reaction..... 69
13. $^{31}P\{^{1}H\}$ NMR spectrum of isomers $(OC)_5Cr[\eta^1\text{-}PPh_2CH_2CH(PPh_2)_2]$ (**6**) and $(OC)_5Cr[\eta^1\text{-}(PPh_2)_2CHCH_2PPh_2]$ (**7**) as they move toward equilibrium.....74
14. $^{13}C\{^{1}H\}$ NMR spectrum of $(OC)_5Cr[\eta^1\text{-}PPh_2CH_2CH(PPh_2)_2]$ (**6**).....75
15. $^{13}C\{^{1}H\}$ NMR spectrum of the mixture of $(OC)_5Cr[\eta^1\text{-}PPh_2CH_2CH(PPh_2)_2]$ (**6**) and $(OC)_5Cr[\eta^1\text{-}(PPh_2)_2CHCH_2PPh_2]$ (**7**).....78

16. ln K vs. 1/T for isomerization of Cr complexes in $CDCl_3$ solution.....81

17. ln K vs. 1/T for isomerization of Cr complexes in toluene-d_8 solution.....82

18. IR spectrum of the mixture of $(OC)_5Cr[\eta^1\text{-}PPh_2CH_2CH(PPh_2)_2]$ (**6**)

and $(OC)_5Cr[\eta^1\text{-}(PPh_2)_2CHCH_2PPh_2]$ (**7**) in the carbonyl region.....83

19. ln {[6]-$[6]_{eq}$} vs. time for isomerization of Cr complexes in $CDCl_3$ at 10 °C.....84

20. ln {[6]-$[6]_{eq}$} vs. time for isomerization of Cr complexes in $CDCl_3$ at 25 °C.....85

21. ln {[6]-$[6]_{eq}$} vs. time for isomerization of Cr complexes in $CDCl_3$ at 40 °C.....86

22. ln {[6]-$[6]_{eq}$} vs. time for isomerization of Cr complexes in toluene-d_8 at 25 °C.....87

23. ln {[6]-$[6]_{eq}$} vs. time for isomerization of Cr complexes in toluene-d_8 at 40 °C.....88

24. ln k_1 vs. 1/T for isomerization of Cr complexes in $CDCl_3$ solution 89

25. ln k_{-1} vs. 1/T for isomerization of Cr complexes in $CDCl_3$ solution 90

26. ln (k_1/T) vs. 1/T for isomerization of Cr complexes in $CDCl_3$ solution 91

27. ln (k_{-1}/T) vs. 1/T for isomerization of Cr complexes in $CDCl_3$ solution 92

28. $^{31}P\{^1H\}$ NMR spectrum of $W(CO)_5PPh_2C(PPh_2)=CH_2$ 93

29. ^1H NMR spectrum of $W(CO)_5PPh_2C(PPh_2)=CH_2$ 95

30. COSY spectrum of $W(CO)_5PPh_2C(PPh_2)=CH_2$ 96

31. $^{13}C\{^1H\}$ NMR spectrum of $W(CO)_5PPh_2C(PPh_2)=CH_2$ 97

32. HETCOR spectrum of $W(CO)_5PPh_2C(PPh_2)=CH_2$ 101

33. DEPT spectrum of $W(CO)_5PPh_2C(PPh_2)=CH_2$ 102

34. Molecular structure of $W(CO)_5PPh_2C(PPh_2)=CH_2$ 103

35. Observed $^{31}P\{^1H\}$ NMR spectrum of $[W(CO)_5PPh_2]_2C=CH_2$ 104

36. Calculated $^{31}P\{^1H\}$ NMR spectrum of $[W(CO)_5PPh_2]_2C=CH_2$.....105

37. IR spectrum of $W(CO)_5NH_2Ph$ in the carbonyl region.....106

38. IR spectrum of $W(CO)_5PPh_2C(PPh_2)=CH_2$ in the carbonyl region.....107

39. IR spectrum of $[W(CO)_5PPh_2]_2C=CH_2$ in the carbonyl region.....108

Chapter I: Kinetic and Thermodynamic Study of Phosphine Exchange in $(OC)_5Cr[\eta^1\text{-}PPh_2CH_2CH(PPh_2)_2]$

A. Introduction

Metal carbonyl complexes and their phosphine derivatives play an important part in organometallic chemistry and in catalysis.[1,2] Catalytic activity is generally related to the tendency of one ligand to be replaced by another and as a result ligand replacement processes have drawn considerable attention. Many previous studies have focused on CO substitution in $M(CO)_6$ (M = Cr, Mo, and W) and $Fe(CO)_5$ complexes by various ligands.[3] Substitution of CO by phosphines in these complexes generally proceeds at elevated temperatures by dissociative (D) loss of CO, although an associative interchange mechanism (I_a) can be important as minor pathway.[4]

D mechanism:

$$M(CO)_6 \underset{k_{-1}}{\overset{k_1}{\rightleftharpoons}} M(CO)_5 + CO$$

$$M(CO)_5 + L \xrightarrow{k_2} M(CO)_5L$$

I_a mechanism:

$$M(CO)_6 + L \underset{}{\overset{k_1}{\rightleftharpoons}} M(CO)_6L \xrightarrow{k_2} M(CO)_5L + CO$$

The well-known ligand $Ph_2PCH_2CH_2PPh_2$ (dppe), was first synthesized in 1960.[5] Since then it has been used to stabilize hundreds of transition metal complexes.[6] It may function as a chelating, bridging, or dangling ligand:

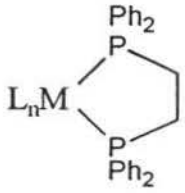

Chelating

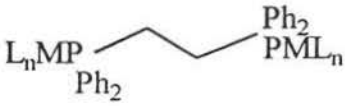

Bridging

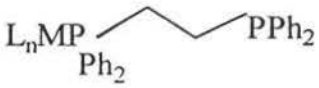

Dangling

Chelated complexes of dppe are especially stable because five-membered rings are relatively strain-free.[7] When heated, dangling and bridged dppe complexes rearrange to chelated complexes (Reaction 1) .[8]

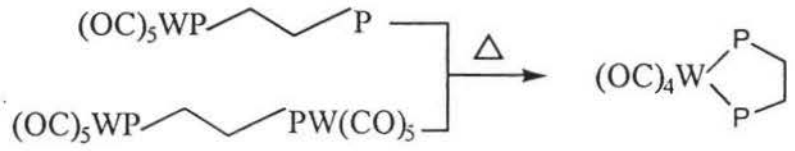

(1)

Although the thermal or photolytic conditions normally employed for carbonyl substitution favor the formation of chelated products, the inertness to substitution of group 6 metal carbonyls allows the possibility of synthesizing complexes of these metals in which dppe serves as a monodentate ligand.

Dangling dppe complexes are the least abundant of the three structural types because of their tendency to undergo chelation, an event which occurs when a vacant coordination site becomes available. The early examples of dangling ligand complexes, all of which are substitutionlly inert, include $[Co(NO)(CO)_2(\eta^1$-dppe)],[9] [Mn(Cp)(CO)(NO)(η^1-dppe)]$^+$,[10] $[Co(CN)_2(\eta^1$-dppe)(η^2-dppe)],[11] $[Fe(Cp)(CO)_2(NO)(\ \eta^1$-dppe)]$^+$,[12] and $\{Mo(Cp)(\ \eta^1$-dppe$)_2\,[C{=}C(CN)_2]\}^+$,[13] and were observed or isolated as unexpected products.

The first dangling dppe complexes to be synthesized by design were reported in 1972 by two different groups, both targeting $M(CO)_5(\eta^1\text{-dppe})$ (M=Cr, Mo, W). One approach was to displace aniline from $M(CO)_5(NH_2Ph)$ with dppe (Reaction 2),[14] while the other utilized strong Lewis acids to assist in the removal of X^- from $[M(CO)_5X]^-$ in the presence of dppe (Reaction 3).[15]

$$M(CO)_5(NH_2Ph) + dppe \longrightarrow M(CO)_5(\eta^1\text{-}dppe) + Ph_2NH_2 \quad (2)$$

$$[M(CO)_5X]^- + [R_3O]^+ + dppe \longrightarrow M(CO)_5(\eta^1\text{-dppe}) + RX + R_2O \quad (3)$$

Both of these methods successfully prevent formation of chelated products because they can be carried out at temperatures below which CO is lost. However, the dppe-bridged complexes, $(CO)_5M(\mu\text{-dppe})M(CO)_5$, form in addition to dangling ligand complexes in both reactions.[16]

The base-catalyzed addition of secondary phosphines to activated carbon-carbon double bonds (hydrophosphination) is an efficient, established pathway for preparing dangling polyphosphine complexes.[17,18] In 1983, Keiter's research group reported that the unidentate diphosphine complexes $Fe(CO)_4(\eta^1\text{-}PPh_2CH_2CH_2PPh_2)$ and *trans*- $Fe(CO)_3(\eta^1\text{-}PPh_2CH_2CH_2PPh_2)_2$ can be prepared by base-promoted addition of PPh_2H to $Fe(CO)_4(PPh_2CH{=}CH_2)$ and *trans*-$Fe(CO)_3(\eta^1\text{-}PPh_2CH{=}CH_2PPh_2)_2$, respectively.[19] It was expected that $Fe(CO)_4(\eta^1\text{-dppe})$ and $Fe(CO)_3(\eta^1\text{-dppe})_2$ would be quite stable with respect to chelation

because the substitution of PPh_3 for CO in $Fe(CO)_4PPh_3$ has a very high activation free energy (Scheme I).[20,21]

$$Fe(CO)_4PPh_3 \underset{+CO}{\overset{-CO(slow)}{\rightleftharpoons}} [Fe(CO)_3PPh_3] \xrightarrow[fast]{PPh_3} \text{trans-}Fe(CO)_3(PPh_3)_2$$

Scheme I

The addition reaction of PPh_2H to $Fe(CO)_{5-n}(PPh_2CH{=}CH_2)_n$ (n=1,2) gave $Fe(CO)_4(\eta^1\text{-}PPh_2CH_2CH_2PPh_2)$ (65%) and gave *trans*- $Fe(CO)_3(\eta^1\text{-}PPh_2CH_2CH_2PPh_2)_2$ (79%) (Scheme II). The addition of the secondary phosphine may also be promoted by the free radical catalyst 2,2'-azobis(isobutyronitrile) (AIBN).[22] Parallel reactions showed that base promotion gave higher yields than the radical pathway.

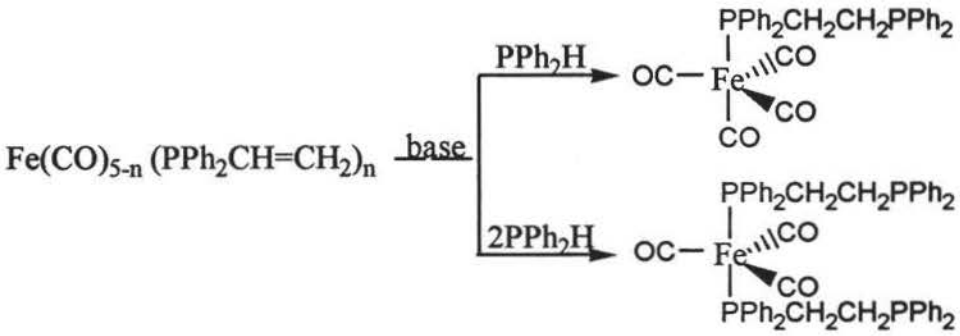

Scheme II

The reaction of $Ph_2PCH{=}CH_2$ with $(OC)_5WPPh_2H$ in the presence of base gives the chelated product, $(OC)_4W(\eta^2\text{-}PPh_2CH_2CH_2PPh_2)$. The chelation occurs because the intermediate $(OC)_5WPPh_2^{\cdot}$ lose CO easily in the presence of

$Ph_2PCH=CH_2$ to form $(OC)_4W(Ph_2CH=CH_2)(Ph_2P)^-$, which subsequently undergoes cyclization (Scheme III).[23]

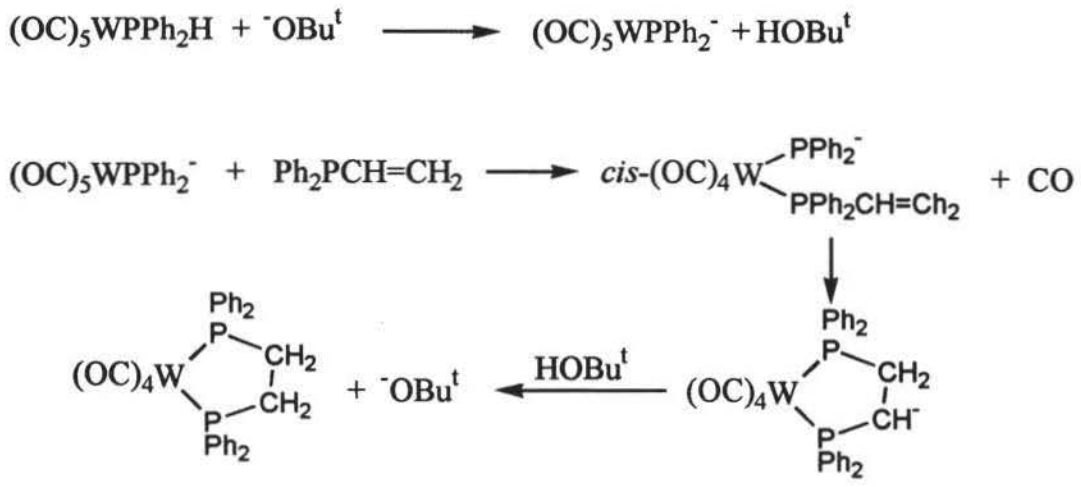

Scheme III

Polyphosphines can also form stable six-membered ring chelated complexes. The reaction of *trans*-$(OC)_4M(PPh_2CH=CH_2)_2$ (M = Cr, Mo,W) with 2 mol of PPh_2H in the presence of AIBN, via isomerization and cyclization gives the chelated product $(OC)_4W$ [PPh_2CH_2 $CH_2CH(PPh_2)$ CH_2 PPh_2] (Scheme IV) .[23]

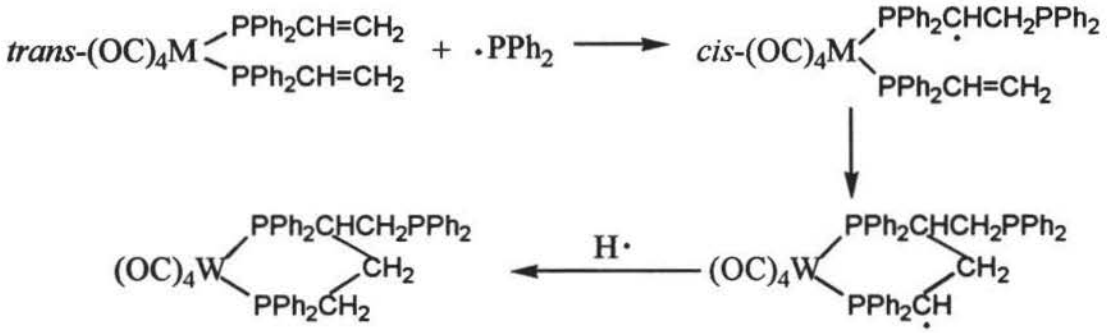

Scheme IV

Dangling ligand complexes have been used in the synthesis of dimetallic compounds bridged by polyphosphine. For example, a recent publication

describes the synthesis and characterization of a number of dimetallic compounds bridged by symmetric diphosphines, $(CO)_5M(\mu\text{-}PPh_2(CH_2)_nPPh_2)M(CO)_5$ (M=Cr, Mo, W; n = 1,2,3).[24] This was a surprising result because it had been previously believed that when n=1, the steric bulk of the phenyl groups combined with the small bite angle of bis(diphenylphosphino)methane (dppm), would make $(CO)_5M(\eta^1\text{-dppm})$ too crowded to coordinate to another $M(CO)_5$ unit. The ^{31}P NMR chemical shifts and coupling constants were inconsistent with the assigned structure and the synthesis was reinvestigated. In 1995, it was found that the dppm-bridged dimetallic species, $(CO)_5M(\mu\text{-dppm})M(CO)_5$ could be synthesized in toluene at 60 °C by displacement of acetonitrile from $(CO)_5W(NCMe)$ in the presence of either $(CO)_5M(\eta^1\text{-dppm})$ or free dppm (Scheme V). The product gave a ^{31}P chemical shift and J_{WP} values that were as expected.[25]

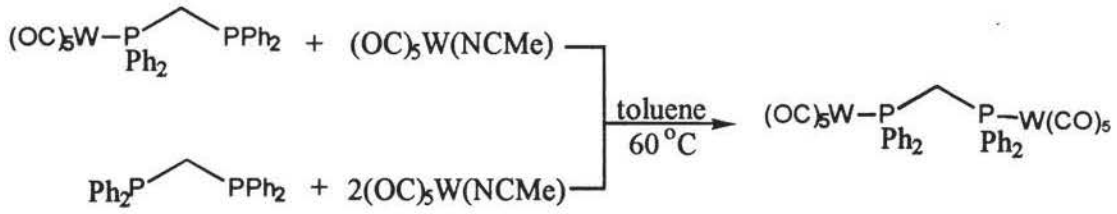

Scheme V

Dangling ligand complexes also have become important precursors for the synthesis of heterobimetallic compounds. Interest in these compounds as

models for surface and catalytic reactions has led to an extensive research area.[26-29] Heterobimetallic complexes are of particular interest because the reactivities of different metals may be exploited in chemical transformations.[30,31]

Some recent examples of heterobimetallic complexes synthesized from dangling ligand complex precursors illustrate a significant interest in this area of research. The reaction of $RuCp(PPh_3)Cl(\eta^1\text{-dppm})$ with $Pt(COD)Cl_2$ gives the heterobinuclear complex $RuCp(PPh_3)Cl(\mu\text{-dppm})PtCl_2$ (Reaction 4) in which the diene has been displaced from platinum.

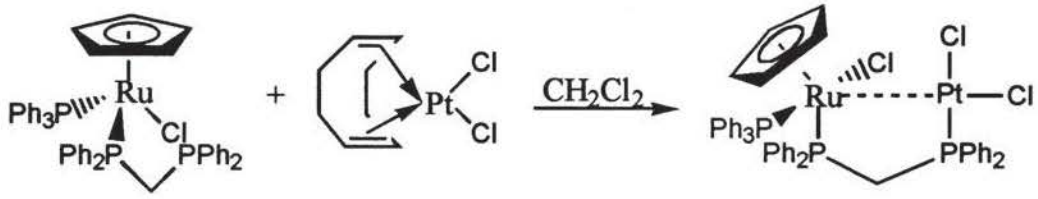

(4)

Reaction of $RuCp(PPh_3)Cl(\mu\text{-dppm})PtCl_2$ with $Tl[PF_6]$ in the presence of CO results in substitution of a single chloride at the ruthenium center to form $[RuCp(CO)(PPh_3)(\mu\text{-dppm})PtCl_2]PF_6$ (Reaction 5). Assignment of the site of CO binding is based on spectroscopic and electrochemical data for the complex. The carbonyl peak in the ^{13}C NMR spectrum shows no platinum satellites. The IR spectrum of $[RuCp(CO)(PPh_3)(\mu\text{-dppm})PtCl_2]PF_6$ shows a CO band (ν_{co} = 1979cm^{-1}). In addition, there is a significant shift in the oxidation potential of the ruthenium center.[32]

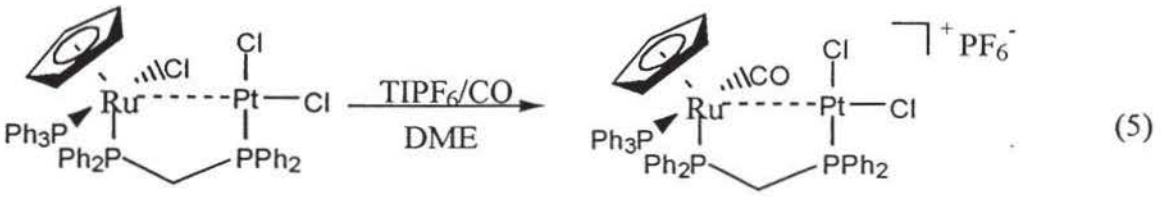

(5)

(DME = ethylene glycol dimethyl ether)

In another paper it was reported that treatment of $(\eta^5\text{-}C_5H_5)_2Rh_2(CO)\{\eta^1\text{-}Ph_2P(CH_2)_nPPh_2\}(\mu\text{-}\eta^1\text{:}\eta^1\text{-}CF_3C_2CF_3)$ with $(\eta^5\text{-}CH_3C_5H_4)Mn(CO)_2(thf)$ or $Cr(CO)_5(thf)$ gives the hetero-trinuclear products $(\eta^5\text{-}C_5H_5)_2Rh_2(CO)\{\mu\text{-}CF_3C_2CF_3\}\{\mu\text{-}\eta^1\text{:}\eta^1\text{-}Ph_2P(CH_2)_nPPh_2\}(\eta^5\text{-}CH_3C_5H_4)Mn(CO)_2$ (I) and $(\eta^5\text{-}C_5H_5)_2Rh_2(CO)\{\mu\text{-}CF_3C_2CF_3\}\{\mu\text{-}\eta^1\text{:}\eta^1\text{-}Ph_2P(CH_2)_nPPh_2\}Cr(CO)_5$ (n=1-4) (II) in good yield.[33] The dangling end of the unidentate attached bisphosphine in the complexes $(\eta^5\text{-}C_5H_5)_2Rh_2(CO)\{\eta^1\text{-}Ph_2P(CH_2)_nPPh_2\}(\mu\text{-}\eta^1\text{:}\eta^1\text{-}CF_3C_2CF_3)$ was the target for the attachment of metal complexes L'M'.

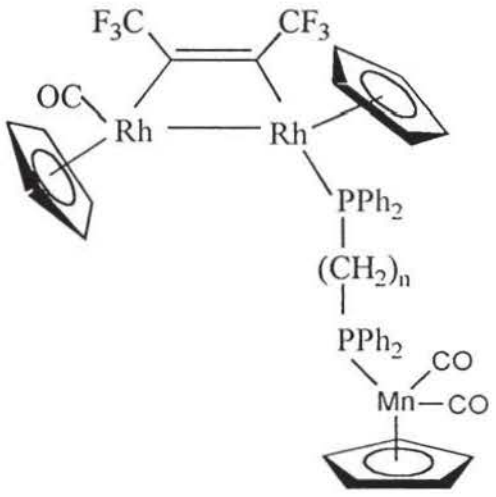

I

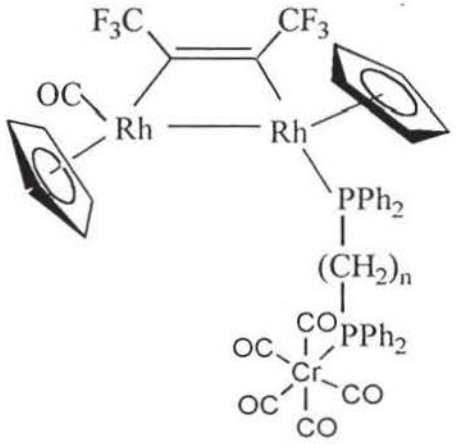

II

The ligand 1,1-bis(diphenylphosphino)ethene (vdpp), which was of importance in our work, was first synthesized in 1982.[34] Since then, its charm has been recognized because the double bond in vdpp provides the opportunity for the preparation of many transition metal complexes by addition reactions (Scheme VI).[35]

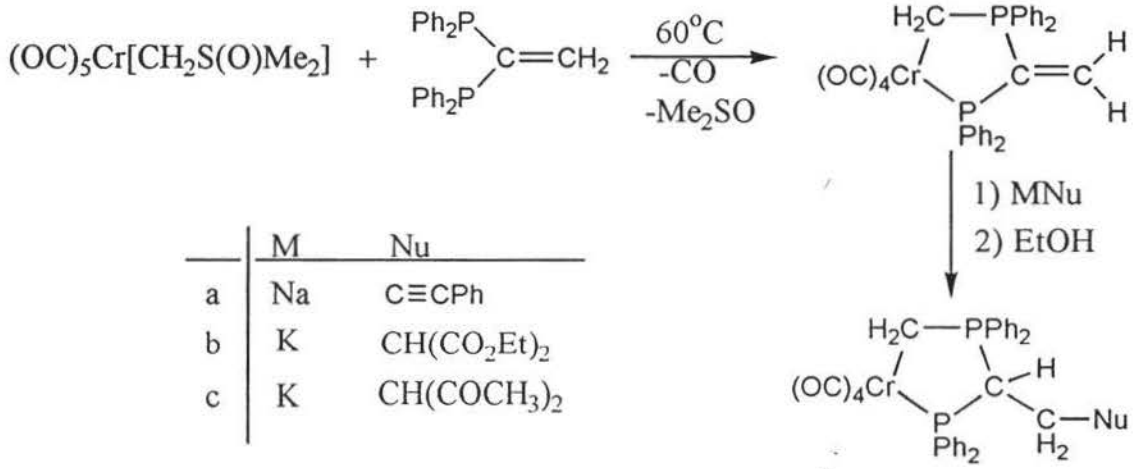

	M	Nu
a	Na	C≡CPh
b	K	$CH(CO_2Et)_2$
c	K	$CH(COCH_3)_2$

Scheme VI

Dangling vdpp complexes can also coordinate to a second metal atom to give a heterometallic complex. For example, treatment of rhenium pentahydride complex $[ReH_5\{P(C_6H_{11})_3\}_2(vdpp\text{-}P)]$ with silver iodide in dichloromethane solution gives $[\{(C_6H_{11})_3P\}_2H_3Re(\mu\text{-}vdpp)(\mu\text{-}H)_2AgI]$ (Reaction 6).

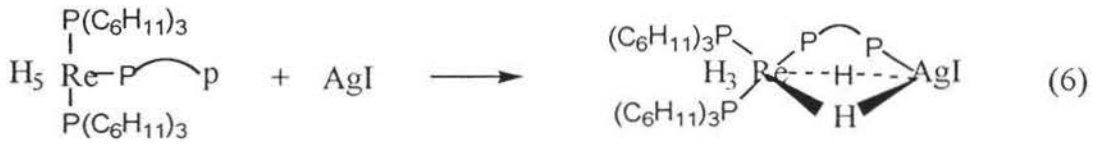

(6)

The $^{31}P\{^{1}H\}$ NMR spectrum of the product at 21 °C consisted of one singlet at δ 33 ppm assigned to the two $P(C_6H_{11})_3$ groups, two multiplets, one at 41ppm assigned to the vdpp phosphorus atom bound to rhenium and a broad resonance at -8.1ppm assigned to the vdpp phosphorus atom bound to silver. The broadness of the latter signal was due to rapid exchange of phosphorus at silver,[36] which is common for silver phosphine complexes.[37]

Coordination of vdpp activates the vinylidene double bond towards nucleophilic (Michael) addition reactions. On coordination to group 6 metal carbonyls, the vinylidene double bond in $[M(CO)_4(vdpp\text{-}PP')]$ can be added to smoothly by a range of amines, hydrazines, or carbon nucleophiles.[38,39]

For example, treatment of $[M(CO)_4(vdpp\text{-}pp')]$ with Li(C≡CPh) in the presence of $Me_2NCH_2CH_2NMe_2$ (tmen) gives $\{M(CO)_4[(PPh_2)_2CHCH_2C{\equiv}CPh]\}$ (M = Cr, Mo, or W) as yellow or orange crystals in excellent yields. The participation of tmen is to increase the carbanion character of the acetylide(Scheme VII).[38]

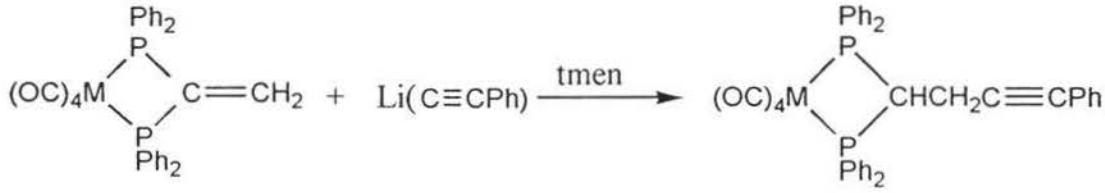

Scheme VII

When coordinated to $PtMe_2$, the vinylidene double bond of vdpp in the complex $[PtMe_2(vdpp\text{-}PP')]$ becomes more activated than when coordinated to

$M(CO)_4$ (M = Cr, Mo, W) because platinum(II) is more polarizing than M(0).[40,41] In other words, the greater electron-withdrawing power of $PtCl_2$ makes the vinylidene double bond more susceptible to nucleophilic attack. These Michael addition reactions were monitored by $^{31}P\{^1H\}$ NMR spectroscopy. A solution of $Cl_2Pt(PPh_2)_2C{=}CH_2$ in CH_2Cl_2-CD_2Cl_2 was cooled to -80 °C and an appropriate amount of hydrazine or amine in CH_2Cl_2 was added by syringe and $^{31}P\{^1H\}$ NMR spectra were taken at intervals. The temperature was increased stepwise and further spectra taken until a reaction occurred. For Me_2NNH_2, the reaction occurred at -40 °C ($t_{1/2}$ = 6 min), for 4-$MeOC_6H_4CH_2NH_2$ at -80 °C($t_{1/2}$ = 2 min) (Scheme VIII). The same reactions were repeated with $I_2Pt(PPh_2)_2C{=}CH_2$ and it was found that Me_2NNH_2 slowly commences reacting at -50 °C, but the reaction did not go to completion until the mixture was warmed up to 0 °C. With 4-$MeOC_6H_4CH_2NH_2$ a slow reaction occurred at -80 °C($t_{1/2}$ = 18 min).[42]

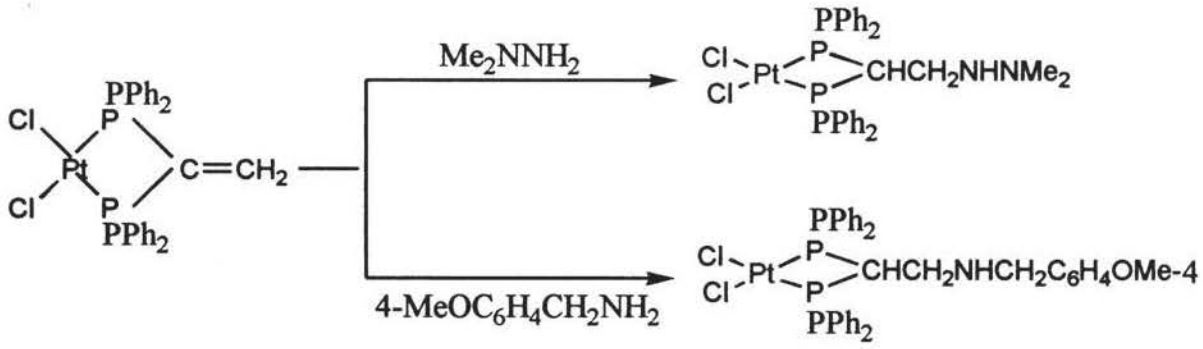

Scheme VIII

The ligand 1,1,2-tris(diphenylphosphino)ethane (tppe), which embodies features of both dppm and dppe in respect of its potential for forming complexes

containing four- and five-membered chelate rings, was prepared in high yield, by the base-catalyzed ($KOBu^t$) addition of diphenylphosphine to the double bond of vdpp (Reaction 7).[43]

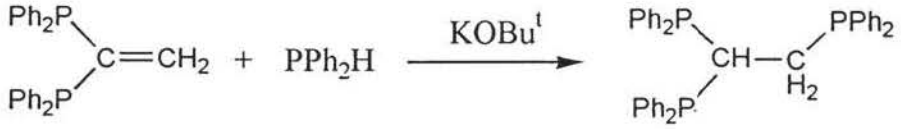

(7)

In principle, tppe can coordinate to a group 6 carbonyl moiety $M(CO)_n$ (n = 3, 4, 5) in five ways.

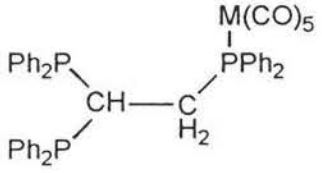

(A)

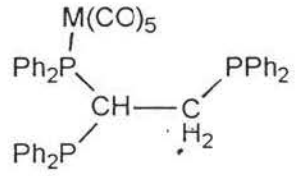

(B)

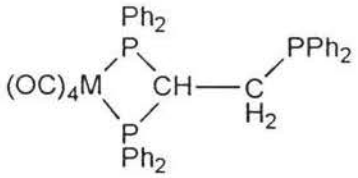

(C)

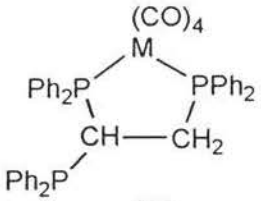

(D)

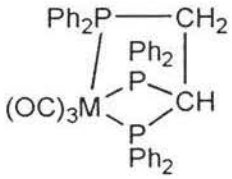

(E)

Among the chelated complexes, ring strain effects should be minimal in (D) due to the presence of a five-membered ring, but could be significant in (C) and substantial in (E). The direct high-temperature {refluxing diglyme[1,1'-oxybis-(2-methoxy ethane)]} reaction between tppe and $M(CO)_6$(M = Cr, W, Mo) is

satisfactory as a preparative route to complexes of the type (D) if the reaction time is controlled. For (E), it was found better (essential for M = Cr) to use tppe to displace EtCN from *fac*-$[M(CO)_3(EtCN)_3]$.[44] The monodentate species (A) and (B) were produced in a *ca.* 4:1 ratio mixture by displacement of tetrahydrofuran (THF) from $\{M(CO)_5(THF)]$ by tppe. There was no pure form of either (A) or (B) obtained from this reaction, but it was found possible to isolate (B) (M = Cr, Mo, W) in pure form indirectly (Reaction 8).

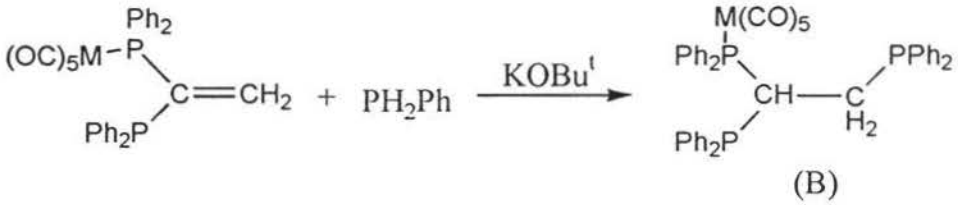

(8)

(B)

Similarly, reaction (9), based on work by Shaw and co-workers for M = W,[45] was used as a preparative route to (C) (M = Cr, Mo, W).

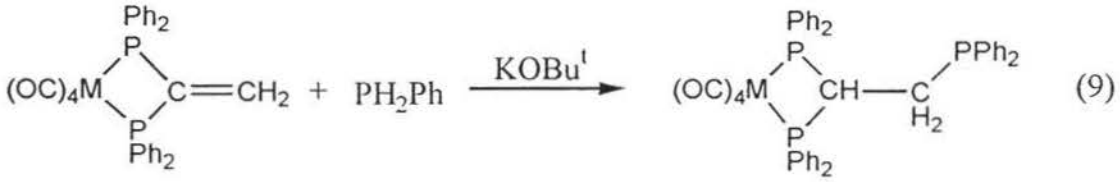

(9)

(C)

A selective synthesis for (A) was later designed by using $PtCl_2$ as a protecting group.[46] The complex $Cl_2Pt(PPh_2)_2CHCH_2PPh_2W(CO)_5$ was prepared , and $(OC)_5W[\eta^1\text{-}PPh_2\,CH_2\,CH(PPh_2)_2]$ was displaced with CN^- (Scheme IX).

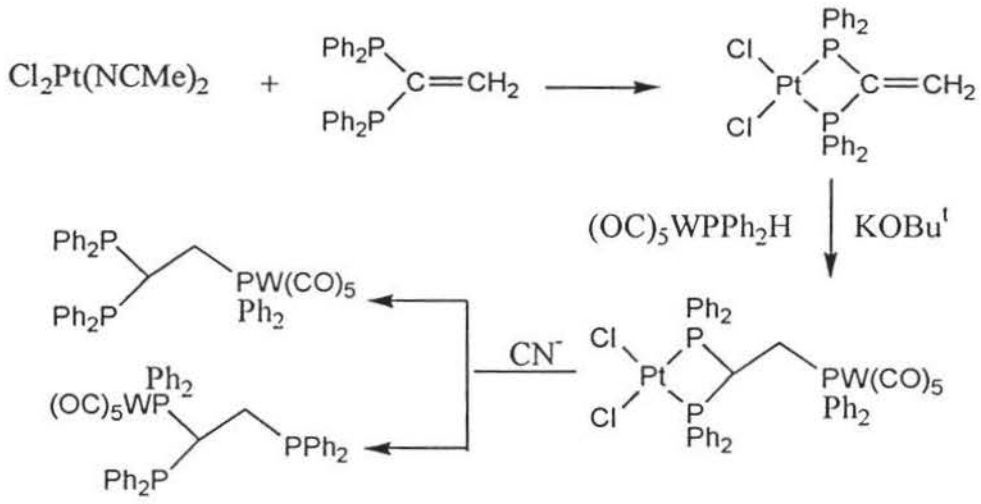

Scheme IX

This reaction sequence also gave a mixture of (A) and (B) and as a result it was concluded that (A) and (B) exist in equilibrium. This work represented the first experimental evidence for the exchange of terminal and coordinated phosphorus groups in pentacarbonyl complexes of group 6.[46] Monitoring the product mixture with $^{31}P\{^{1}H\}$NMR spectroscopy revealed that (A), which formed first, slowly converted to (B) (reaction 10).[46]

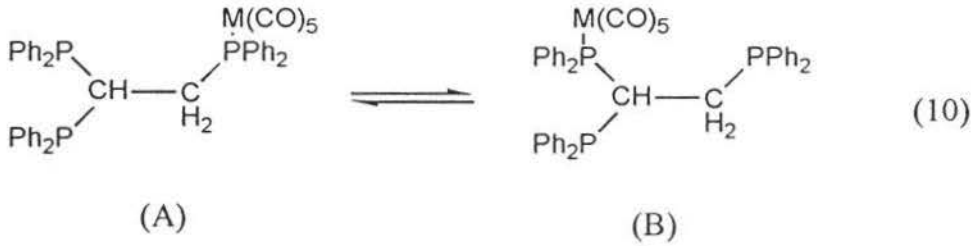

(A) (B) (10)

Intrigued by this highly unusual behavior, a kinetic and thermodynamic study was initiated. The results showed that isomer (B) is more stable than isomer (A) (ΔG_{298} = -3.86kJ/mol) even though the more sterically demanding end of the phosphine ligand is coordinated in (B). The entropy of activation ($\Delta S^{\neq}$ = -28.2JK^{-1} mol^{-1}) and enthalpy of activation ($\Delta H^{\neq}$ = 92.6 kJ/mol) for the forward reaction strongly suggested a transition state which is associative in nature. The rate constant for the forward reaction at 55 °C was determined to be 3.7 x 10^{-4} s^{-1}. For purposes of comparison phosphorus exchange in $(OC)_5W[\eta^1$-$PPh_2CH_2\,CH_2P(p\text{-}tol)_2]$ was also studied and it was found that the rate constant for isomerization was 3.3 x 10^{-8} s^{-1} (four orders of magnitude slower than reaction 10), suggesting a reaction which is dissociative in nature. To account for the unusually fast rate of phosphine exchange in reaction 10, a mechanistic model was postulated in which the transition state consisted of interaction of one phosphine arm with the cis carbonyl groups of tungsten, while the second phosphine arm displaces the labile coordinated phosphine (Scheme X).[47] It is significant that $^4J_{PC}$ in (B) between the phosphorus atom of the short dangling phosphine and the carbonyl groups of tungsten was observed, suggesting a though-space interaction.

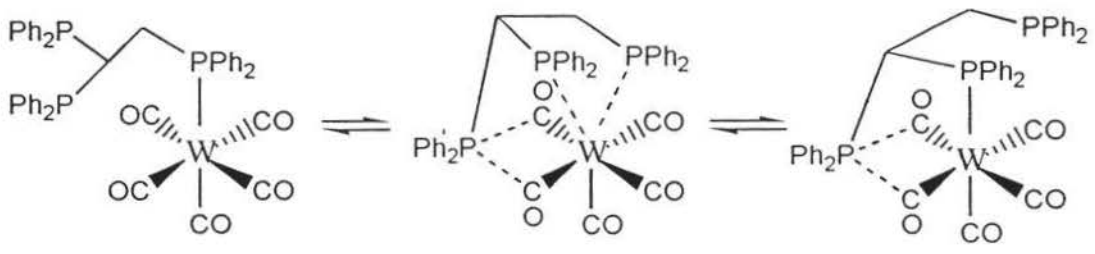

Scheme X

The work in this thesis continues the thermodynamic and kinetic studies of phosphine exchange in dangling phosphine complexes by extending and completing the studies previously initiated for chromium. The purpose of the work is to gain further insight into the mechanism of isomerization, and to determine the extent to which the solvent medium influences rates of exchange and isomer stability.

Chromium atoms are much smaller than tungsten atoms. If substitution of L' for L, $L_6M + L' = L_5ML' + L$ (M = Cr, W), proceeds by associative mechanism, it would be expected that the reaction would go faster for the tungsten complex because a 7-coordinate transition state would be more stable when tungsten is the central metal atom than when the smaller chromium atom is present. If the reaction proceeds by a dissociative mechanism, it would be expected that isomerization of the chromium complex would be faster than that of the tungsten complex because tungsten-phosphorus bonds are stronger than chromium-phosphorus bonds. Thus, by comparing the reaction rates of tungsten and chromium complexes, we can provide experimental evidence in support of an associative or dissociative mechanism.

Furthermore, a comparison of the activation parameters of tungsten and chromium complexes will provide additional mechanistic information. If the activation enthalpy for chromium is larger than for tungsten, it would suggest that the mechanism has a significant associative component because the smaller chromium atom would be less likely to support a 7-coordinate complex. But, if it

is larger for tungsten, it would suggest a significant dissociative component because the W-P bond is stronger than the Cr-P bond.

The choice of solvent may also be of considerable importance as it could have a large influence on both the thermodynamics and kinetics of isomerization. If the lone electron pairs on the dangling phosphines are significantly solvated, the isomerization reaction would be influenced by the extent of lone pair-solvent interaction. Previous work on the isomerization of tungsten complexes was carried out in $CDCl_3$, a solvent which could affect reaction rates by hydrogen bonding (weakly) between the solvent and dangling phosphorus lone pairs. Toluene, a solvent less polar than chloroform, might interact with the dangling phosphorus ligand less than chloroform and lead to significantly different reaction rates and positions of equilibrium.

B. Results and discussion

1. Synthesis of $(OC)_5Cr[\eta^1\text{-}PPh_2CH_2CH(PPh_2)_2]$

1,1-Bis(diphenylphosphino)ethene (vdpp) was prepared from Ph_2PLi in dry THF according to the literature method.[34]

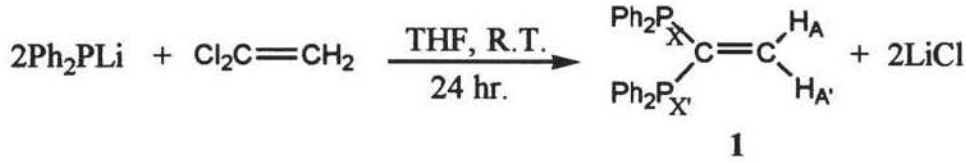

(1)

1

The ^1H NMR spectrum of **1** (Fig.1) showed a triplet at δ 5.9 ppm, which is assigned to the $C=CH_2$ protons. This is a second order AA'XX' spin system in which H_A and $H_{A'}$ are chemically equivalent and magnetically nonequivalent. The observed triplet is a deceptively simple spectrum, in which the separation of the two outer lines is $|\,^3J_{P(X)H(A)} + {}^3J_{P(X')H(A)}|$. The $^{13}C\{^1H\}$ NMR spectrum (Fig.2) showed a triplet at δ 135.7 ppm ($^1J_{PC'} = 9.4$ Hz) assigned to C' of vinyl carbons ($C'=C''H_2$), a triplet at δ 136.1 ppm ($^2J_{PC''} = 4.9$ Hz) assigned to the terminal carbon C'' of $C'=C''H_2$, and multiplets (from δ 128.2 ppm to 134.5 ppm) assigned to the phenyl carbons. The $^{31}P\{^1H\}$NMR spectrum (Fig.3) showed a single peak at δ -2.9 ppm. Comparing with McFarlane's report,[34] we agree with the chemical shifts of P (δ -3.9 ppm), the terminal carbon C''(δ 135.5 ppm) and the phenyl carbons (δ 128.5 to 136.0 ppm), but we do not agree with the chemical shift of C' (δ 148.4 ppm) or the coupling constants ($^1J_{PC'} = 36.4$ Hz, $^2J_{PC''} = 8.1$ Hz).

The preparation of $(OC)_5CrPPhH$ was carried out from the substitution of THF in $Cr(CO)_5THF$ by PPh_2H, while $Cr(CO)_5THF$ came from the UV irradiation of $Cr(CO)_6$ in THF.[48]

$$Cr(CO)_6 + THF \xrightarrow[8\ hr]{UV} Cr(CO)_5THF + CO \qquad (2)$$

$$Cr(CO)_5THF + PPh_2H \xrightarrow{1\ hr} \mathbf{2} + THF \qquad (3)$$

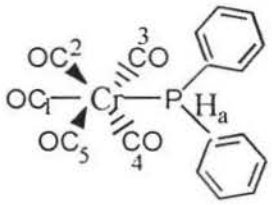

2

The ^1H NMR spectrum of complex **2** showed a doublet at δ 6.5 ppm (J_{PH} = 338.9 Hz), which was assigned to proton H_a (Fig.4). The $^{13}C\{^1H\}$ NMR spectrum of complex **2** showed a doublet at δ 221.0 ppm ($^2J_{PC}$ = 7.1 Hz) assigned to C_1, and a doublet at δ 216.2 ppm ($^2J_{PC}$ = 13.4 Hz) assigned to $C_{2\text{-}5}$. The ipso carbons of the two phenyl groups gave a doublet at δ 132.6 ppm ($^1J_{PC}$ = 38.8 Hz), the ortho carbons gave a doublet at δ 131.9 ppm ($^2J_{PC}$ = 11.3 Hz), the para carbons gave a doublet at δ 130.4 ppm ($^4J_{PC}$ = 1.5 Hz), and the meta carbon gave a doublet at δ 129.0 ppm ($^3J_{PC}$ = 9.6 Hz) (Fig.5). These assignments have been supported by J. H. Nelson's spectroscopy book.[48b] The $^{31}P\{^1H\}$ NMR spectrum is also consistent with the structure of **2** (Fig.6).

For $(OC)_5CrPPh_2H$ the IR[ν(CO)(cm^{-1})] data ($A_1^{(1)}$:1945, $A_1^{(2)}$:2067, E:1988) suggested that the π-acidity of PPh_2H is relatively high compared with H_3P and Ph_3P, but lower than $(EtO)_3P$, $(PhO)_3P$, and X_3P (X is halogen) (Fig.7).

A $Cr(CO)_5L$ complex has C_{4v} symmetry, and gives rise to three allowed IR absorptions (two non-degenerate and one doubly degenerate), having the symmetry labels $A_1^{(1)}$, $A_1^{(2)}$ and E. The important one to focus on is $A_1^{(1)}$, which corresponds to the symmetrical stretching motion of the CO group lying opposite the ligand L. It is this CO that competes most directly with L for available π electron density and therefore is in a position to best reflect the π acidity of L. In the case of the phosphorus ligands, the π acidity increases as the electronegativity of any substitutent on P increases. As these ligands become more and more competitive for π electrons, CO receives less and less electron density and the C≡O stretching frequency increases accordingly.[49]

The preparation of $Cl_2Pd(Ph_2P)_2C{=}CH_2$ was carried out from the displacement of NCPh from $Cl_2Pd(NCPh)_2$ by $(Ph_2P)_2C{=}CH_2$.

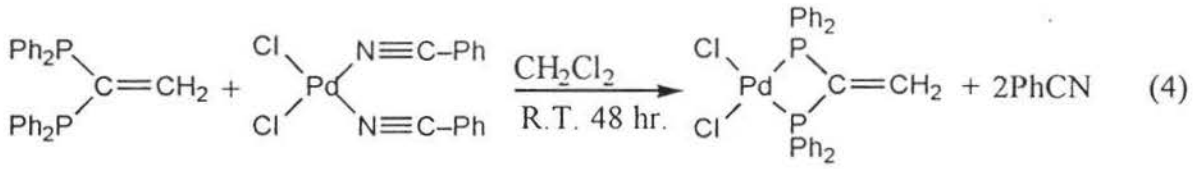

(4)

3

Complex **3** is quite insoluble and its formation was accompanied by the formation of an unidentified byproduct. The $^{31}P\{^1H\}$ NMR spectrum of compound **3** and its byproduct showed singlets at δ -20.6 ppm and -41.4 ppm (Fig.8), while the analogous platinum compound $Cl_2Pt(Ph_2P)_2C{=}CH_2$ had a signal at δ -31.7 ppm with J_{PtP} = 3,244 Hz.[42] Although it was not possible to assign the signal for **3** with

certainty, previous work has shown that ^{31}P chemical shifts for palladium complexes are in general downfield from the platinum complexes. Therefore, we believe the signal at -20.6 belongs to compound **3**. Although palladium has an isotope with a nuclear spin, ^{105}Pd (22.23%), for which I = -5/2, the quadropolar property of this nucleus makes the palladium and phosphorus coupling unobservable under our experimental conditions.[50] The ^{1}H NMR spectrum showed a set of signals at δ 6.4 ppm which was assigned to the AA' portion of the AA'XX' ($P_2C=CH_2$) spin system (Fig.9), and is consistent with the ^{1}H NMR spectrum of $Cl_2Pt(Ph_2P)_2\,C=CH_2$.[42] Attempts to purify compound **3** by recrystallization and column chromatography were not successful. The $^{31}P\{^{1}H\}$ NMR spectrum showed a signal at δ -41.4 ppm which was not identified. As most of the sample remained undissolved, we concluded that perhaps the sample was much more pure than the NMR spectra indicated. Therefore, we continued on to the next reaction and it was successful.

The new compound $Cl_2Pd(Ph_2P)_2CHCH_2PPh_2Cr(CO)_5$ was synthesized by adding $(OC)_5CrPPh_2H$ across the carbon-carbon double bond of compound **3** in the presence of $KOBu^t$.

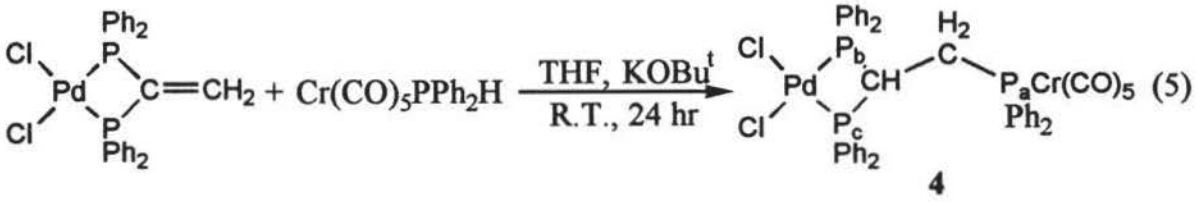

4 (5)

The $^{31}P\{^1H\}$ NMR spectrum of **4** showed a doublet at δ -27.2 ppm ($^3J_{PP}$ = 3.2 Hz) and a triplet at δ 57.4 ppm ($^3J_{PP}$ = 3.6 Hz) (Fig.10). The IR spectrum, ν(C≡O), showed signals at 1939 (vs), 2065 (m) and 2059 (m) (Fig.11). Compared with $Cl_2Pt(Ph_2P)_2CHCH_2PPh_2Cr(CO)_5$,[51] the chemical shift of the phosphorus atom bound to Pd is further downfield than that of the corresponding phosphorus atom bound to Pt, but the chemical shift of phosphorus bound to chromium remains essentially unchanged. The C≡O stretching frequencies were not affected by the differences in the remote Pt and Pd atoms. Recrystallization and column chromatography were applied to purify **4**, but still the signals at δ -38.6 ppm, -20.8 ppm and δ 49.9 ppm were observed in $^{31}P\{^1H\}$ NMR spectrum.

This reaction successfully avoided the formation of chelated product **5** which occurs when $(OC)_5CrPPh_2H$ reacts directly with $(Ph_2P)_2C{=}CH_2$.[46]

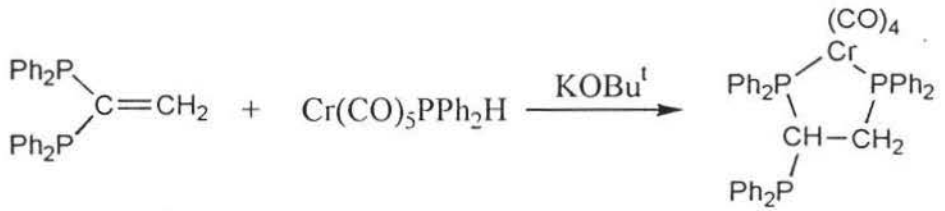

(6)

5

Potassium cyanide was employed to remove the Cl_2Pd from compound **4** and to release $(OC)_5Cr[\eta^1\text{-}PPh_2CH_2CH(PPh_2)_2]$ **6**, which partially isomerized to $(OC)_5Cr[\eta^1\text{-}(PPh_2)_2CHCH_2PPh_2]$ 7.

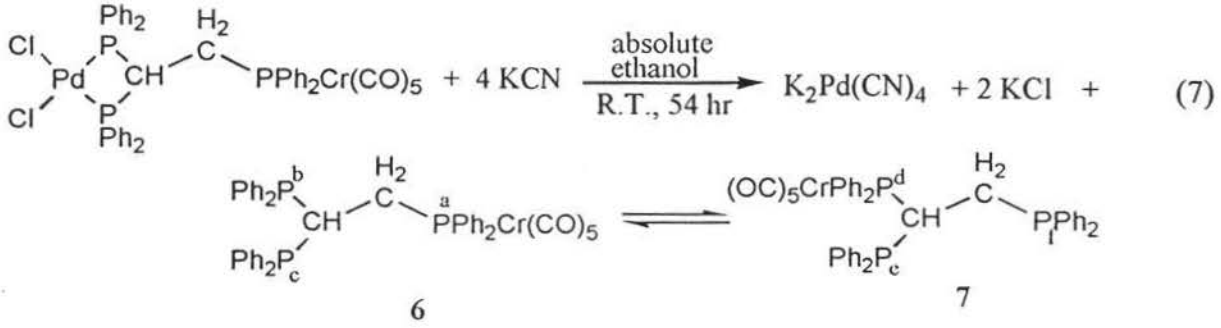

6 7

The $^{31}P\{^1H\}$ NMR spectrum showed that this reaction first gave the product **6** (Fig.12), and then slowly converted to **7** at room temperature (Fig.13). The spectrum of compound **6** showed a triplet at δ 51.8 ppm ($^3J_{PaPb,c}$ = 2.6 Hz) and a doublet at δ-2.8 ppm ($^3J_{PaPb,c}$ = 2.4 Hz). The spectrum of compound **7** gave a doublet of doublets at δ 68.8 ppm ($^2J_{PdPe}$ = 193.2 Hz, $^3J_{PdPf}$ = 21.2 Hz), a doublet at δ -10.9 ppm ($^2J_{PdPe}$ = 193.1Hz), and a doublet at δ -16.0 ppm ($^3J_{PdPf}$ = 21.2 Hz). Coupling between P_e and P_f was not observed.

Typically, a P-C(ax) coupling constant is greater than a P-C(eq) coupling constant for phosphine substituted tungsten pentacarbonyl complexes. The $^{13}C\{^1H\}$ NMR spectrum of **6** shows that the reverse is true for analogous chromium complexes, as the P-C(eq) coupling constant (12.9 Hz) is larger than P-C(ax) coupling constant (6.9 Hz) (Fig.14). Similar coupling constant behavior of chromium complexes was reported in 1980.[52a] A general statement was made that the magnitude of the $^2J_{PC}$ through-metal nuclear spin-spin coupling to the trans CO in $LM(CO)_5$ complexes of Mo and W is significantly larger than that of the analogous coupling to the cis CO, whereas in $LCr(CO)_5$ complexes the converse is true.[52b] The $^{13}C\{^1H\}$NMR spectrum of a similar compound, $(OC)_5CrPPh_2Et$, gave

$J_{P-(eq)}$ = 13.7 Hz, and $J_{P-(ax)}$ = 6.8 Hz, which was in agreement with the assignment for compound **6**. The $^{13}C\{^1H\}$ NMR spectrum of **7** gave a doublet of doublets at δ 216.3 ppm ($^2J_{CP}$ = 12.5 Hz, $^4J_{CP}$ = 3.4 Hz) assigned to the equatorial carbonyl carbons (Fig.15). This long-range coupling was also reported for compound **9** ($^4J_{PC}$ = 3.89 Hz).[51]

Our attempts to carry out free radical reactions to synthesize complex **6** were not successful. It was expected that $(OC)_5CrPPh_2H$ and $(Ph_2P)_2C{=}CH_2$ in the presence of AIBN at elevated temperatures (50 °C or 60 °C), would give complex **6**, but the $^{31}P\{^1H\}$ NMR spectrum showed only a trace of desired product.

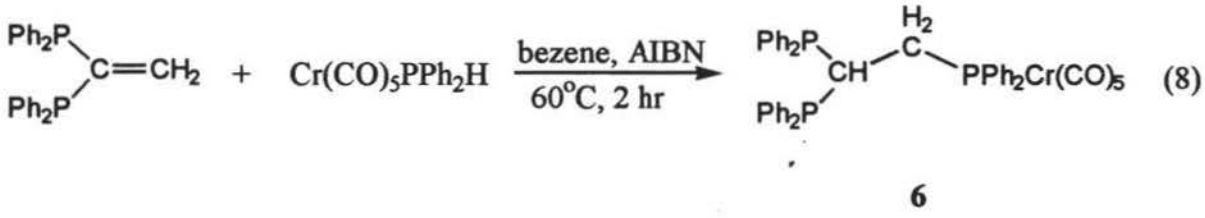

(8)

6

2. Equilibrium Studies of Isomerization of 6 and 7

(9)

6 **7**

The equilibrium studies were carried out in $CDCl_3$ and toluene-d_8 solutions at various temperatures. The equilibrium concentration of isomers **6** and **7** were determined by the integration of $^{31}P\{^1H\}$ NMR spectra. Meaningful integrations

were obtained by using a delay time of 15 s and a pulse width of 16 usec (83 degree). A one pulse decoupling during acquisition was not applied to eliminate NOE (Nuclear Overhauser Enhancement) effects on ^{31}P signal intensities. The equilibrium constants, K = [7]/[6], are found in Table 1. For comparison, the K values of reaction 10 in $CDCl_3$ solution from literature are also listed in Table 1.

(10)

Table 1. The equilibrium constants, K, of reactions A, B and C. A is reaction 10 in $CDCl_3$; B is reaction 9 in $CDCl_3$; C is reaction 9 in toluene-d_8 solution.

K	10 °C	25 °C	40 °C	53 °C	Ref.
A	6.14 ± 0.04	4.74 ± 0.01	3.76 ± 0.05	3.01 ± 0.02	51
B	3.60 ± 0.04	2.61 ± 0.04	2.04 ± 0.04	1.67 ± 0.02	this work
C	N/A	2.18 ± 0.02	1.72 ± 0.04	1.58 ± 0.01	this work

The equilibrium constant, K, of each reaction decreases when the reaction temperature increased, which indicates that the forward reactions are exothermic. This is confirmed by the negative ΔH values shown in Table 3. Among the reactions at the same temperature, the values of K decrease from A to C, and equilibrium positions correspondingly shift from right to left. For the tungsten reaction (A) the product is more stable than the reactant at all temperatures. If the reactant and product isomers were equally stable, the equilibrium constant would

be 2 because there are two possible attachments in the product isomer. For chromium (B) at 53 °C we see that **7** is less stable than **6**, at 40 °C the two isomers are equally stable, and at 25 °C, **7** is more stable than **6**. In toluene **7** is less stable than **6** at temperature above 25 °C.

Insight into the magnitudes of K are given by the determination of ΔH, ΔS, and ΔG for the reactions. Standard equations (eq-1 and eq-2) shown below were used to determine thermodynamic parameters.

$$\Delta G = -RT \ln K = \Delta H - T\Delta S \qquad \text{(eq-1)}$$

$$\ln K = -\Delta H/(RT) + \Delta S/R \qquad \text{(eq-2)}$$

In these equations, R is the gas constant, ΔG, ΔH, ΔS are the change of free energy, the change of enthalpy, and the change of entropy, respectively. The values of ΔH and ΔS can be calculated from the van't Hoff plot (lnK vs. 1/T) (Table 2).

$$\text{Slope} = -\Delta H/R \qquad \text{(eq-3)}$$

$$\text{Intercept} = \Delta S/R \qquad \text{(eq-4)}$$

The plots of lnK vs. 1/T were manipulated (Fig.16-17), and the values of ΔH and ΔS were obtained from equations 3 and 4. The values of ΔG at 25 °C were obtained from the equation, $\Delta G_{(298K)} = \Delta H - T\,\Delta S$. The results are shown in Table 3.

Table 2. The values of lnK and 1/T of reactions A, B and C. A is reaction 10 in $CDCl_3$; B is reaction 9 in $CDCl_3$; C is reaction 9 in toluene-d_8 solution.

1/T (K^{-1})	3.53×10^{-3}	3.36×10^{-3}	3.19×10^{-3}	3.07×10^{-3}	Ref.
lnK (A)	1.81 ± 0.01	1.56	1.32 ± 0.01	1.10 ± 0.01	51
lnK (B)	1.28 ± 0.01	0.96 ± 0.02	0.71 ± 0.02	0.51 ± 0.01	this work
lnK (C)	N/A	0.78 ± 0.01	0.54 ± 0.02	0.46 ± 0.01	this work

Table 3. The values of ΔH, ΔS, and $\Delta G_{(298K)}$ of reactions A, B and C. A is reaction 10 in $CDCl_3$; B is reaction 9 in $CDCl_3$; C is reaction 9 in toluene-d_8 solution.

	ΔH (kJ mol^{-1})	ΔS (J mol^{-1} K^{-1})	$\Delta G_{(298K)}$(kJ mol^{-1})	Ref.
A	-12.25 ± 0.1	-28.2 ± 0.3	-3.86 ± 0.14	51
B	-13.63 ± 0.39	-37.62 ± 1.28	-2.42 ± 0.38	this work
C	-9.41 ± 1.90	-25.25 ± 6.10	-1.88 ± 2.63	this work

For reaction B, both ΔH and ΔS are more negative than for reaction A. The difference in the entropy change is most striking. The large negative ΔS values in both cases suggest that as **6** isomerizes to **7** a significant restriction in freedom of movement results. It might be expected that there would be greater steric congestion in the chromium product than in the tungsten leading to a more negative ΔS.

It is apparent that the solvent plays an important role in these reactions. In toluene both ΔH and ΔS are less negative than in $CDCl_3$. This might suggest that toluene interacts more strongly with dangling phosphine groups than chloroform. Isomer **6** may be somewhat stabilized relative to **7** as a result of this interaction.

The large decrease in entropy for these reactions is overcome by the negative enthalpy value leading to an overall favorable (negative) free energy of reaction. The negative free energy change is the driving force of the spontaneous reaction. The magnitude of the free energy becomes less negative from A to C, which is also consistent with the trend of the values of K.

Complex **7** is more themodynamically stable than **6** at lower temperatures even though the more sterically congested end of the phosphine ligand is coordinated in **7**. An intramolecular interaction between the short phosphine arm and the carbonyl groups is postulated to explain this abnormal phenomenon (see scheme X).[51] Supporting experimental evidence for this phosphine-carbonyl interaction, in addition to the large entropy decrease for the reaction, is also given by the presence of long-range phosphorus-carbon coupling in **7** ($^4J_{PC}$ = 3.4 Hz) (Fig.15), which we believe is largely a through-space interaction. The similar long-range P-C coupling in compound **9** ($^4J_{PC}$ = 3.8 Hz)[51] is larger than that of **7** and this is in good agreement with the K values indicating that tungsten complex **9** is more stable than chromium complex **7**.

The IR spectrum of **7** in the carbonyl region is consistent with C_{4v} symmetry suggesting that the interaction between the short arm phosphine of **7** and carbonyl groups is not localized (Fig.18). It has been reported that electronic differences in $LW(CO)_5$ ($L=PMe_nPh_{3-n}$) are too small to be determined by vibrational spectroscopy.[52C] Therefore, it is not surprising that the IR spectra of **6** and **7** are superimposable.

3. Kinetic Studies of Isomerization of 6 and 7 in $CDCl_3$ and Toluene-d_8.

6 **7** (9)

This is a first-order reaction in which the net rate of disappearance of **6** is given by

$$-d[6]/dt = k_1[6] - k_{-1}[7] \quad \text{(eq-5)}$$

where k_1 and k_{-1} are rate constants of the forward and backward reactions, respectively.

When the reaction reaches equilibrium,

$$-d[6]/dt = 0 \quad \text{(eq-6)}$$

$$k_1[6]_{eq} = k_{-1}[7]_{eq} \quad \text{(eq-7)}$$

$$[7]_{eq}/[6]_{eq} = K = k_1/k_{-1} \quad \text{(eq-8)}$$

Also if **6** and **7** are the only complexes in the reaction system, it is true that

$$[6] + [7] = [6]_{in} + [7]_{in} = [6]_{eq} + [7]_{eq} \quad \text{(eq-9)}$$

Where $[6]_{in}$ and $[7]_{in}$ are the initial concentrations of **6** and **7** and $[6]_{eq}$ and $[7]_{eq}$ are the equilibrium concentrations of **6** and **7**, respectively.

Substitution of equations 8 and 9 into equation 5, and rearrangement, gives the relation

$$-d[6]/dt = (k_1 + k_{-1})\{[6] - [6]_{eq}\} \quad \text{(eq-10)}$$

Integration of equation 10 gives

$$\ln\{[6] - [6]_{eq}\} = -(k_1 + k_{-1})\, t + \ln\{[6]_{in} - [6]_{eq}\} \quad \text{(eq-11)}$$

Therefore, a plot of $\ln\{[6] - [6]_{eq}\}$ versus t gives

$$\text{slope} = -(k_1 + k_{-1})$$

From the slope and equilibrium constant K, the individual forward and backward rate constants can be obtained.

$$k_1 = (\text{-slope})(K)/(1 + K)$$

$$k_{-1} = (\text{-slope})/(1 + K)$$

Also, the half life to reach equilibrium can be calculated by

$$t_{1/2} = (\ln 2)/k \qquad \text{(eq-12)}$$

The time to go half way to equilibrium is given by

$$t_{1/2}' = (\ln 2)/(k_1 + k_{-1}) \qquad \text{(eq-13)}$$

Reaction 9 was carried out at 40 °C in $CDCl_3$, and at 25 °C and 40 °C in toluene-d_8. The change of concentration of **6** was detected by running $^{31}P\{^1H\}$ NMR spectra and taking integrals at appropriate time intervals.

The plots of $\ln\{[6] - [6]_{eq}\}$ versus time at 10 °C, 25 °C (the first two data points are from Lin's thesis[54]), 40 °C in $CDCl_3$, and the plots of $\ln\{[6] - [6]_{eq}\}$ versus t at 25 °C and 40 °C in toluene-d_8 were manipulated (Fig. 19-23).[53] The values of k_1, k_{-1} and $t_{1/2}'$ were obtained, and shown in Table 4.

Table 4. Rate constants and half-lives to equilibrium for isomerization reactions of A, B and C. A is reaction 10 in $CDCl_3$; B is reaction 9 in $CDCl_3$; C is reaction 9 in toluene-d_8 solution.

	Temp. (K)	k_1 (s^{-1})	k_{-1} (s^{-1})	$t'_{1/2}$	Ref.
A	283	$(1.60 \pm 0.04) \times 10^{-6}$	$(2.61 \pm 0.06) \times 10^{-7}$	4.3 days	51
	298	$(1.18 \pm 0.01) \times 10^{-5}$	$(2.50 \pm 0.01) \times 10^{-6}$	13.5 hours	51
	313	$(7.95 \pm 0.30) \times 10^{-5}$	$(2.11 \pm 0.10) \times 10^{-5}$	2.4 hours	51
B	283	$(2.04 \pm 0.02) \times 10^{-7}$	$(5.64 \pm 0.20) \times 10^{-8}$	30.8 days	54
	298	$(2.10 \pm 0.02) \times 10^{-6}$	$(8.03 \pm 0.29) \times 10^{-7}$	2.8 days	54
	313	$(1.68 \pm 0.02) \times 10^{-5}$	$(8.22 \pm 0.17) \times 10^{-6}$	7.7 hours	this work
C	298	$(2.26 \pm 0.14) \times 10^{-6}$	$(1.04 \pm 0.06) \times 10^{-6}$	2.4 days	this work
	313	$(1.02 \pm 0.05) \times 10^{-5}$	$(5.92 \pm 0.31) \times 10^{-6}$	11.9 hours	this work

If the rate constants are known, the activation energy E_a can be obtained from the Arrhenius equation

$$k = A \cdot e^{[-E_a/(RT)]} \qquad \text{(eq-14)}$$

$$\ln k = \ln A - E_a/(RT) \qquad \text{(eq-15)}$$

where A is a preexponential factor. A plot of lnk versus 1/T gives

$$\text{slope} = - E_a/R$$

The plots of $\ln k_1$ vs. 1/T and $\ln k_{-1}$ vs. 1/T were manipulated for reaction 9 in $CDCl_3$ (Fig.24, 25).[53] The values of E_a are shown in Table 5.

Table 5. The activation energy of reactions A, B and C. A is reaction 10 in $CDCl_3$; B is reaction 9 in $CDCl_3$; C is reaction 9 in toluene-d_8 solution.

	E_a (forward) (kJ mol^{-1})	E_a (backward) (kJ mol^{-1})	Ref.
A	95.3 ± 1.8	107.0 ± 1.6	51
B	108.31 ± 0.43	122.34 ± 1.12	this work
C	77.76	90.01	this work

The free energy of activation, $\Delta G^{\neq}$, is also related to the rate constant, k,

$$k = (k'T/h)\cdot e^{[-\Delta G^{\neq}/(RT)]} \qquad \text{(eq-16)}$$

where k' is Boltzmann's constant and h is Planck's constant. Taking the logarithm of both sides gives

$$\ln(k/T) = -\Delta G^{\neq}/(RT) + \ln(k'/h)$$

Recognizing that $\Delta G^{\neq} = \Delta H^{\neq} - T\,\Delta S^{\neq}$ (eq-17)

we have

$$\ln(k/T) = \Delta H^{\neq}/(RT) + \Delta S^{\neq}/R + \ln(k'/h) \qquad \text{(eq-18)}$$

Therefore, the Eyring plot [the plot of ln(k/T) versus 1/T] gives $\Delta H^{\neq}$ from the slope and $\Delta S^{\neq}$ from the intercept.[53]

$$\text{slope} = -\Delta H^{\neq}/R$$

$$\text{intercept} = \Delta S^{\neq}/R + \ln(k'/h)$$

The values of $\Delta S^{\neq}$ are of interest because values below -10 eu indicate an associative reaction, while values greater than +10 eu indicate a dissociative reaction.[4c,55a, 56]

The plots of ln(k/T) versus 1/T were manipulated for reaction 9 in $CDCl_3$ (Fig. 26, 27). The values of $\Delta H^{\neq}$,$\Delta S^{\neq}$, and $\Delta G^{\neq}$ are shown in Table 6. Because of the incomplete data for reaction 9 in toluene-d_8, the activation parameters for this reaction are questionable.

Table 6. The values of $\Delta H^{\neq}$,$\Delta S^{\neq}$, and $\Delta G^{\neq}$ for the reactions of A, B, and C. A is reaction 10 in $CDCl_3$; B is reaction 9 in $CDCl_3$; C is reaction 9 in toluene-d_8 solution.

	A	B	C
$\Delta H^{\neq}_f$ (kJ mol^{-1})	92.6 ± 1.9	105 ± 0.46	75.22
$\Delta H^{\neq}_b$ (kJ mol^{-1})	104.5 ± 1.8	119.87 ± 1.16	87.48
ΔH (kJ mol^{-1})	-11.9 ± 2.6	-14.87 ± 1.25	-12.26
$\Delta S^{\neq}_f$ (J mol^{-1}K^{-1})	-28.2 ± 6.2	1.41 ± 1.58	-100.60
$\Delta S^{\neq}_b$ (J mol^{-1}K^{-1})	-1.0 ± 6	40.41 ± 3.91	-65.93
ΔS (J mol^{-1}K^{-1})	-27.2 ± 8.6	-39 ± 4.22	-34.67
$\Delta G^{\neq}_f$ (kJ mol^{-1})	101.0 ± 2.6	105.42 ± 0.66	105.20
$\Delta G^{\neq}_b$ (kJ mol^{-1})	104.8 ± 2.5	107.83 ± 1.64	107.13
ΔG (kJ mol^{-1})	-3.8 ± 3.6	-2.41 ± 1.77	-1.93
Ref.	51	this work	this work

The reaction rates of the tungsten complexes are faster than those of the chromium complexes. As discussed in the introduction, this result is consistent with a reaction that proceeds by an associative mechanism because it would be expected that a 7-coordinate transition state would be more stable when tungsten

is the central metal atom than when the smaller chromium atom is present. A comparison of the entropy of activation shows that values are significantly more positive for the chromium than for the tungsten complexes in chloroform. It can be concluded that the isomerization for the chromium complexes proceeds with a greater dissociative component than for the tungsten complexes. It makes sense that an associative mechanism may become less favorable as the central metal atom becomes smaller.

Both the tungsten and chromium reactions are unexpectedly fast for d^6 low-spin complexes. Many works have confirmed the substitutionally inert nature of d^6 complexes.[53] For example, the dissociative rate constant (k_1) for CO substitution by phosphine in $W(CO)_6$ at 30 °C is 1×10^{-14} s^{-1}.[55a] The rate constant for PPh_3 dissociation from $(OC)_5CrPPh_3$ is 3×10^{-11} s^{-1} at 30 °C,[55b] about six orders of magnitude slower than the rate of isomerization in reaction 9.

The mechanistic model presented in scheme X (Page 15) can explain the dramatic acceleration of the reaction. The interaction of the dangling phosphine arm with a carbonyl ligand leads to a weakening of the metal-phosphorus bond, allowing the other dangling phosphine arm to displace the coordinated phosphine. The isomerization of $(OC)_5W[\eta^1\text{-}PPh_2CH_2CH_2P(p\text{-tol})_2]$, lacking an accelerating arm, proceeds at the expected slower rate ($k_1 = 2.03 \times 10^{-8}$ s^{-1}, $k_{-1} = 1.25 \times 10^{-8}$ s^{-1} at 55 °C).[51] The isomerization of $(OC)_5Cr[\eta^1\text{-}PPh_2CH_2CH_2P(p\text{-tol})_2]$ is also very slow ($k_1 = 1.22 \times 10^{-8}$ s^{-1}, $k_{-1} = 0.65 \times 10^{-8}$ s^{-1} at 55 °C).[55c]

The activation energy of chromium complexes in $CDCl_3$ solution is larger than that of tungsten complex in the same solution, which is in agreement with the

difference in their reaction rates. The activation enthalpy of chromium (-14.87 ± 1.25 kJ mol^{-1}) is not significantly different from that of tungsten (-11.9 ± 2.6 kJ mol^{-1}). Both of the reactions are accompanied with a large decrease of entropy (-27.2 ± 8.6 J $mol^{-1}K^{-1}$ for W complexes, -39 ± 4.22 J $mol^{-1}K^{-1}$ for Cr complexes), again a sign that the products of isomerization have less freedom to move. The activation free energy of chromium (-2.41 ± 1.77 kJ mol^{-1}) is slightly less negative than that of tungsten (-3.8 ± 3.6 kJ mol^{-1}).

The solvent can influence both rates and mechanisms of reactions. Sometimes the solvent alters the rate without influencing the mechanism by changing the force between reacting particles and hence altering the readiness with which they approach each other. But it would be unusual if the solvent changed the mechanism without changing the rate.[57] In this study, the replacement of $CDCl_3$ with toluene-d_8 does not influence the rates much, but dramatically decreases the activation energies. Toluene-d_8 also changes the activation entropy of the forward reaction from 1.41 ± 1.58 eu to -69.93 eu, although the overall ΔS (-34.67 eu) is very close to that of isomerization in $CDCl_3$ (-39 ± 4.22 eu). How toluene-d_8 makes such a big difference is not clear. Unfortunately only two data points were obtained and it is possible that a great deal of experimental error exists in these measurements.

These results suggest that complex reactivity may be greatly influenced by the intramolecular interaction, the central metal atom and the solvent. Further studies are necessary to understand the nature of solvent interaction in these systems.

C. Experimental Section

Reactions were carried out under a nitrogen atmosphere as many of the reactants and products are air-sensitive. Tetrahydrofuran(THF) was dried by sodium metal in the presence of benzophenone, and was freshly distilled under N_2 before use. All other solvents were used without further purification. The other chemicals were obtained from Sigma-Aldrich and other commercial suppliers and also used without further purification.

The infrared spectra ($CHCl_3$) of the carbonyl groups in the complexes were recorded on a Nicolet 20 DXB Fourier Transform Spectrometer.

Phosphorus-31 nuclear magnetic resonance spectroscopy (NMR) was used to characterize the compounds, determine equilibrium constants and measure the rates of isomerization. The instrument used was a General Electric QE-300 NMR spectrometer.

All melting points were taken by a capillary melting point apparatus (Arthur H. Thomas Company).

Irradiation was carried out in a quartz vessel equipped with a 400 watt ultraviolet lamp.

Elemental analyses were done by the microanalytical laboratory in University of Illinois at Urbana-Champaign. Structural analyses performed at the Chemistry Department at University of Delaware.

Preparation of PPh_2Li

Syringes were used to transfer PPh_2H (21.8 mL, 0.125 mol) and BuLi (62.5 mL, 0.125 mol) to 150 mL of dry THF. The PPh_2H was added followed by dropwise addition of BuLi over 0.5 hour. The solution turned red after the addition of BuLi. The reaction mixture was stirred for 36 hours.

Preparation of $(Ph_2P)_2C=CH_2$ (vdpp)

The above solution was added via syringe over 45 min to 150 ml of dry THF containing $Cl_2C=CH_2$ (5.00 mL, 0.0625 mol). The dark red solution was stirred for 24 hours. Diluted HCl (100 mL, 2 M) was added to the reaction mixture causing the red color to disappear and two layers to develop. The yellow top layer was separated from the colorless bottom layer with a separatory funnel. The top layer was dried with $MgSO_4$ after which the solvent was removed under high vacuum. The yellow residue crystallized from CH_2Cl_2/CH_3OH giving white crystals of $(Ph_2P)_2C=CH_2$ (11.282 g , 45.5%). mp 110-113 °C. $^{31}P\{^1H\}$NMR: δ -2.9 ppm, ^1H NMR: δ 5.9 ppm $\{J_{P\text{-}H\ (trans)} + J_{P\text{-}H\ (cis)} = 29.4\ Hz\}$, $^{13}C\{^1H\}$ NMR: δ 136.1 ppm ($^2J_{P\text{-}C} = 4.9$ Hz), δ 135.7 ppm ($^1J_{P\text{-}C} = 9.4$ Hz), δ 128.2 ppm to 134.5 ppm (multiplet of phenyl group).

Preparation of $(OC)_5CrPPh_2H$

A solution of $Cr(CO)_6$ (5.000 g, 22.7 mmol) in 250 mL dry THF was irradiated for 8 hours with UV light. The colorless solution turned to red. To this red solution, Ph_2PH (3.95 mL, 22.7 mmol) was added via a syringe. This

mixture was allowed to stir for 1.5 hour. The color changed from red to yellow, and became white-greenish at the end. The solvent was removed under vacuum. Unreacted $Cr(CO)_6$ as confirmed by IR, separated from the green oily residue when CH_3OH was added. The green filtrate obtained by filtration was taken to dryness under vacuum. The product, flat green crystals, was recrystallized from CH_2Cl_2/CH_3OH. Yield: 0.756 g, 8.8%; mp: 59-65 °C; IR[ν(C≡O) (cm^{-1})]: 1945 (vs), 2067 (m); $^{31}P\{^1H\}$ NMR: δ 33.4 ppm; ^1H NMR: δ 6.5 ppm ($^1J_{P-H}$ = 338.9 Hz), 7.4 to 7.6 ppm (multiplet of phenyl group); $^{13}C\ \{^1H\}$ NMR: δ 129.0 ppm ($^3J_{P-C}$ = 9.6 Hz), 130.4 ppm ($^4J_{P-C}$ = 1.5 Hz), 131.9 ppm ($^2J_{P-C}$ = 11.3 Hz), 132.6 ppm ($^4J_{P-C}$ = 38.8 Hz), 216.2 ppm{$^2J_{P-C(ax)}$ = 13.4 Hz}, 221.0 ppm {$^2J_{P-C(eq)}$ = 7.1 Hz}.

Preparation of $Cl_2Pd(Ph_2P)_2C=CH_2$

A mixture of $(C_6H_5CN)_2PdCl_2$ (1.000 g, 2.61 mmol) and $(Ph_2P)_2C=CH_2$ (1.034 g, 2.61 mmol) were stirred in 25 mL CH_2Cl_2 for 48 hours. A yellow solid formed and was collected by filtration. Yield: 1.270 g, 84.8%; $^{31}P\{^1H\}$ NMR: δ -20.6 ppm; ^1H NMR: δ 6.4 ppm (AA' part of AA'XX' second order spectrum from $P_2C=CH_2$ proton), 7.4 ppm to 7.9 ppm (multiplet of phenyl group).

Preparation of $Cl_2Pd(PPh_2)_2CHCH_2PPh_2Cr(CO)_5$

The mixture of $Cl_2Pd(PPh_2)_2C=CH_2$ (1.270 g, 2.20 mmol) and $CrPPh_2H$ (0.837 g, 2.20 mmol) were stirred in 40 mL dry THF for 24 hours with 0.112 g (1.0 mmol) of catalytic potassium tert-butoxide ($KOBu^t$). The red solution was

refluxed at 80 °C for 2 hours and cooled to room temperature. The solvent was removed under vacuum and the dark brown residue was recrystallized with CH_2Cl_2/CH_3OH. A brown solid was obtained by filtration. Yield: 1.275 g, 60.9%; IR[ν(C≡O) (cm^{-1})]: 1939(vs), 2065(m); $^{31}P\{^1H\}$NMR: δ -27.2 ppm ($^3J_{P-P}$ = 3.2 Hz), 57.4 ppm ($^3J_{P-P}$ = 3.6 Hz).

Synthesis of $(CO)_5Cr[\eta^1\text{-}PPh_2CH_2CH(PPh_2)_2]$ (6) and $(OC)_5Cr[\eta^1\text{-}PPh_2CH(PPh_2)CH_2PPh_2]$ (7)

A mixture of $Cl_2Pd(PPh_2)_2CHCH_2PPh_2Cr(CO)_5$ (0.700 g, 0.735 mmol) and KCN (0.191 g, 2.94 mmol) were stirred in 50 mL absolute ethanol for 54 hours. The solvent was removed under vacuum. The residue was recrystallized with CH_2Cl_2/CH_3OH, and separated by filtration. The yellow filtrate was taken to dryness. A yellow solid was obtained from repeated crystallization from CH_2Cl_2/CH_3OH. Yield: 0.170 g, 29.9%. IR[ν(C≡O) (cm^{-1})]: 1940 (vs), 2062 (m); The $^{31}P\{^1H\}$ NMR spectrum showed that the product was a mixture of isomer **6** and 7. The $^{31}P\{^1H\}$ NMR spectrum of **6**: δ -2.8 ppm ($^3J_{P-P}$ = 2.4 Hz), 51.8 ppm ($^3J_{P-P}$ = 2.6 Hz); The $^{31}P\{^1H\}$NMR spectrum of isomer 7: δ -16.0 ppm ($^3J_{P-P}$ = 21.2 Hz), -10.9 ppm ($^2J_{P-P}$ = 193.1 Hz), 68.8 ppm ($^2J_{P-P}$ = 193.2 Hz, $^3J_{P-P}$ = 21.2 Hz); The $^{13}C\{^1H\}$ NMR spectrum of **6**: δ 216.4 ppm ($^2J_{P-C(eq)}$ = 12.9 Hz), 221.8 ppm ($^2J_{P-C(ax)}$ = 6.9 Hz); The $^{13}C\{^1H\}$ NMR spectrum of 7: δ 216.3 ppm ($^2J_{P-C(eq)}$ = 12.5 Hz, $^4J_{P-C(eq)}$ = 3.4 Hz), 221.7 ppm ($^2J_{P-C(ax)}$ = 5.1 Hz). Isomer 7 was less soluble, and was isolated from the filtrate by further recrystallization. But the more soluble isomer **6** was not successfully purified, although it was

formed initially from this reaction, it partially isomerized to isomer **7** once it existed in the solution.

Synthesis of $(OC)_4Cr[\eta^2\text{-}PPh_2CH(PPh_2)CH_2PPh_2]$

The chelate complex formed at 53 °C from the mixture of $(CO)_5Cr[\eta^1\text{-}PPh_2CH_2CH(PPh_2)_2]$ and $(OC)_5Cr[\eta^1\text{-}PPh_2CH(PPh_2)CH_2PPh_2]$ in $CDCl_3$ solution. $^{31}P\{^1H\}$NMR spectrum: δ -14.4 ppm ($^2J_{P\text{-}P}$ = 24.1Hz), 70.7 ppm ($^3J_{P\text{-}P}$ = 21.0Hz), 88.3 ppm ($^2J_{P\text{-}P}$ = 23.6Hz, $^3J_{P\text{-}P}$ = 21.2Hz) which was consistent with the chelated complex, $(OC)_4Cr[\eta^2\text{-}PPh_2CH(PPh_2)CH_2PPh_2]$.[43] Also, there were other signals in the $^{31}P\{^1H\}$NMR spectrum which were not identified: δ -96.5 ppm, 14.3 ppm, 30.3 ppm, 47.8 ppm, 55.1 ppm and 55.9 ppm. No chelation products were observed in toluene-d_8 solution under the same conditions.

Equilibrium and Kinetic Measurements

A mixture of isomers **A** and **B** (40.0 mg, 0.0516 mmol) was dissolved in 0.50 mL of $CDCl_3$ and separately in 0.50 mL toluene-d_8, frozen in liquid nitrogen and flame sealed under vacuum. The sample in $CDCl_3$ was investigated at 40 °C and at 53 °C, while the sample in toluene-d_8 was studied at 15 °C, 25 °C, 40 °C and 53 °C. A constant temperature bath was used to maintain a constant temperature. The NMR probe was brought to the corresponding temperature and $^{31}P\{^1H\}$NMR spectra were recorded in appropriate time intervals. In an effort to optimize the quantitative study a delay time of 15 sec (D5 = 15 s) and a pulse width of 16 usec (P2 = 16 us, 83 degree) were used. Integrations were carried out following

standard procedures in which the width at half-height was obtained for each signal and multiplied by ± 31.8 to give an integral that included 99% of the intensity. Four integrations were averaged to avoid bias in the measurement of the isomer ratio. Equilibrium was assumed to have been reached when the integral ratio of isomers remained stable after three consecutive runs at reasonable time intervals for each specific temperature.

Chapter II: Synthesis of $[(OC)_5WPPh_2]_2C=CH_2$ and crystal structure of $(CO)_5WPPh_2C(PPh_2)=CH_2$

A. Introduction

The diphosphine ligand, bis(diphenylphosphino)methane (dppm), is a very important ligand in organometallic chemistry and homogeneous catalysis.[7] The two available coordination sites of dppm makes it possible to chelate a single metal center to stablize a catalyst fragment or to bridge two metal centers to allow cooperative catalytic reactions to occur at adjacent sites. These bridging systems require a second bridging atom or molecule, or a metal-metal bond as a single dppm ligand is not sufficient to hold the metals together. A third role of dppm is forming a monodentate ligand complex with one phosphine remaining uncoordinated. This coordination of one phosphine end does not significantly reduce the reactivity of the unbound end of phosphine, which is indicated by its ability to undergo chelation, protonation, quaternization and even coordination to a second metal fragment.[14a, 58]

The coordination of a second metal fragment to the free end of $(OC)_5M(\eta^1$-dppm) (M = Cr, Mo, W) does not occur at room temperature because of the steric hindrance of the phenyl groups. However, the preparation of $(OC)_5W(\mu$-dppm)-$W(CO)_5$ can be carried out from either $(OC)_5W$(NCMe) and dppm or from $(OC)_5W$ (NCMe) and $(OC)_5W(\eta^1$-dppm) at 60 °C. The thermal dissociation of a carbonyl ligand is not likely under these reaction conditions (Scheme V in chapter

I).[24, 25] Likewise, the dppm bridged complex, $[Ru_2(\eta^5\text{-}C_5H_5)_2(1,10\text{-phenanthroline})_2(\mu\text{-dppm})]^{2+}$, forms in refluxing EtOH, while only the monodentate complex forms at room temperature.[59] On the other hand, the ethylene-bridged ligand, bis (diphenylphosphino)ethane (dppe), readily formed bimetallic complexes at room temperature or below.[12, 14a, 60]

The solid state structures of $(OC)_5W(\eta^1\text{-dppm})$ **(10)** and $(OC)_5W(\mu\text{-dppm})\text{-}W(CO)_5$ **(11)** are very interesting.[61] The lone pair of electrons on the dangling phosphine in **10** is oriented toward the $W(CO)_5$ unit in the solid state, and the $^{31}P\{^1H\}$ and $^{13}C\{^1H\}$ NMR data indicate that this is also the major conformation of **10** in solution. Formation of **11** from **10** requires rotation about both P-C bonds in $Ph_2PCH_2PPh_2$ and an extreme increase in the P-C-P bond angle from 111.5° to 133.1° (Scheme XI).

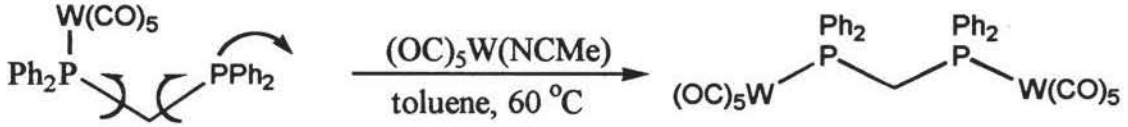

10 **11**

Scheme XI

Of interest in our work is the ligand, 1,1-bis(diphenylphosphino)ethene (vdpp), as a dangling or bridging ligand coordinated with $W(CO)_5$ units. Based on the presence of the rigid carbon-carbon double bond, we predicted that in the dangling complex, $(CO)_5WPPh_2C(PPh_2)=CH_2$ **(12)**, the lone electron pair on the dangling end of vdpp would not be directed toward equatorial carbonyl groups in

the solid state or in solution. If this were true, the addition of a second $W(CO)_5$ to **12** forming $[(OC)_5WPPh_2]_2C{=}CH_2$ **(13)** might take place at room temperature, because the lone electron pair on the dangling phosphine of **12** is in an exposed position, and could readily attack the incoming tungsten metal center. Contrary to the formation of **11** from **10**, the change of configuration of vdpp would be small during the formation of **13** from **12**. Both **12** and **13** were synthesized in this study, and the x-ray crystal structure of **12** was determined.

B. Results and discussion

1. Synthesis and Characterization of $(CO)_5WPPh_2C(PPh_2)=CH_2$ (12)

Compound **12** was synthesized from a 1.4:1 ratio of $W(CO)_5NH_2Ph$ and $(Ph_2P)_2C=CH_2$ in toluene at room temperature, The excess of $W(CO)_5NH_2Ph$ was used because the unreacted $(Ph_2P)_2C=CH_2$ was hard to remove from the products. The product was recrystallized from CH_2Cl_2/CH_3OH and the $^{31}P\{^1H\}$ NMR spectrum revealed that a mixture of **12** and **13** was present. This showed that, **13** can be formed at room temperature and that the dangling phosphine in compound **12** is accessible.

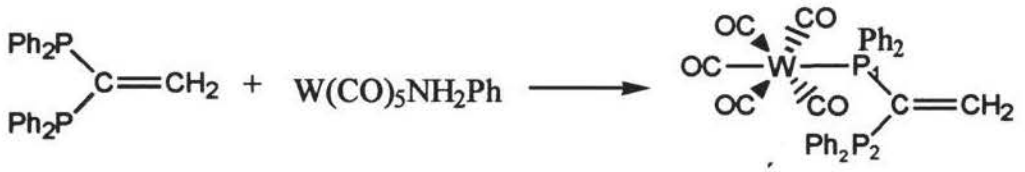

(11)

12

The $^{31}P\{^1H\}$ NMR spectrum of **12** showed a doublet at δ -12.1 ppm ($^2J_{P\text{-}P}$ = 68.4 Hz), which was assigned to P_2 and a doublet with tungsten satellite signals at δ 30.2 ppm ($^1J_{P\text{-}W}$ = 245.9 Hz, $^1J_{P\text{-}P}$ = 68.4 Hz) assigned to P_1. In addition the signals of oxidized P were observed at δ 27.9 ppm (Fig. 28). The ^1H NMR spectrum showed a doublet of doublets at δ 5.9 ppm {$J_{P\text{-}H(trans)}$ = 44.0 Hz, $J_{P\text{-}H(cis)}$ = 6.2 Hz} assigned to the $C=CH_2$ proton. Geminal proton-proton coupling was not observed (Fig. 29). Assignments were supported by a COSY (COrrelated SpectroscopY) spectrum of **12** (Fig.30). The $^{13}C\{^1H\}$ NMR spectrum (Fig.31)

showed a doublet at δ 199.2 ppm {$^2J_{P\text{-}C(ax)}$ = 22.5 Hz}, which was assigned to the axial carbonyl carbon. The expected satellite signals from the coupling of this carbon to W were too weak to be observed under our experimental conditions. A doublet and its satellite signals, assigned to the equatorial carbonyl carbons, were observed at δ 197.3 ppm {$^2J_{P\text{-}C(eq)}$ = 7.0 Hz, $^1J_{CW}$ = 126.3 Hz}. Benson's $^{13}C\{^1H\}$ NMR data of $(OC)_5WPPh_2CH_2PPh_2$ gave a doublet of doublets for the analogous carbons at δ 197.6 ppm {$^2J_{C\text{-}P}$ = 6.9 Hz, $^4J_{C\text{-}P}$ = 3.0 Hz},[61] indicating that the dangling end of the phosphine ligand is directed toward the equatorial carbonyl carbon of its $W(CO)_5$ unit. However, there is no evidence of this long-range C-P coupling in our spectrum. This is consistent with our prediction that the lone electron pair of the dangling phosphine P in **12** is not oriented toward equatorial carbons in solution. The downfield signals at δ 144.7ppm, 144.5 ppm were examined carefully and assigned to the vinyl carbons ($C=CH_2$). Two dimensional NMR spectra were run on **12**. The HETCOR (HETeronuclear chemical shift-CORrelation) spectrum showed the cross-link between δ 5.9 ppm in the ^1H NMR spectrum and δ 144.5 ppm in the $^{13}C\{^1H\}$ NMR spectrum; therefore, the signals at δ 144.5 ppm were assigned to the vinyl carbons. The APT (Attached Proton Test) gave more information that the investigated carbon had two protons attached. Therefore, this carbon was specified as the terminal carbon of the vinyl group (Fig. 32). The DEPT spectrum (Distortionless Enhancement by Polarization Transfer) gave a small doublet at about δ 144.5 ppm in the CH_2 subspectrum, although the peak list did not include these two peaks because of our parameter setting (Fig. 33). In addition, the expansion of the $^{13}C\{^1H\}$ NMR spectrum in this

region was in agreement with the structure (Fig. 31b). The $^{13}C\{^1H\}$ NMR data of **12** are given in (Table 7). The notations of the atoms are consistent with those in the molecular structure (Fig.34).

Table 7. The $^{13}C\{^1H\}$ chemical shifts and spin couplings of compound **12**.

Atoms	δ (ppm)	Coupling Constants (Hz)
C_1	199.2	$^2J_{C\text{-}P(1)} = 22.5$
$C_{2\text{-}5}$	197.3	$^2J_{C\text{-}P(1)} = 7.0$, $^1J_{C\text{-}W} = 126.3$
C_{18}	144.7	$^1J_{C\text{-}P(1)} = 19.5$, $^1J_{C\text{-}P(2)} = 46.5$
C_{19}	144.5	$^2J_{C\text{-}P(1)} = 1.1$, $^2J_{C\text{-}P(2)} = 15.5$
$C_{11,17}$	134.3	$^1J_{C\text{-}P(1)} = 12.9$, $^3J_{C\text{-}P(2)} = 2.8$
$C_{25,31}$	133.4	$^1J_{C\text{-}P(2)} = 42.2$, $^3J_{C\text{-}P(1)} = 2.8$
$C_{6,10,12,16}$	133.0	$^2J_{C\text{-}P(1)} = 12.0$, $^4J_{C\text{-}P(2)} = 1.7$
$C_{20,24,26,30}$	133.7	$^2J_{C\text{-}P(2)} = 20.8$
$C_{7,9,13,15}$	128.3	$^3J_{C\text{-}P(1)} = 7.3$
$C_{21,23,27,29}$	128.0	$^3J_{C\text{-}P(2)} = 9.7$
$C_{8,14}$	129.0	singlet
$C_{22,28}$	130.2	$^4J_{C\text{-}P(1)} = 1.2$

2. Structure of compound 12 in the solid state

The structure of compound **12** is shown in (Fig. 34). The figure gives a clear view that the lone electron pair of the uncoordinated end of vdpp is not directed toward the equatorial carbonyl groups in solid state. Selected bond distances and angles are given in (Table 8). The tungsten atom is coordinated to five carbonyl ligands and one phosphine in approximate C_{4v} symmetry; the P-W-$C_{(ax)}$ angle is 175.3° and the P-W-$C_{(eq)}$ angles range from 87.6° to 97.0°, averaging 91.2°. Bond distances about tungsten atom are typical for monosubstituted tungsten pentacarbonyl complexes, range from 1.989 Å to 2.042 Å, and averaging 2.027 Å. The CO bond trans to the P atom has the shortest W-C distance, as expected for a carbonyl group trans to a weaker π-acid.

Table 8. Selected bond distances and bond angles of $C_{31}H_{22}O_5P_2W$

W-C(1)	1.989(7)	W-C(5)	2.033(7)
W-C(2)	2.039(8)	W-C(3)	2.031(7)
W-C(4)	2.042(8)	W-P(1)	2.530(2)
P(1)-C(17)	1.828(6)	P(1)-C(18)	1.835(6)
P(1)-C(11)	1.833(6)	P(2)-C(31)	1.823(6)
P(2)-C(25)	1.824(6)	P(2)-C(18)	1.851(6)
O(1)-C(1)	1.145(8)	O(2)-C(2)	1.122(8)
O(3)-C(3)	1.133(7)	O(4)-C(4)	1.131(9)
O(5)-C(5)	1.141(8)	C(18)-C(19)	1.309(8)

Continue of table 8.

C(1)-W-C(5)	90.4(3)	C(1)-W-C(2)	87.4(3)
C(5)-W-C(2)	89.9(3)	C(1)-W-C(3)	90.8(3)
C(5)-W-C(3)	177.7(2)	C(2)-W-C(3)	88.2(3)
C(1)-W-C(4)	86.6(3)	C(5)-W-C(4)	88.8(3)
C(2)-W-C(4)	173.8(3)	C(3)-W-C(4)	93.2(3)
C(1)-W-P(1)	175.3(2)	C(5)-W-P(1)	91.3(2)
C(2)-W-P(1)	97.0(2)	C(3)-W-P(1)	87.6(2)
C(4)-W-P(1)	89.1(2)	C(17)-P(1)-C(18)	101.0(3)
C(17)-P(1)-C(11)	104.3(3)	C(18)-P(1)-C(11)	101.3(3)
C(17)-P(1)-W	116.3(2)	C(18)-P(1)-W	118.7(2)
C(11)-P(1)-W	113.1(2)	C(31)-P(2)-C(25)	102.1(3)
C(31)-P(2)-C(18)	102.2(3)	C(25)-P(2)-C(18)	101.3(3)
O(1)-C(1)-W	179.5(6)	O(2)-C(2)-W	176.9(7)
O(3)-C(3)-W	178.6(5)	O(4)-C(4)-W	178.4(6)
O(5)-C(5)-W	178.6(5)	P(1)-C(18)-P(2)	114.5(3)
C(6)-C(11)-P(1)	117.4(4)	C(10)-C(11)-P(1)	123.9(4)
C(12)-C(17)-P(1)	122.5(5)	C(16)-C(17)-P(1)	118.3(5)
C(19)-C(18)-P(1)	120.4(5)	C(19)-C(18)-P(2)	124.7(5)
C(20)-C(25)-P(2)	125.8(5)	C(24)-C(25)-P(2)	116.7(5)
C(26)-C(31)-P(2)	125.2(5)	C(30)-C(31)-P(2)	116.4(5)

Table 9. Crystallographic data for $C_{31}H_{22}O_5P_2W$

formula	$C_{31}H_{22}O_5P_2W$
formula weight	720.28
space group	$P2_1/c$
a, Å	13.412(5)
b, Å	9.556(11)
c, Å	22.435(8)
β, deg	92.77(3)
V, Å^3	2872(4)
Z	4
cryst color, habit	colorless block
D(calc), g cm^3	1.666
μ(MoKα), cm^{-1}	41.72
temp, K	248(2)
T(max)/T(min)	0.308/0.251
diffractometer	Siemens P4
radiation	MoKα(λ = 0.71073 Å)
$R(F)$, %[a]	3.06
$R(wF^2)$, %[a]	6.81

[a] Quantity minimized = $R(wF^2) = \Sigma[w(F_o^2-F_c^2)^2]/\Sigma[wF_o^2)^2]^{1/2}$;
$R = \Sigma\Delta/\Sigma(F_o)$, $\Delta = |(F_o - F_c)|$

3. Synthesis and Characterization of $[(OC)_5WPPh_2]_2C=CH_2$ (13)

Compound **13** was synthesized from a 3:1 ratio of $W(CO)_5NH_2Ph$ and $(Ph_2P)_2C=CH_2$ in toluene at room temperature. The product was a mixture of **12** and **13**. The synthesis of **13** was also carried out from a 2:1 ratio of $W(CO)_5$-NH_2Ph and $(Ph_2P)_2C=CH_2$ in toluene at 55 °C. This reaction gave some unexpected crystals of **12** which were separated with tweezers from a mixture of **12** and **13**.

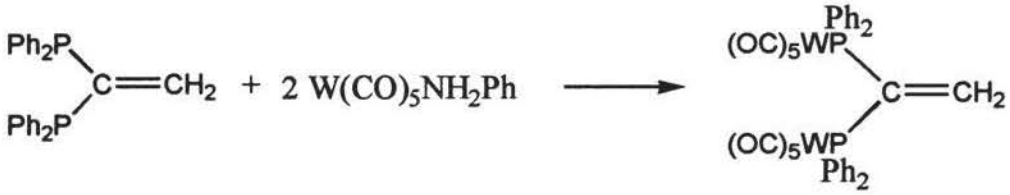

(12)

13

The $^{31}P\{^1H\}$NMR spectrum of **13** showed a central line and a second order ABX pattern (Fig. 35). The satellite pattern consists of two ab subspectra indicated by lines 1, 3, 5, 7 and by lines 2, 4, 6, 8, but as lines 2 and 5, line 4 and 7 are overlapping, only 6 satellite lines are shown in this pattern instead of the expected 8 lines.[25] The satellite pattern was analyzed and the coupling constants were calculated.[34,62,63] The coupling constants are as follows: $^2J_{P\text{-}P'}$ = 20.2 Hz, $^1J_{P\text{-}W}$ = 248.8 Hz, $^3J_{P\text{-}W}$ = 1.6 Hz. These magnitudes are comparable to those found in $(OC)_5W(\mu\text{-}PPh_2CH_2PPh_2)W(CO)_5$, a similar compound in which both ends of the phosphorus ligand are coordinated with a $W(CO)_5$ unit.[25] The $^1J_{P\text{-}W}$ of 248.8 Hz observed for **13** is also similar to that of **12** (245.9 Hz). It is well known that the magnitude of $^1J_{P\text{-}W}$ increases as the electronegativities of the substituents on phosphorus increase.[25,64]

The ABX pattern of spectrum of **13** was simulated (Fig.36). In the ABX pattern, the number of spin nuclei is 3 and the calculated coupling constants were entered as: $J_{(1,2)}$ = 20.2 Hz, $J_{(1,3)}$ = 248.8 Hz, $J_{(2,3)}$ = 1.6 Hz. The model spectrum perfectly fits the real spectrum. The big surprise was, when the value of $J_{(2,3)}$ was slightly adjusted, it was revealed that only a tiny range of $J_{(2,3)}$ values (1.4 - 1.9 Hz) gave a 6 line ABX pattern. Value outside of this range gave an 8 line pattern.

C. Experimental Section

Preparation of $W(CO)_5NH_2Ph$

The mixture of $W(CO)_6$ (10 g, 28.4 mmol) and aniline (10.35 mL, 113.6 mmol) were irradiated in 400 mL dry THF for 9 hours. The solution turned to yellow. The THF was removed completely by rotavaporation. The oily residue was coagulated by adding dilute HCl, and washed with deionized water. The yellow solid was collected by filtration and was sublimed under vacuum at 35 °C for 24 hours to remove unreacted $W(CO)_6$. Yield: 9.53 g, 80.5%. mp: 109-111 °C. IR[ν(C≡O) (cm^{-1})]: 1933 (vs), 1978 (m).

Preparation of $(CO)_5WC(PPh_2)_2{=}CH_2$

A mixture of $(Ph_2P)_2C{=}CH_2$ (0.951 g, 2.4 mmol) and $W(CO)_5NH_2Ph$ (1.420 g, 3.4 mmol) was stirred in 30 mL of toluene for 24 hours. The solvent was removed under vacuum. The yellow residue was recrystallized from CH_2Cl_2 / CH_3OH, and sand-colored crystals were chromatographed over silica. The first band was eluted by a 1:9 volume ratio of ethyl acetate/petroleum ether. The solvent was removed and the product was recrystallized with CH_2Cl_2/CH_3OH, faint yellow crystals. Yield: 0.713 g, 41.2%. mp: 146-150 °C. IR [ν(C≡O) (cm^{-1})]: 1940 (vs), 2071 (m); ^{1}H NMR: δ 5.9 ppm {$J_{P\text{-}H(trans)}$ = 44.0 Hz, $J_{P\text{-}H(cis)}$ = 6.2 Hz}; $^{31}P\{^1H\}$NMR: δ -12.1 ppm($^2J_{P\text{-}P}$ = 68.4 Hz), 30.2 ppm($^2J_{P\text{-}P}$ = 68.4 Hz, $^1J_{P\text{-}W}$ = 245.9 Hz); $^{13}C\{^1H\}$NMR: δ199.2 ppm {$^2J_{P\text{-}C(ax)}$ = 22.5 Hz}, 197.3 ppm {$^2J_{P\text{-}C(eq)}$ = 7.0 Hz, $^1J_{CW}$ = 126.3 Hz}, 144.7 ppm ($^1J_{PC}$ = 46.5 Hz, $^1J_{PC}$ = 19.5 Hz), 144.5 ppm ($^2J_{PC}$ =

15.5 Hz, $^2J_{PC}$ = 1.1 Hz), 134.3 ppm ($^1J_{PC}$ = 12.9 Hz, $^3J_{PC}$ = 2.8 Hz), 133.4 ppm ($^1J_{PC}$ = 42.2 Hz, $^3J_{PC}$ = 2.8 Hz), 133.7 ppm ($^2J_{PC}$ = 20.8 Hz), 133.0 ppm ($^2J_{PC}$ = 12.0 Hz, $^4J_{PC}$ = 1.7 Hz), 130.2 ($^4J_{PC}$ = 1.2 Hz), 129.0 ppm (singlet), 128.3 ppm ($^3J_{PC}$ = 7.3 Hz), 128.0 ppm ($^3J_{PC}$ = 9.7 Hz).

Growing Crystals of $(CO)_5WC(PPh_2)_2{=}CH_2$

Pure $(CO)_5WC(PPh_2)_2{=}CH_2$ was dissolved in a minimal amount of CH_2Cl_2 and a pipette was used to transfer the saturated solution to a clean 5 mm NMR tube. Approximate the same amount of CH_3OH was slowly dribbled into the tube so that CH_2Cl_2 and CH_3OH formed the discrete layers. The tube was placed in the dark and not disturbed for 2 days. A yellow crystal formed and was collected by filtration. The quality of the single crystal was evaluated with a polarizing microscopy.

Preparation of $[(CO)_5WPPh_2]_2C{=}CH_2$

The mixture of $(Ph_2P)_2C{=}CH_2$ (0.476 g, 1.2 mmol) and $W(CO)_5NH_2Ph$ (1.501g, 3.6 mmol) were stirred in 15 mL toluene for 7 days. The solvent was removed under vacuum. The dark green oil was recrystallized with CH_2Cl_2/ CH_3OH. The faint yellow solid obtained was chromatographed over silica. With a 1:9 ethyl acetate/ petroleum ether eluant, a first faint yellow band of $(CO)_5WC(PPh_2)_2{=}CH_2$ appeared first. A second yellow band, $[(CO)_5WPPh_2]_2$- $C{=}CH_2$, was obtained, and a third strong yellow band was not identified. The second fraction was recrystallized from CH_2Cl_2/CH_3OH. The product, faint yellow crystal, was obtained with considerable loss.

Yield: 0.217 g, 17.3%. mp: 178-180 °C. IR[ν(C≡O) (cm^{-1})]:1944 (vs), 2071 (m); $^{31}P\{^{1}H\}$NMR: δ 36.2 ppm ($^{2}J_{P\text{-}P}$ = 20.2 Hz, $^{2}J_{P\text{-}W}$ = 248.8 Hz, $^{3}J_{P\text{-}W}$ = 1.6 Hz). Anal. Calcd. for $C_{36}H_{22}O_{10}P_2W_2$: C, 41.41%; H, 2.12%. found: C, 40.56%; H, 2.24%.

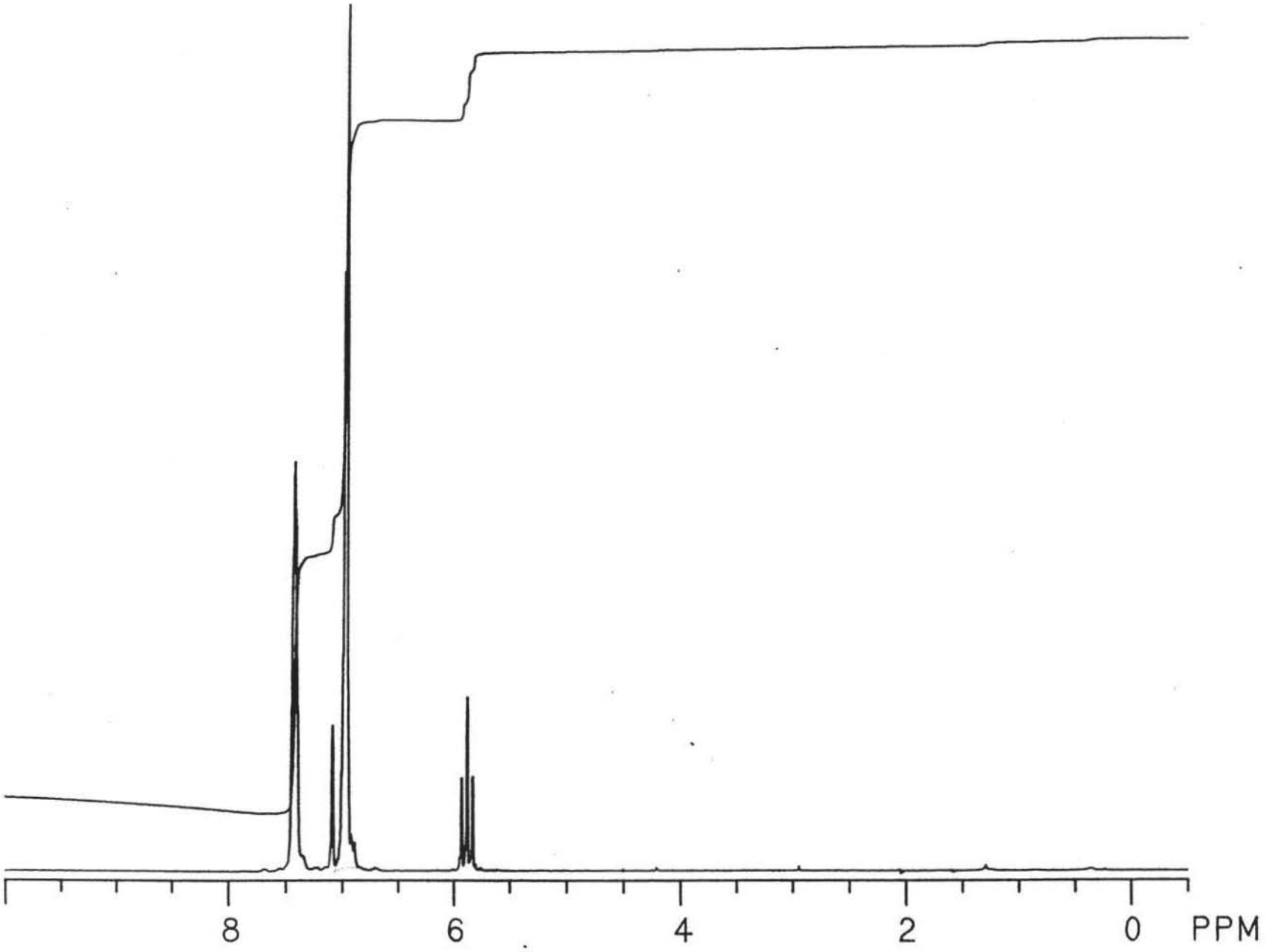

Figure 1. The ^{1}H NMR spectrum of $(Ph_2P)_2C{=}CH_2$ in C_6D_6

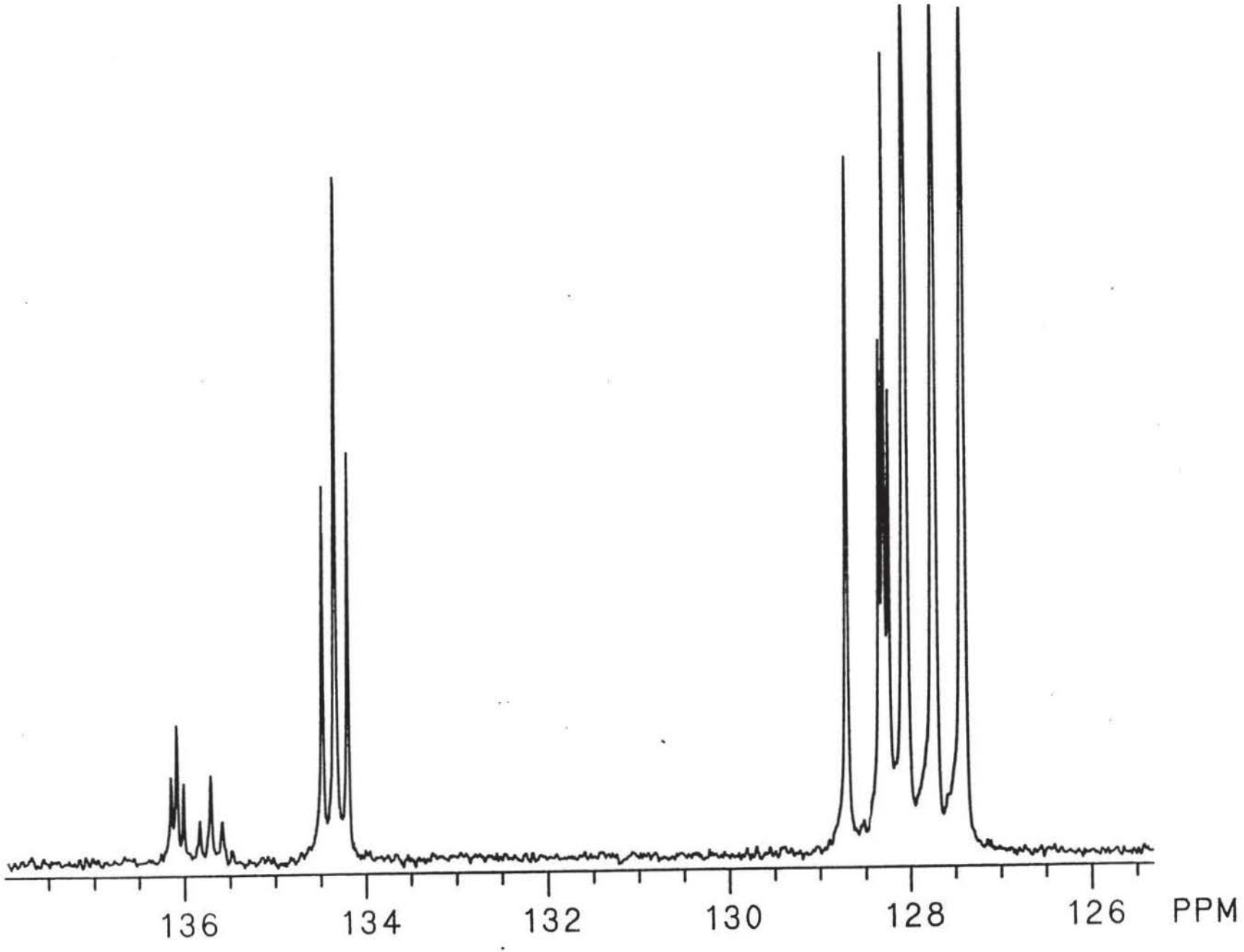

Figure 2. The $^{13}C\{^{1}H\}$ NMR spectrum of $(Ph_2P)_2C{=}CH_2$ in C_6D_6

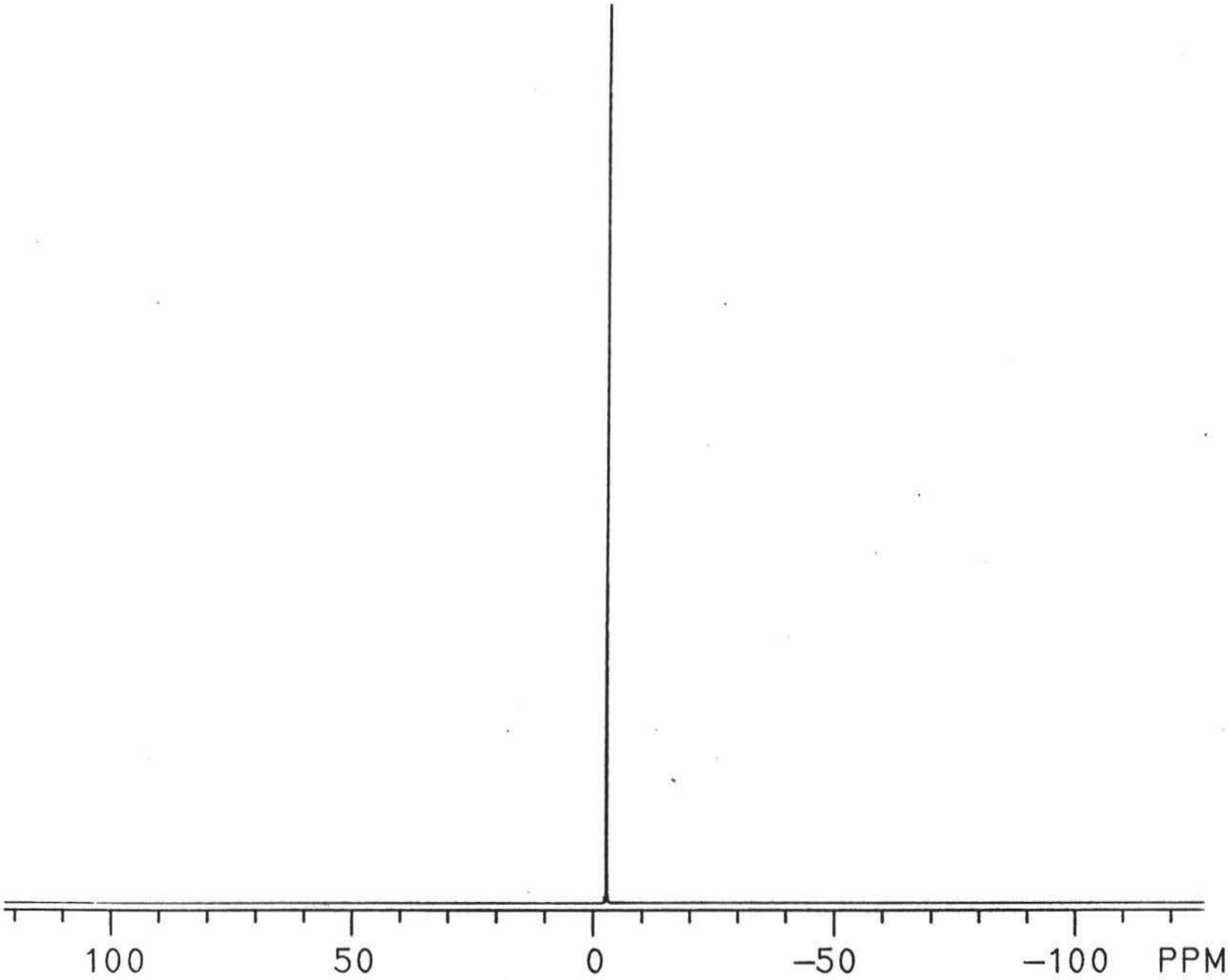

Figure 3. The $^{31}P\{^{1}H\}$ NMR spectrum of $(Ph_2P)_2C{=}CH_2$ in C_6D_6

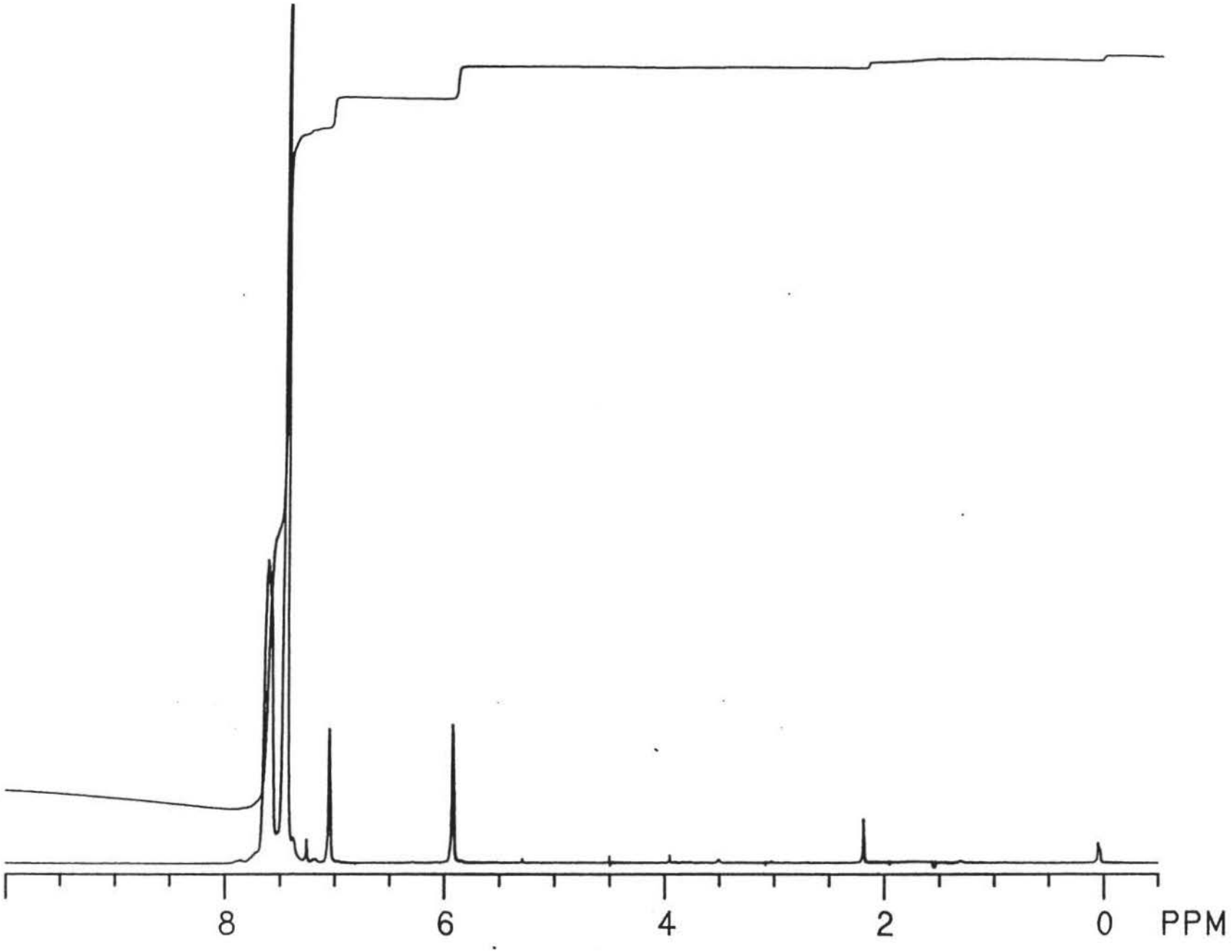

Figure 4. The ^{1}H NMR spectrum of $(OC)_5CrPPh_2H$ in $CDCl_3$

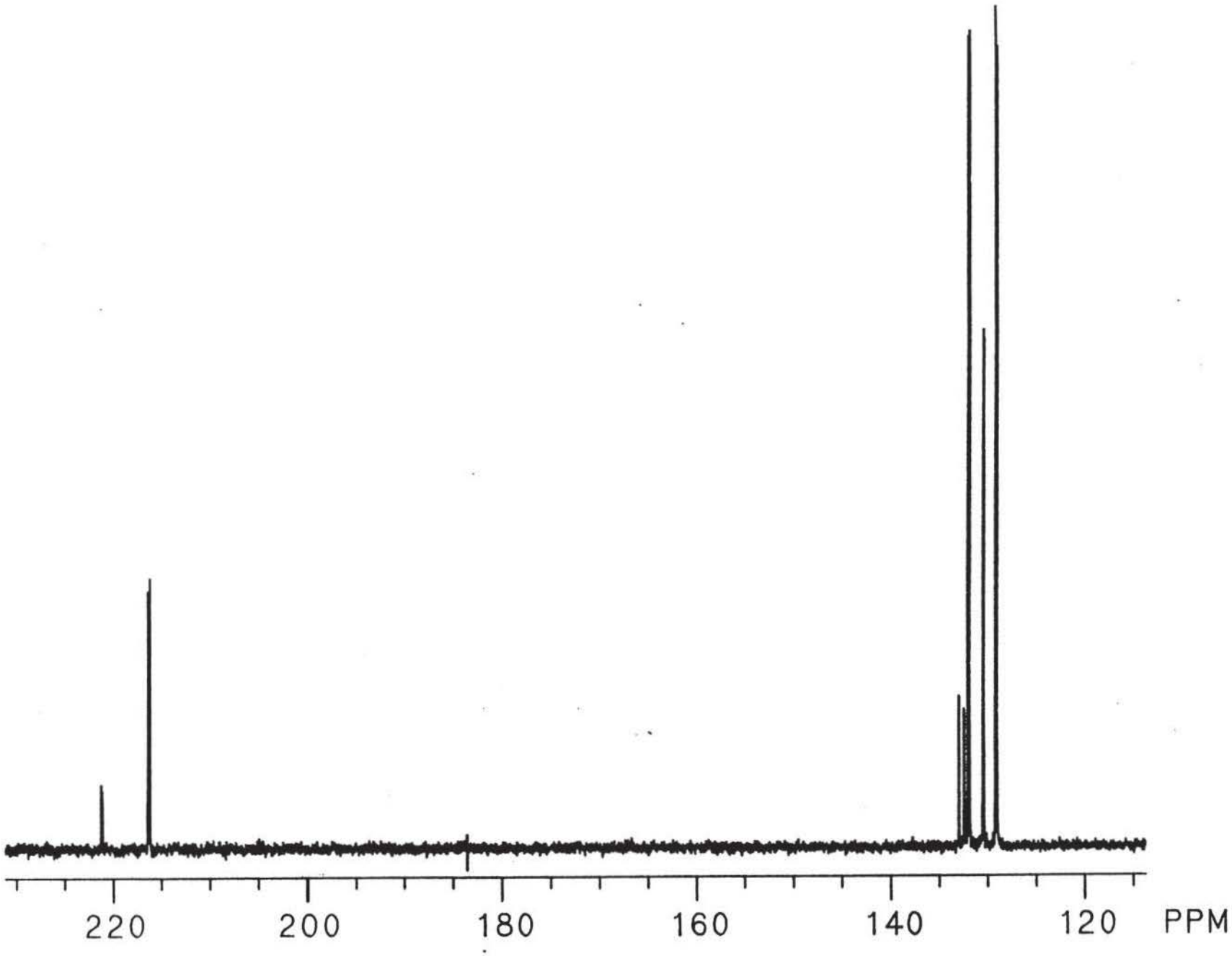

Figure 5. The $^{13}C\{^{1}H\}$ NMR spectrum of $(OC)_5CrPPh_2H$ in $CDCl_3$

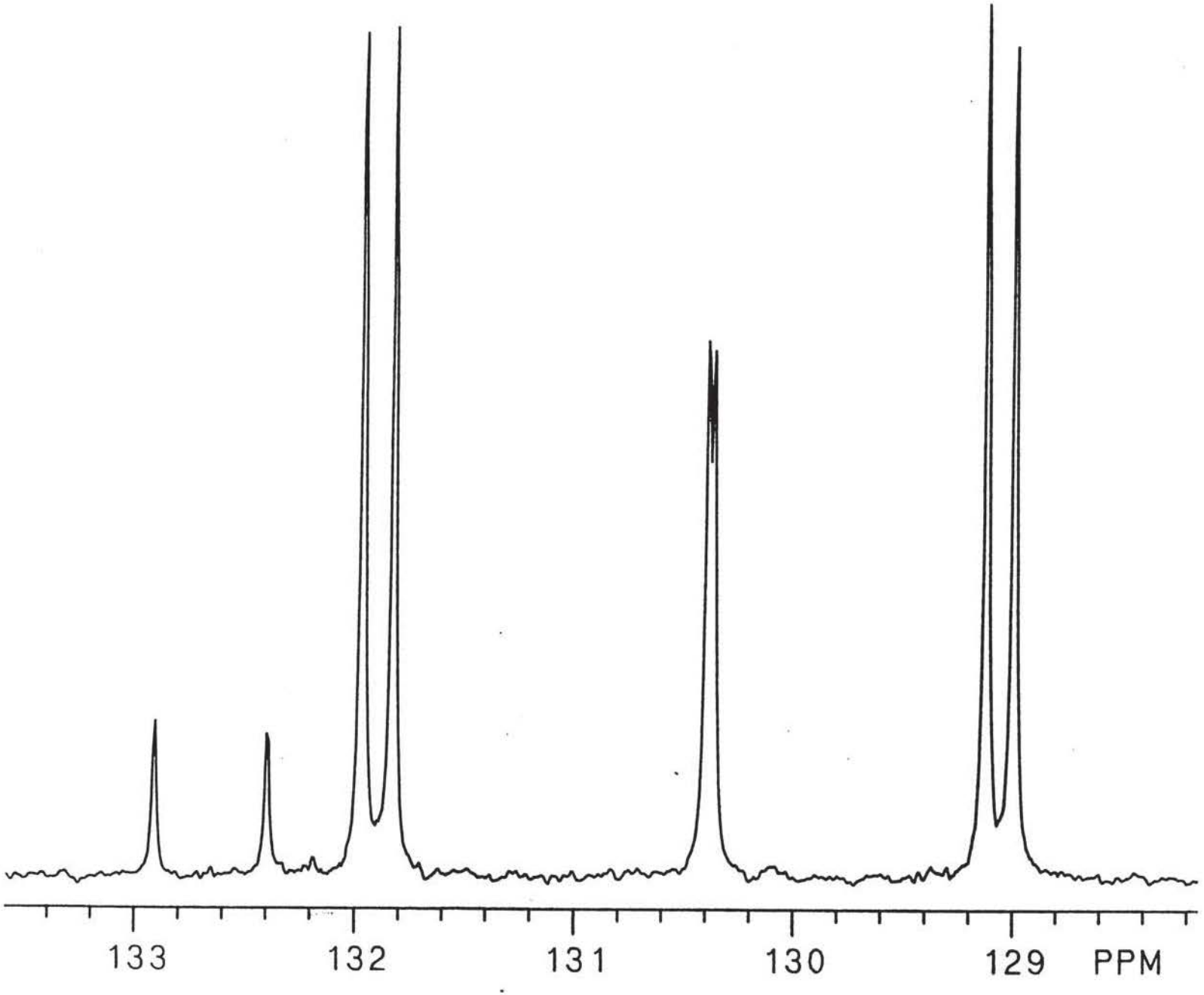

Figure 5a. The expansion of phenyl region of $(OC)_5CrPPh_2H$

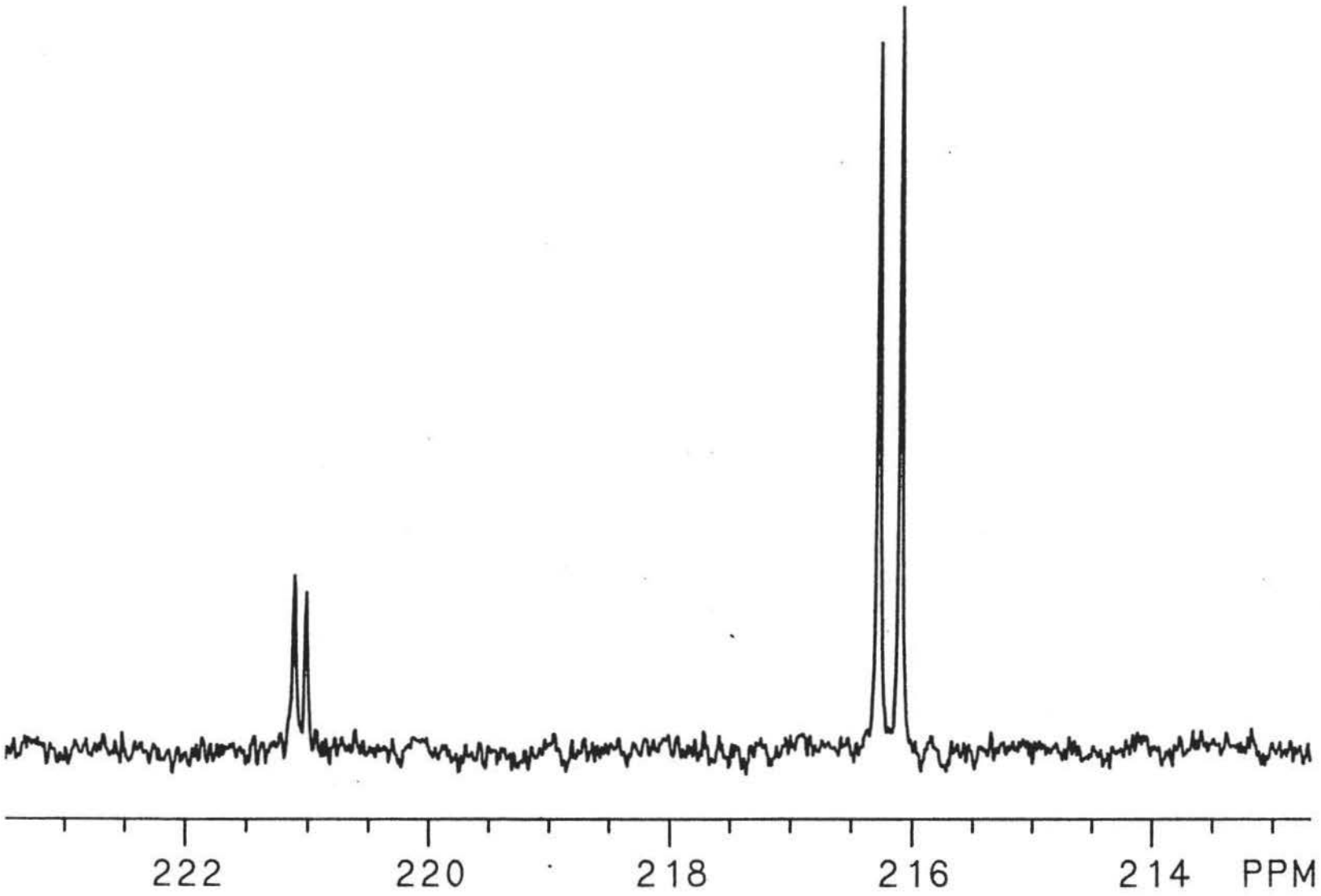

Figure 5b. The expansion of carbonyl region of $(OC)_5CrPPh_2H$

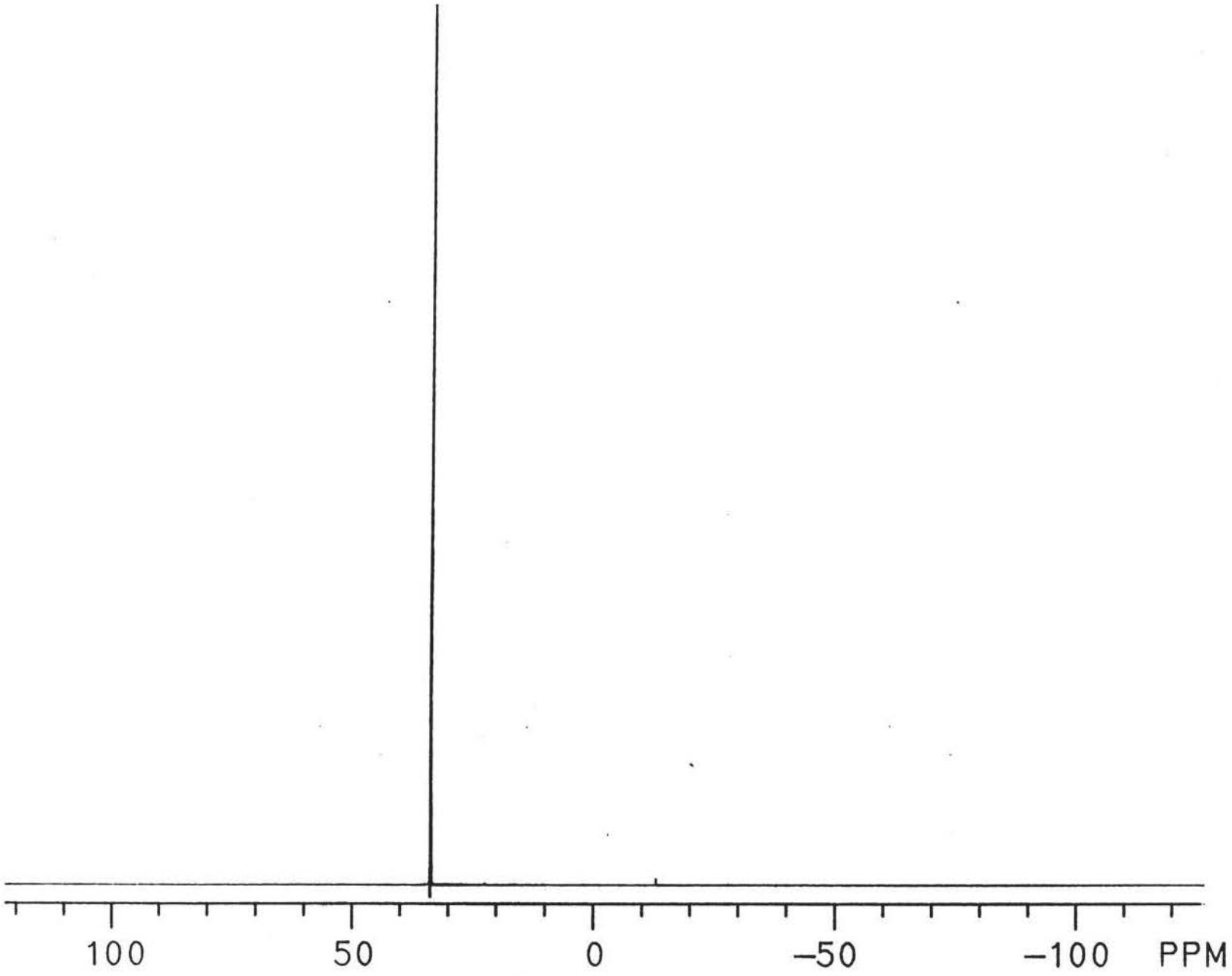

Figure 6. The $^{31}P\{^{1}H\}$ NMR spectrum of $(OC)_5CrPPh_2H$ in $CDCl_3$

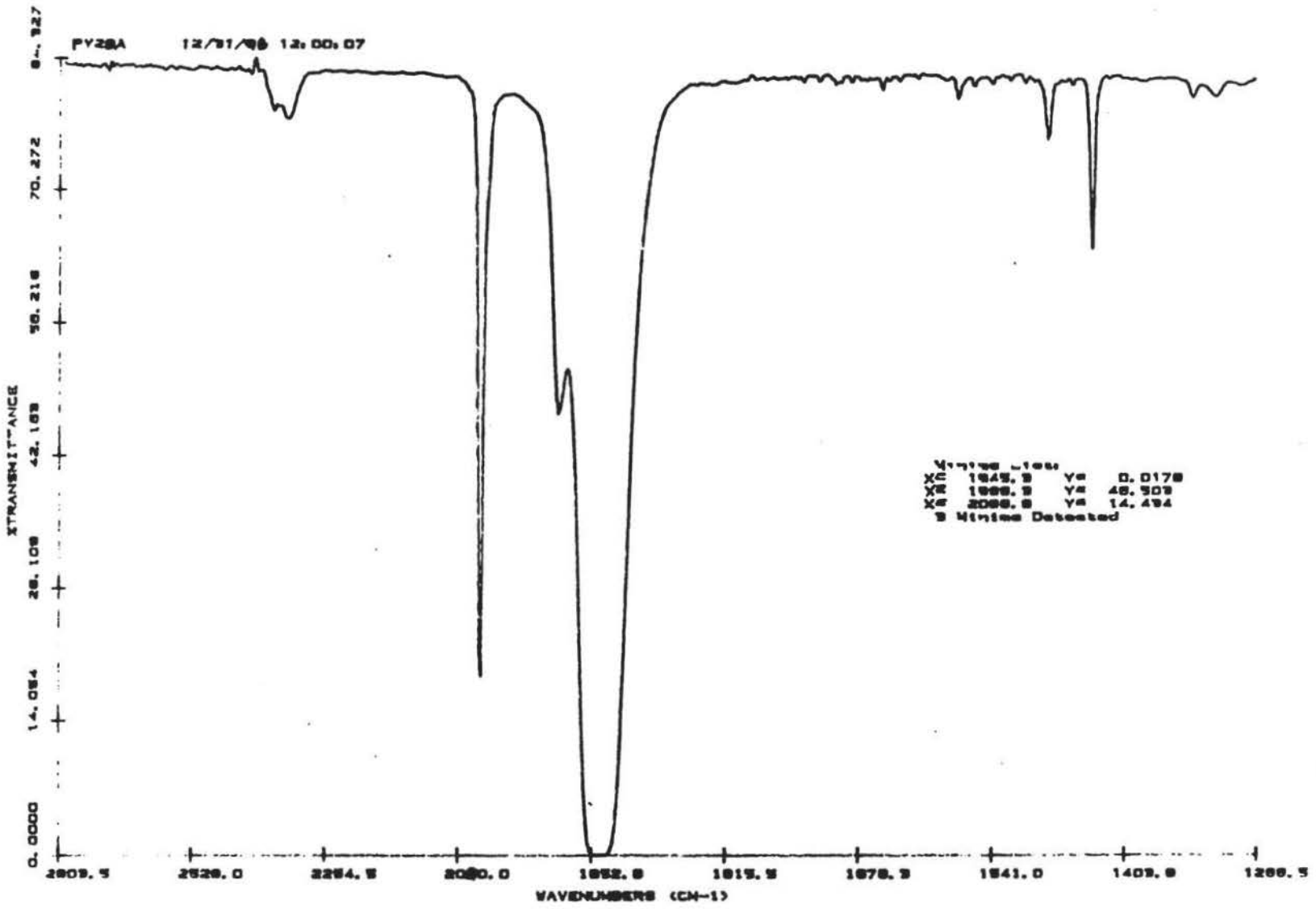

Figure 7. The IR spectrum of $(OC)_5CrPPh_2H$ in carbonyl region in $CHCl_3$

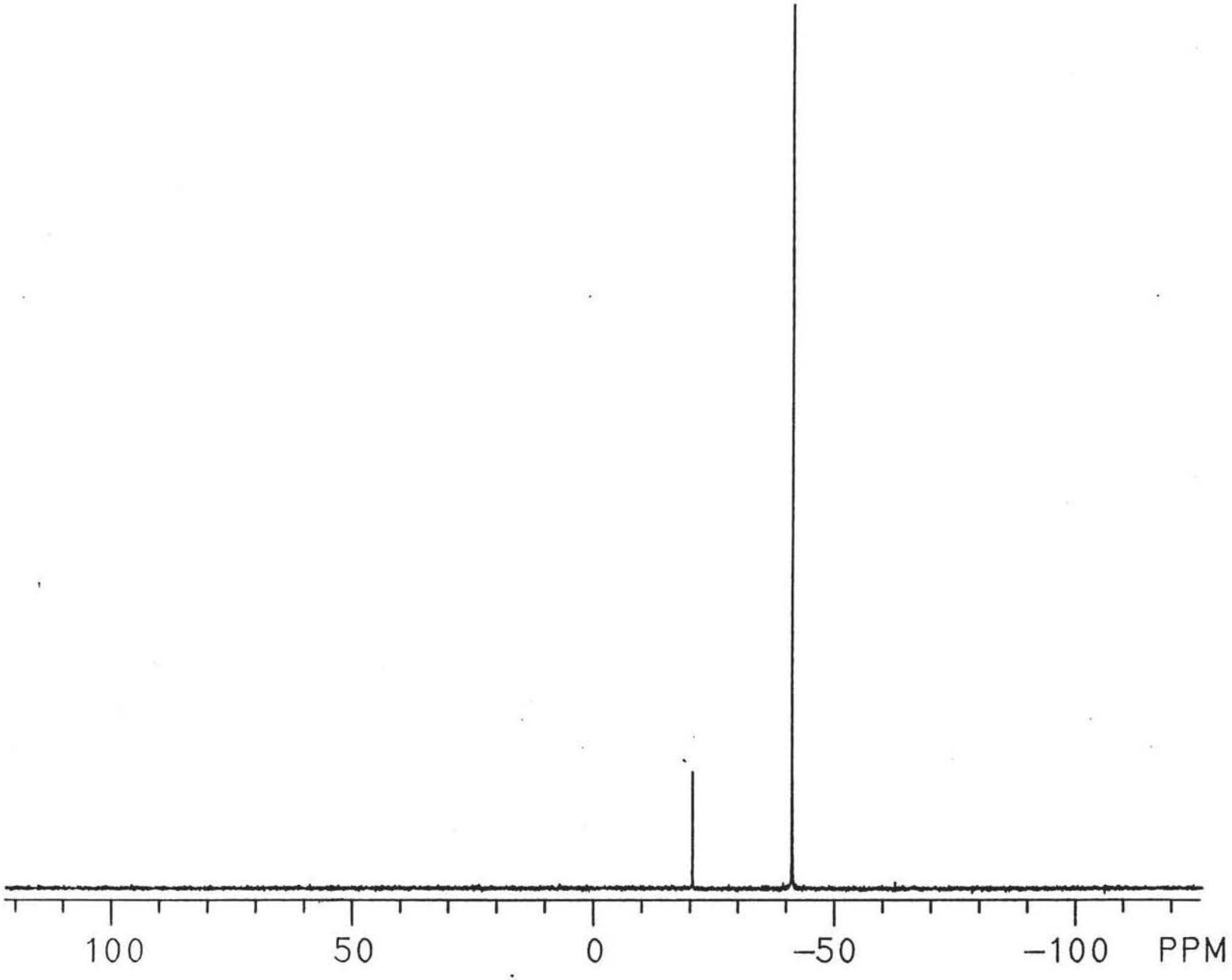

Figure 8. The $^{31}P\{^{1}H\}$ NMR spectrum of $Cl_2Pd(PPh_2)_2C{=}CH_2$ in $CDCl_3$

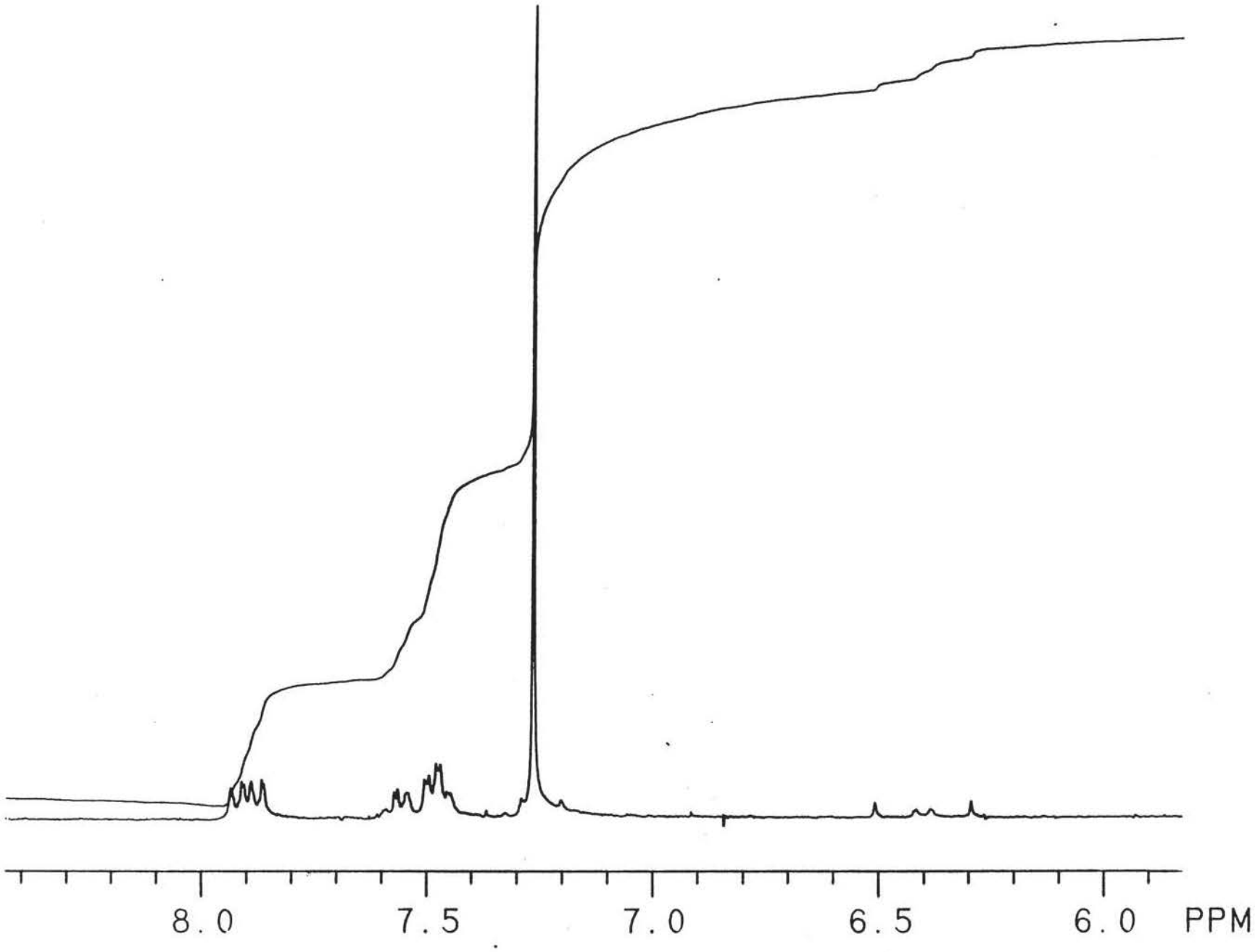

Figure 9. The ^1H NMR spectrum of $Cl_2Pd(PPh_2)_2C{=}CH_2$ in $CDCl_3$

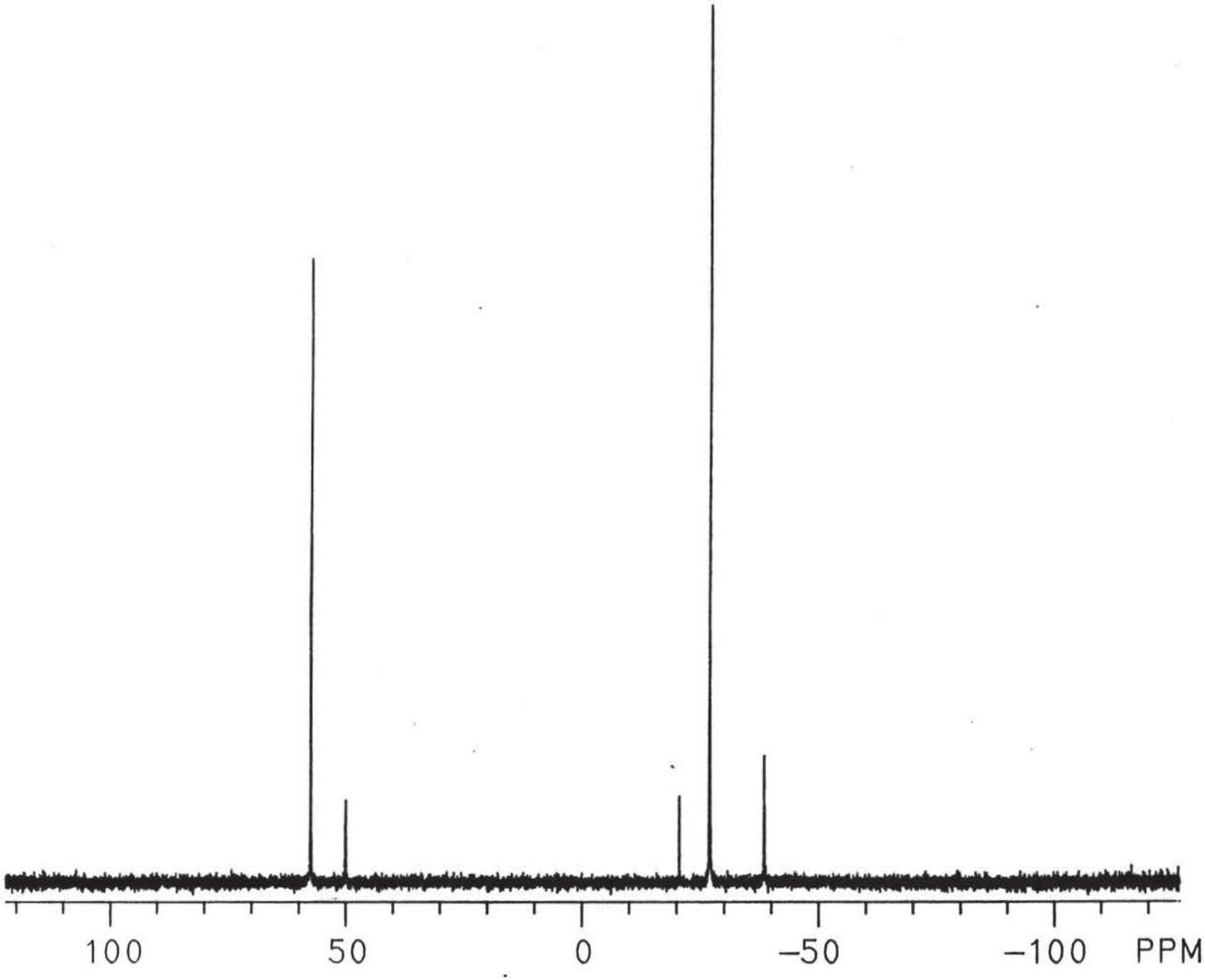

Figure 10. The $^{31}P\{^{1}H\}$ NMR spectrum of $Cl_2Pd(PPh_2)_2CHCH_2PPh_2Cr(CO)_5$ in $CDCl_3$

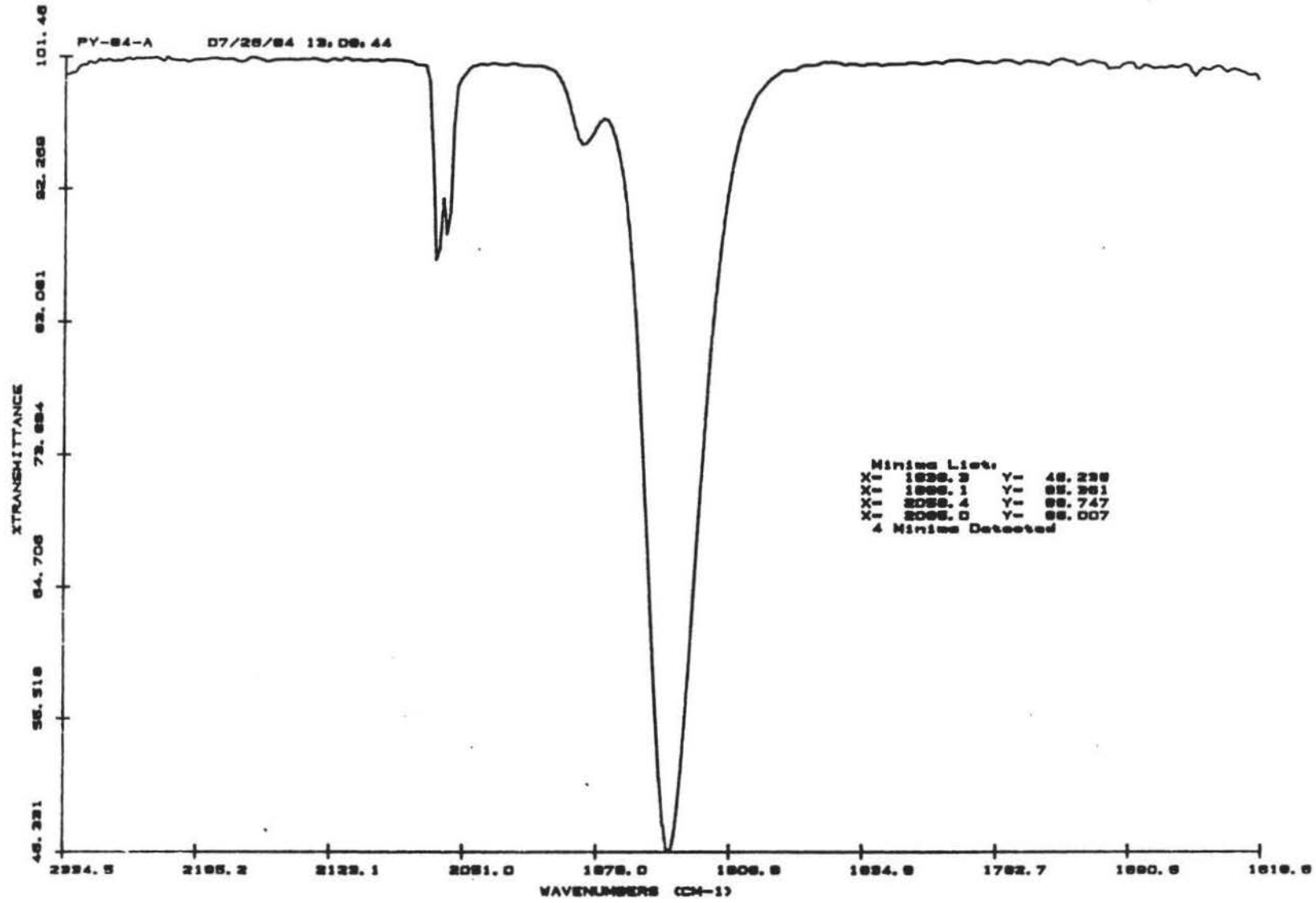

Figure 11. The IR spectrum of $Cl_2Pd(PPh_2)_2CHCH_2PPh_2Cr(CO)_5$ in carbonyl region in $CHCl_3$

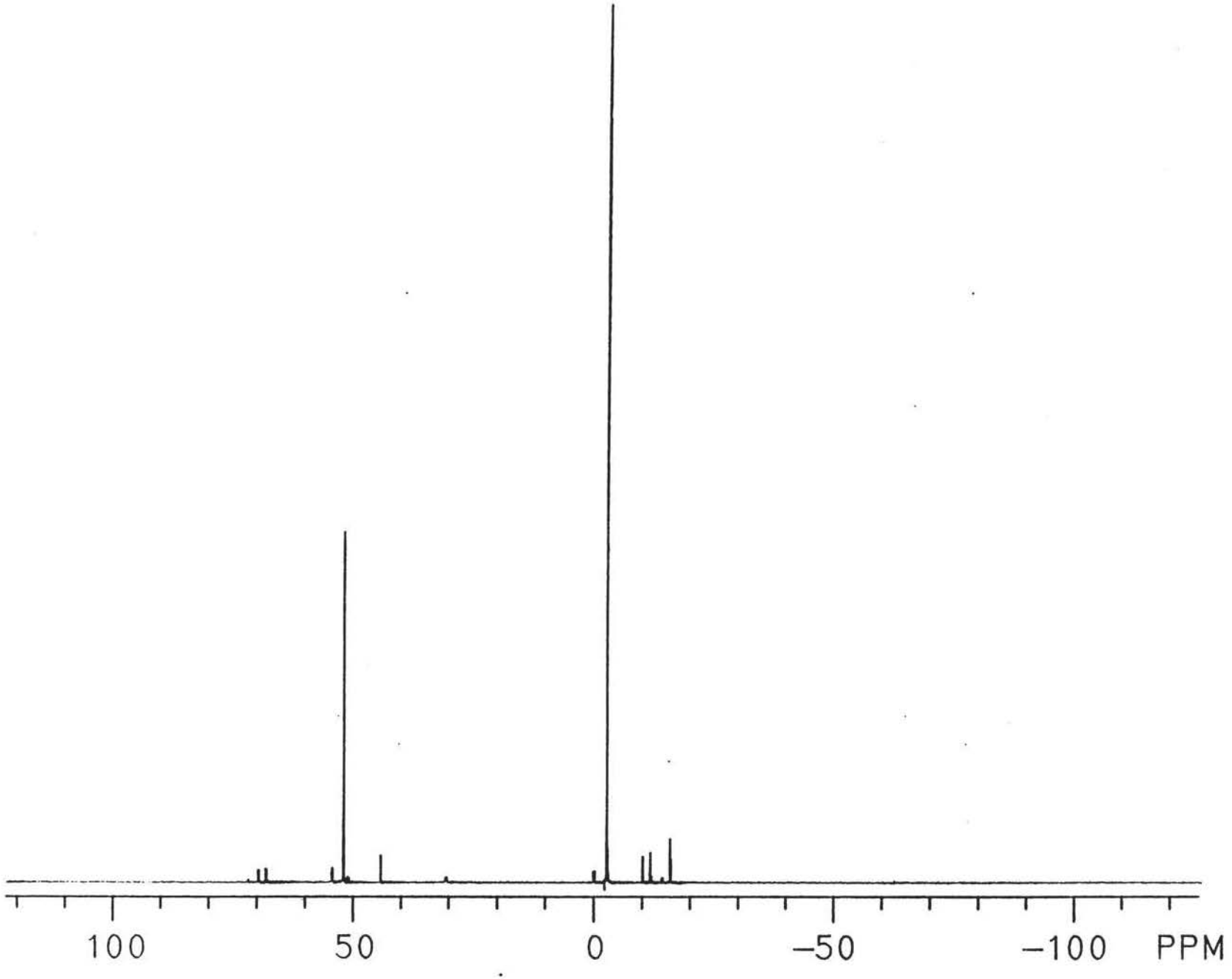

Figure 12. The $^{31}P\{^{1}H\}$ NMR spectrum of isomers $(OC)_5Cr[\eta^1\text{-}PPh_2CH_2CH(PPh_2)_2]$ (6) and $(OC)_5Cr[\eta^1\text{-}(PPh_2)_2CHCH_2PPh_2]$ (7) in $CDCl_3$, showing that the compound 6 is first formed from the reaction

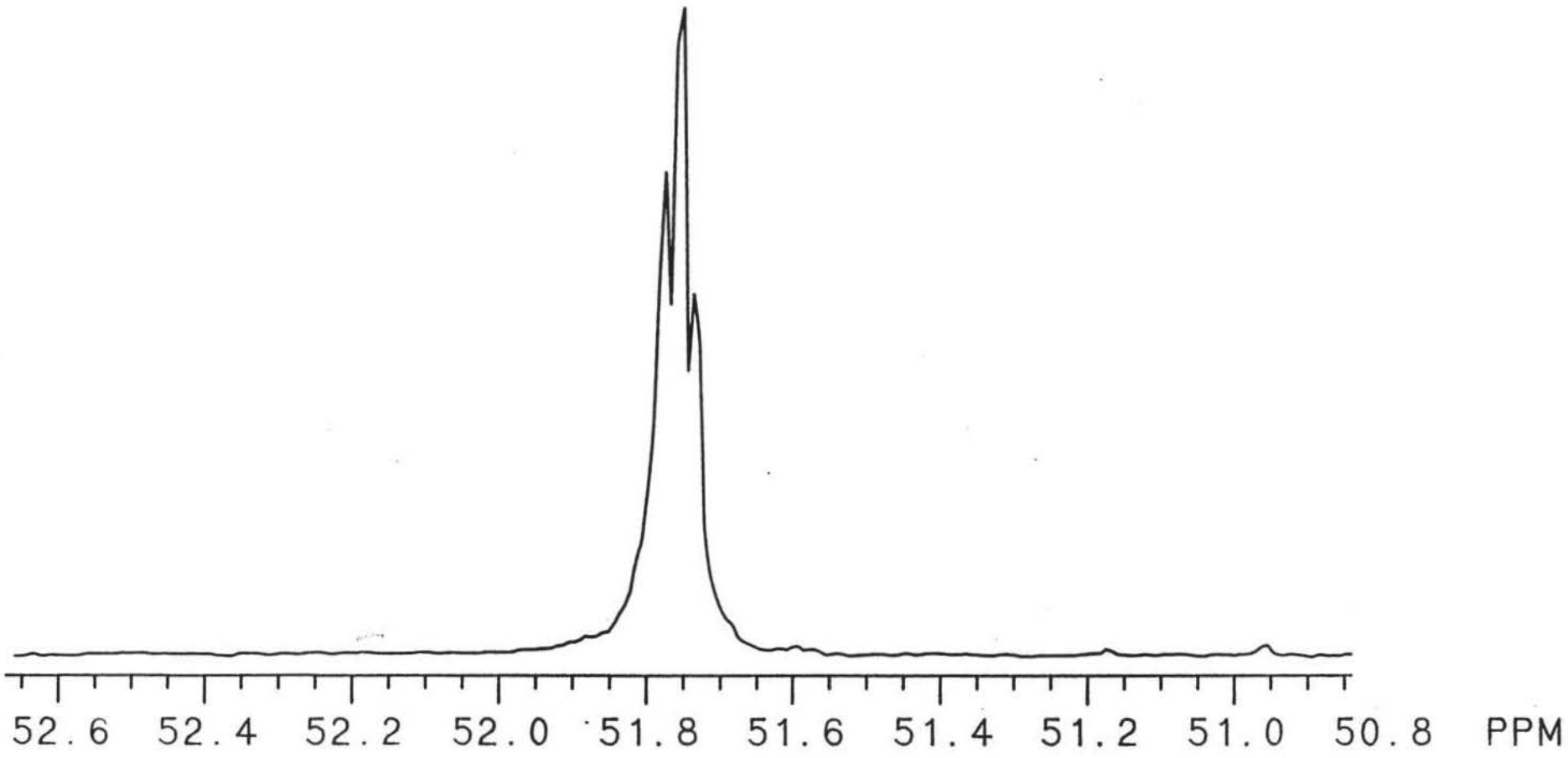

Figure 12a. The expansion of the $^{31}P\{^{1}H\}$ NMR of compound 6

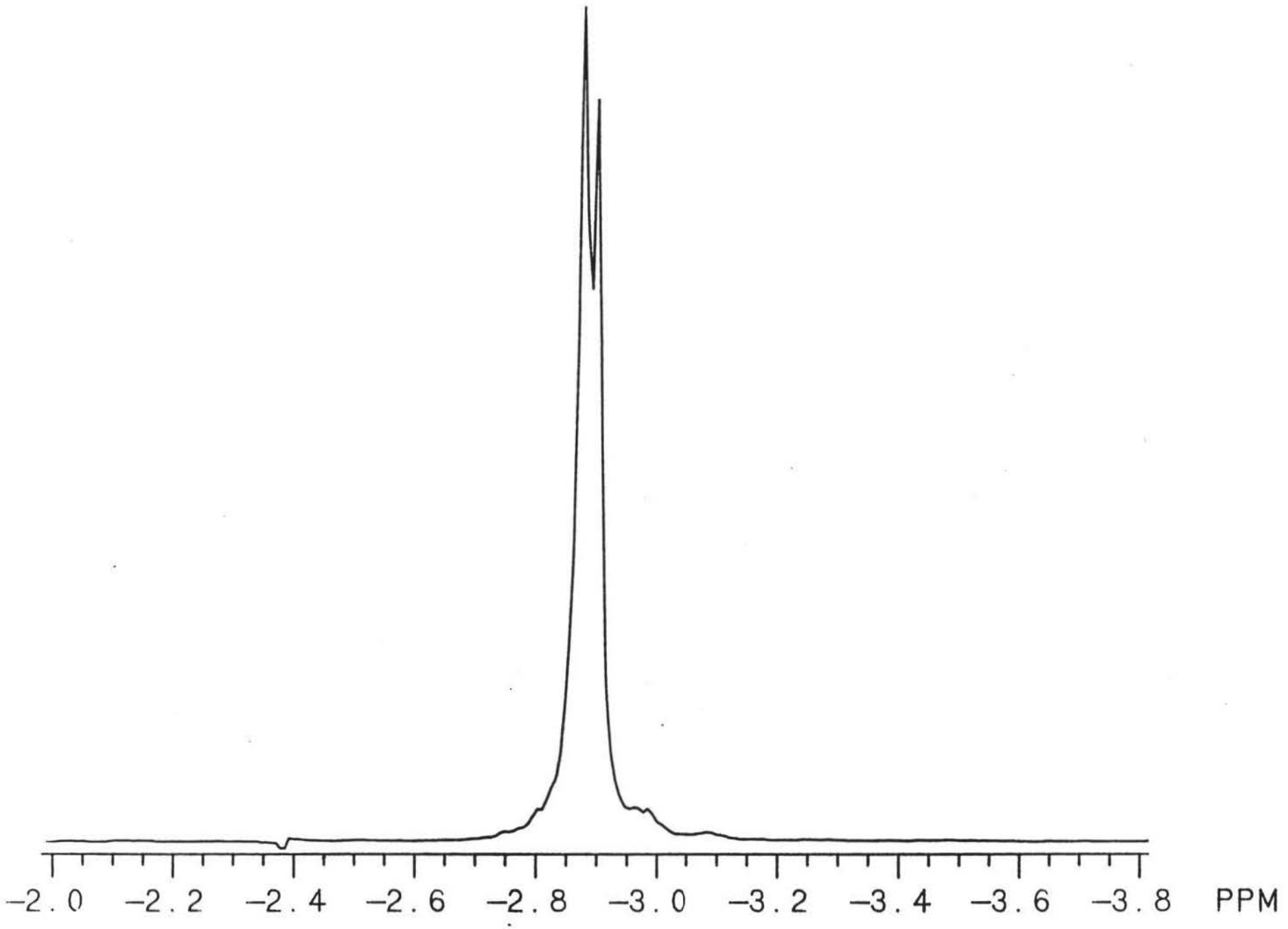

Figure 12b. The expansion of the $^{31}P\{^{1}H\}$ NMR of compound 6

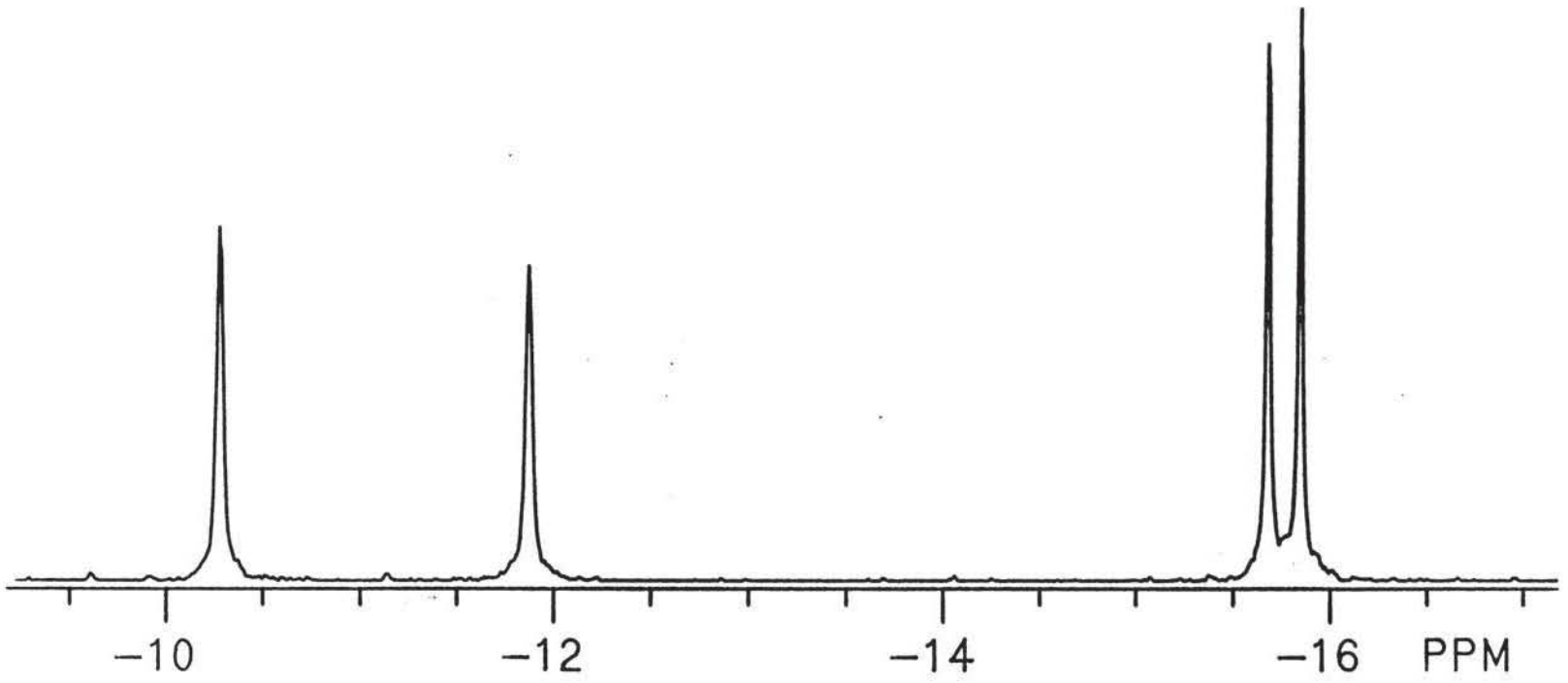

Figure 12c. The expansion of the $^{31}P\{^{1}H\}$ NMR of compound 7

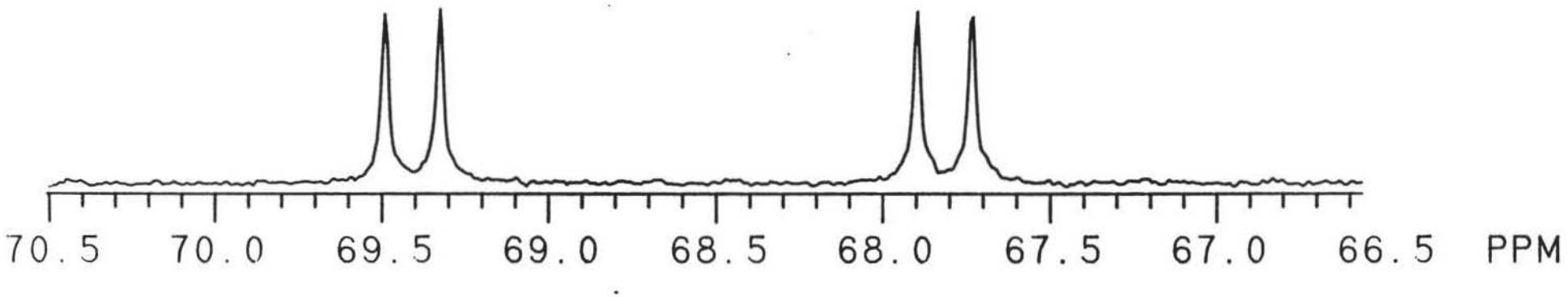

Figure 12d. The expansion of the $^{31}P\{^{1}H\}$ NMR of compound 7

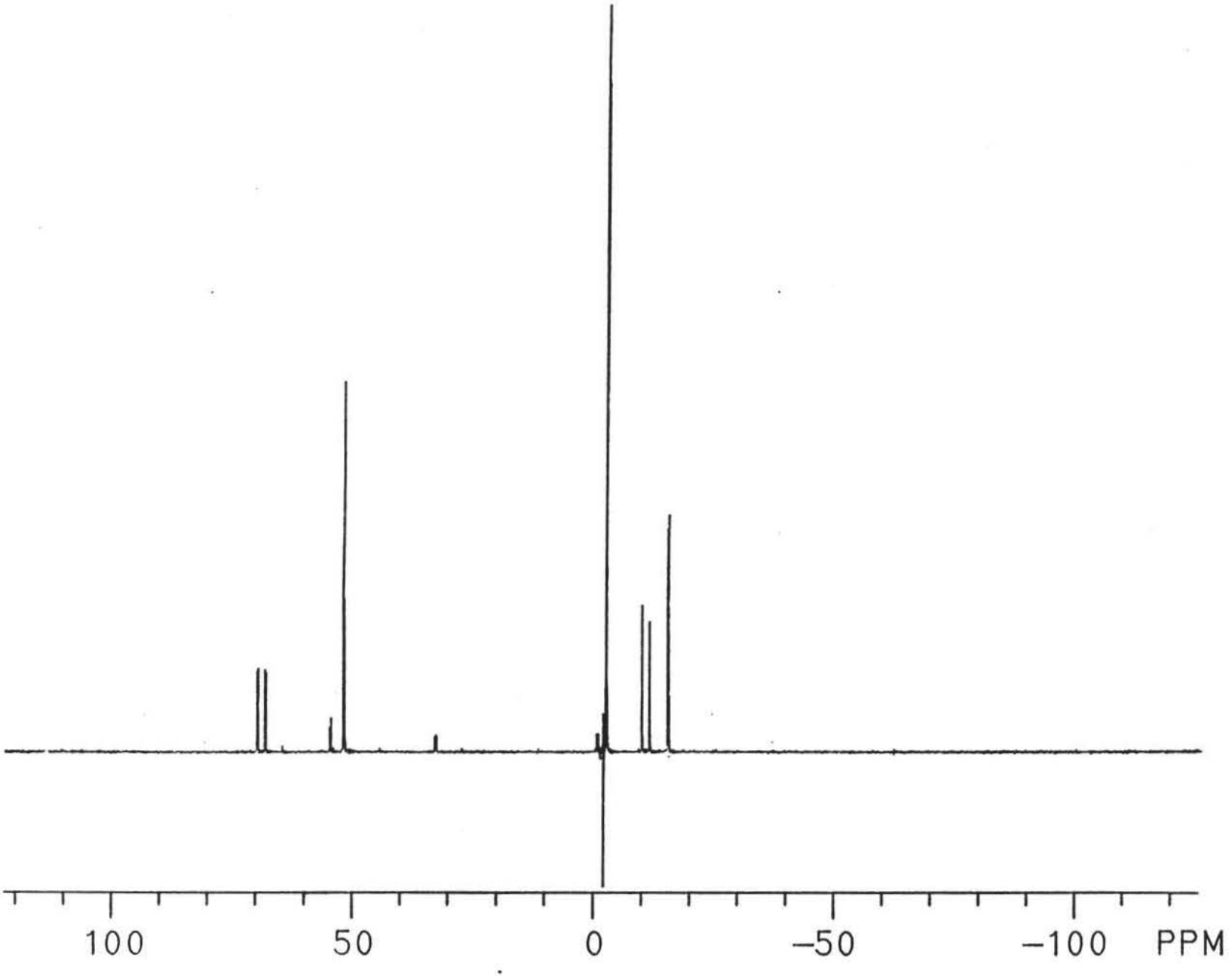

Figure 13. The $^{31}P\{^{1}H\}$ NMR spectrum of isomers $(OC)_5Cr[\eta^1\text{-}PPh_2CH_2CH(PPh_2)_2]$ (6) and $(OC)_5Cr[\eta^1\text{-}(PPh_2)_2CHCH_2PPh_2]$ (7) as they move toward equilibrium

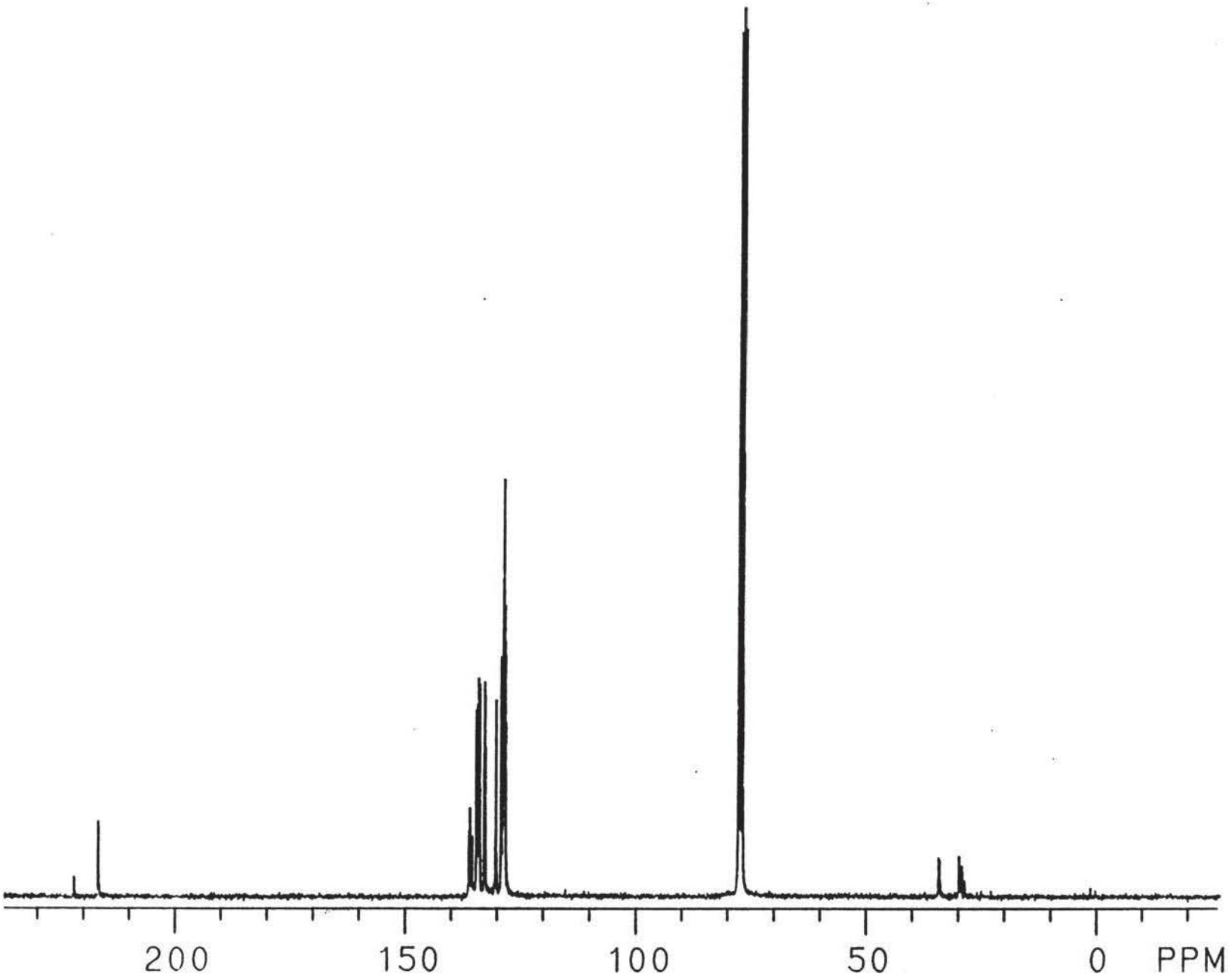

Figure 14. The $^{13}C\{^{1}H\}$ NMR spectrum of $(OC)_5Cr[\eta^1\text{-}PPh_2CH_2CH(PPh_2)_2]$ (6) in $CDCl_3$

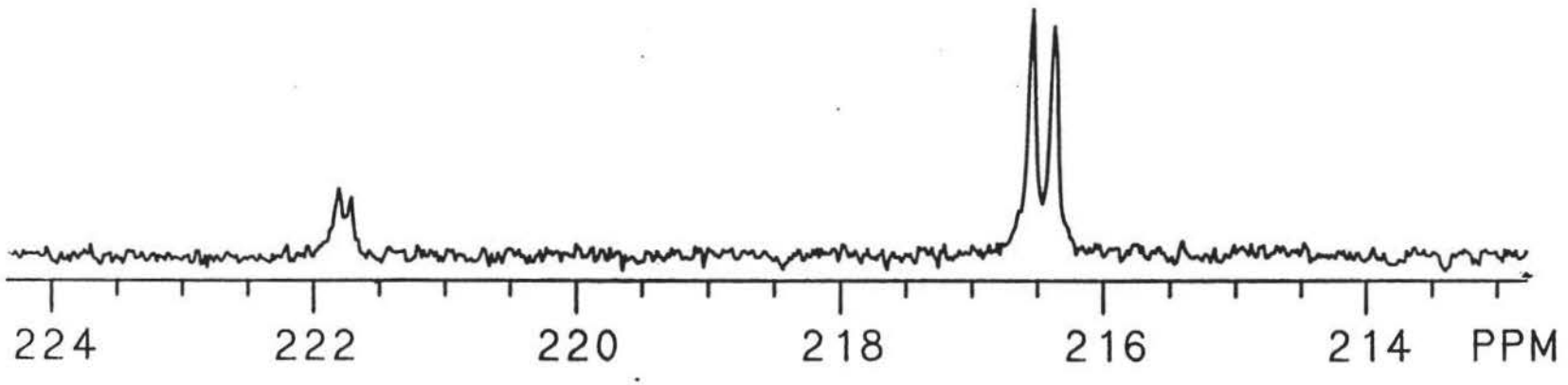

Figure 14a. The expansion $^{13}C\{^{1}H\}$ NMR spectrum of (6) in carbonyl region

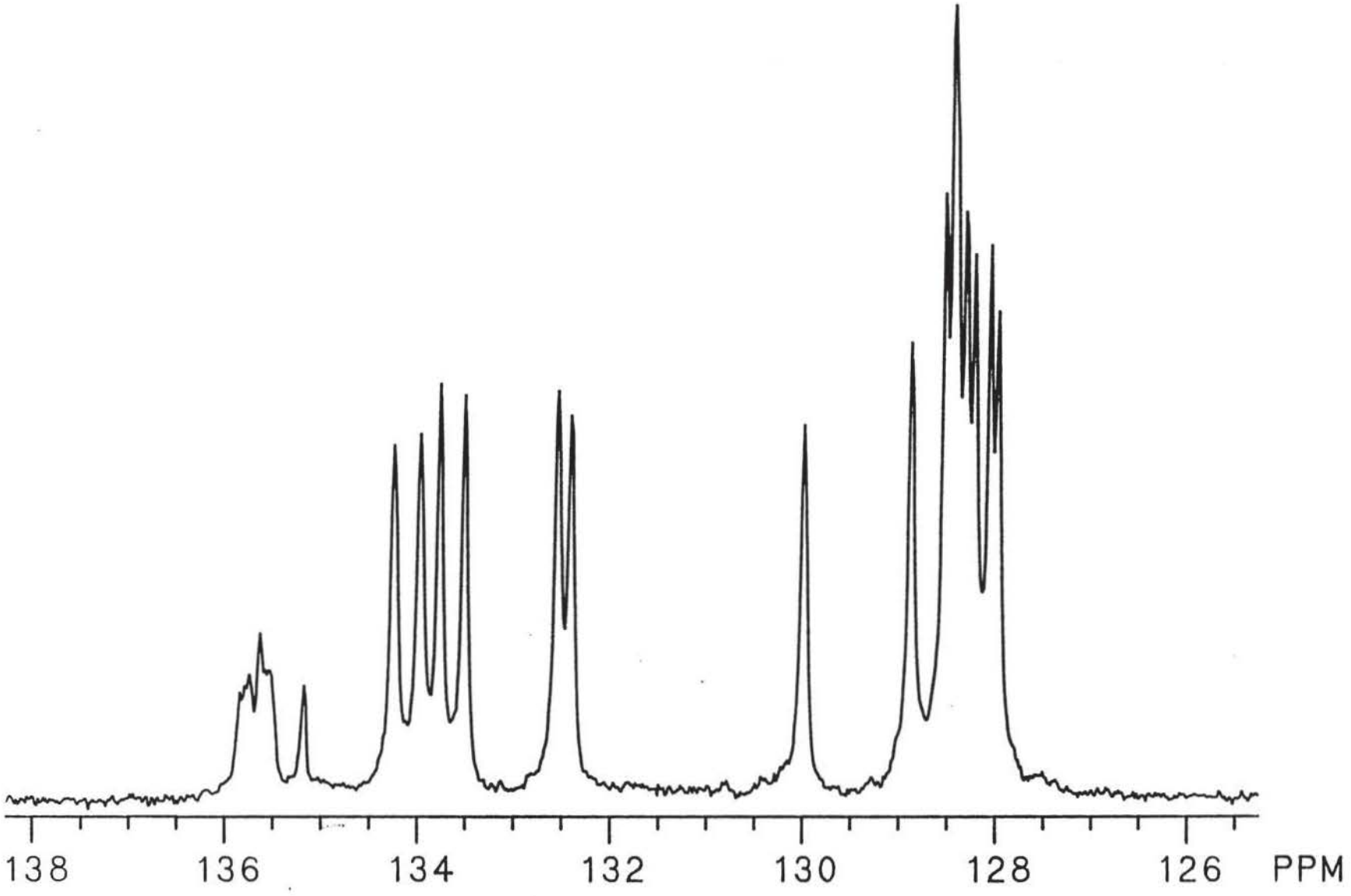

Figure 14b. The expansion $^{13}C\{^{1}H\}$ NMR spectrum of (6) in phenyl region

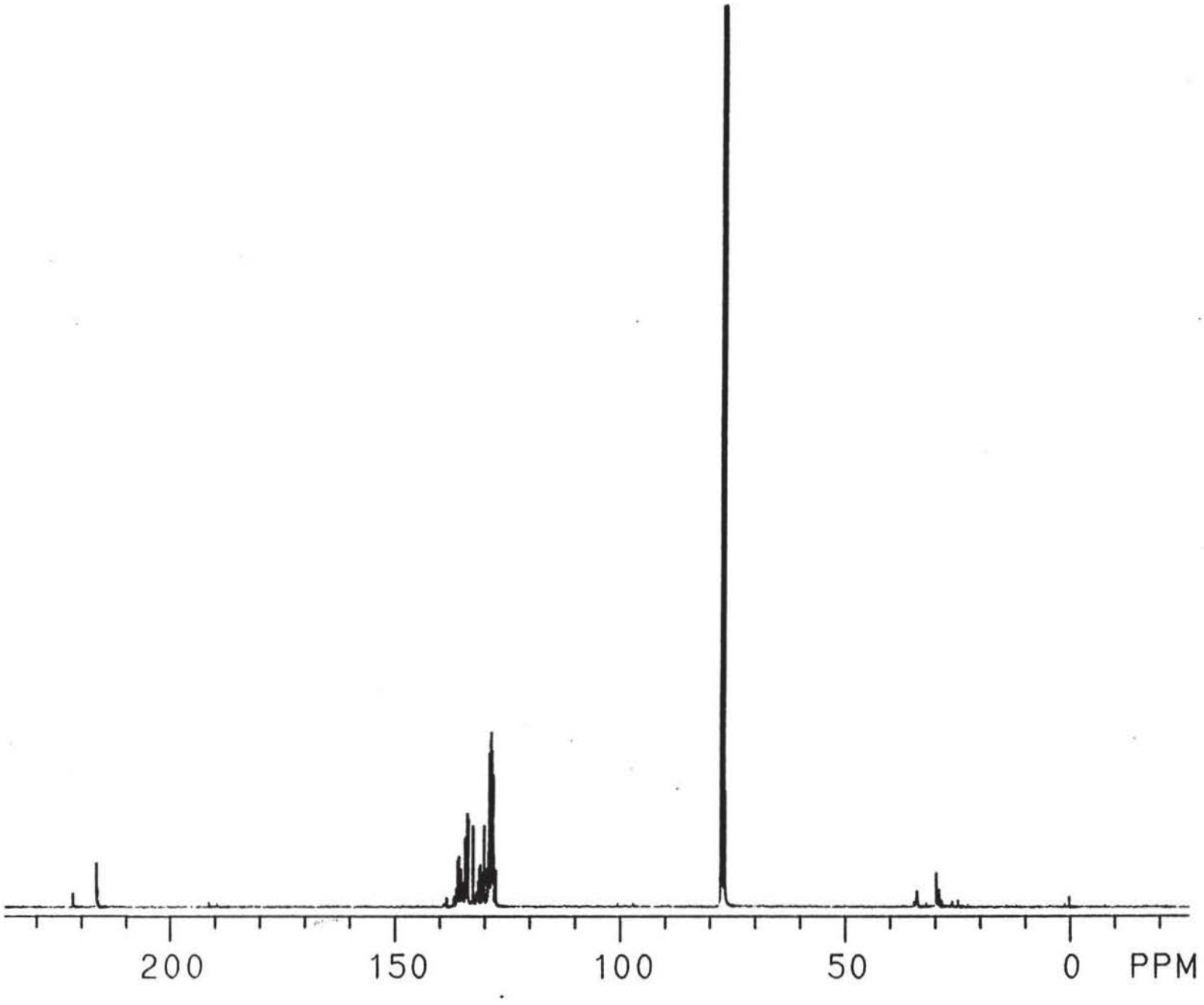

Figure 15. The $^{13}C\{^{1}H\}$ NMR spectrum of the mixture of 6 and 7 in $CDCl_3$

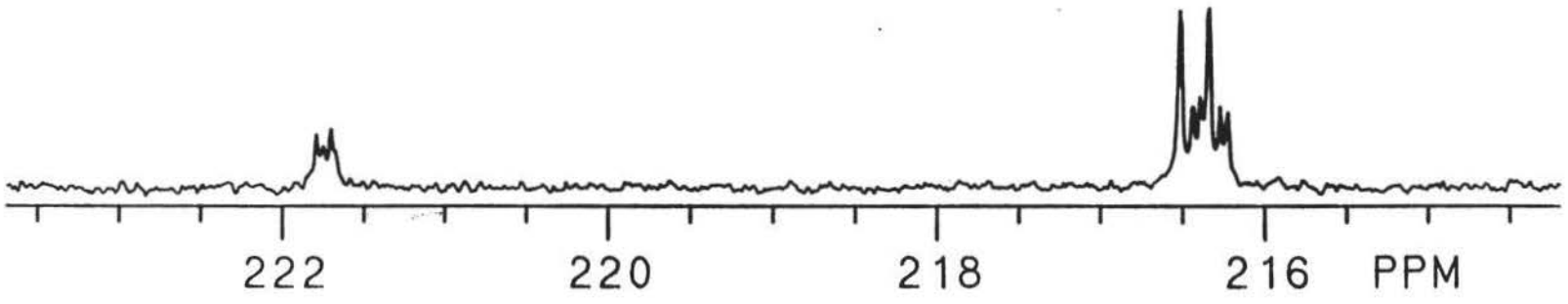

Figure 15a. The expansion of carbonyl region

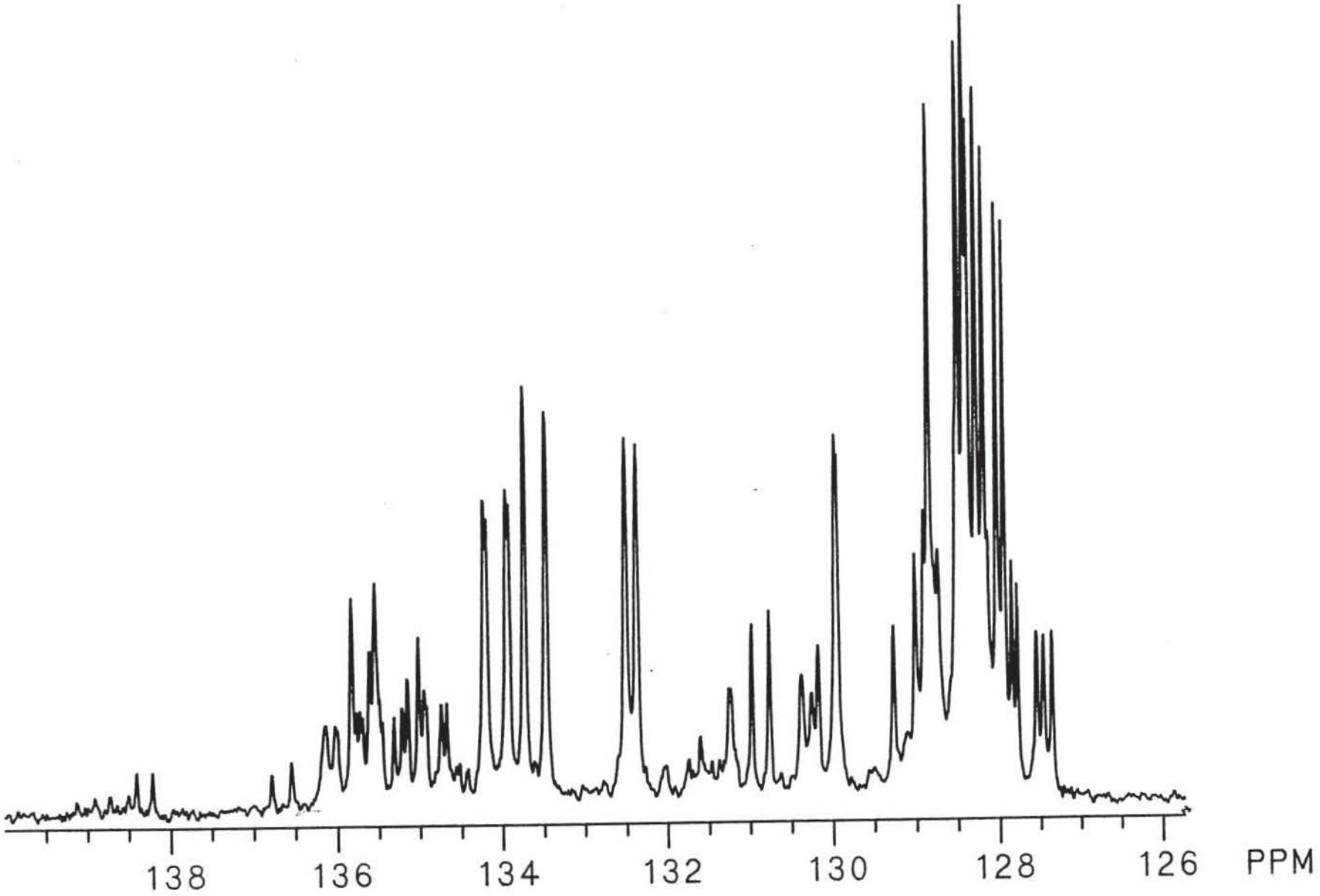

Figure 15b. The expansion of phenyl region

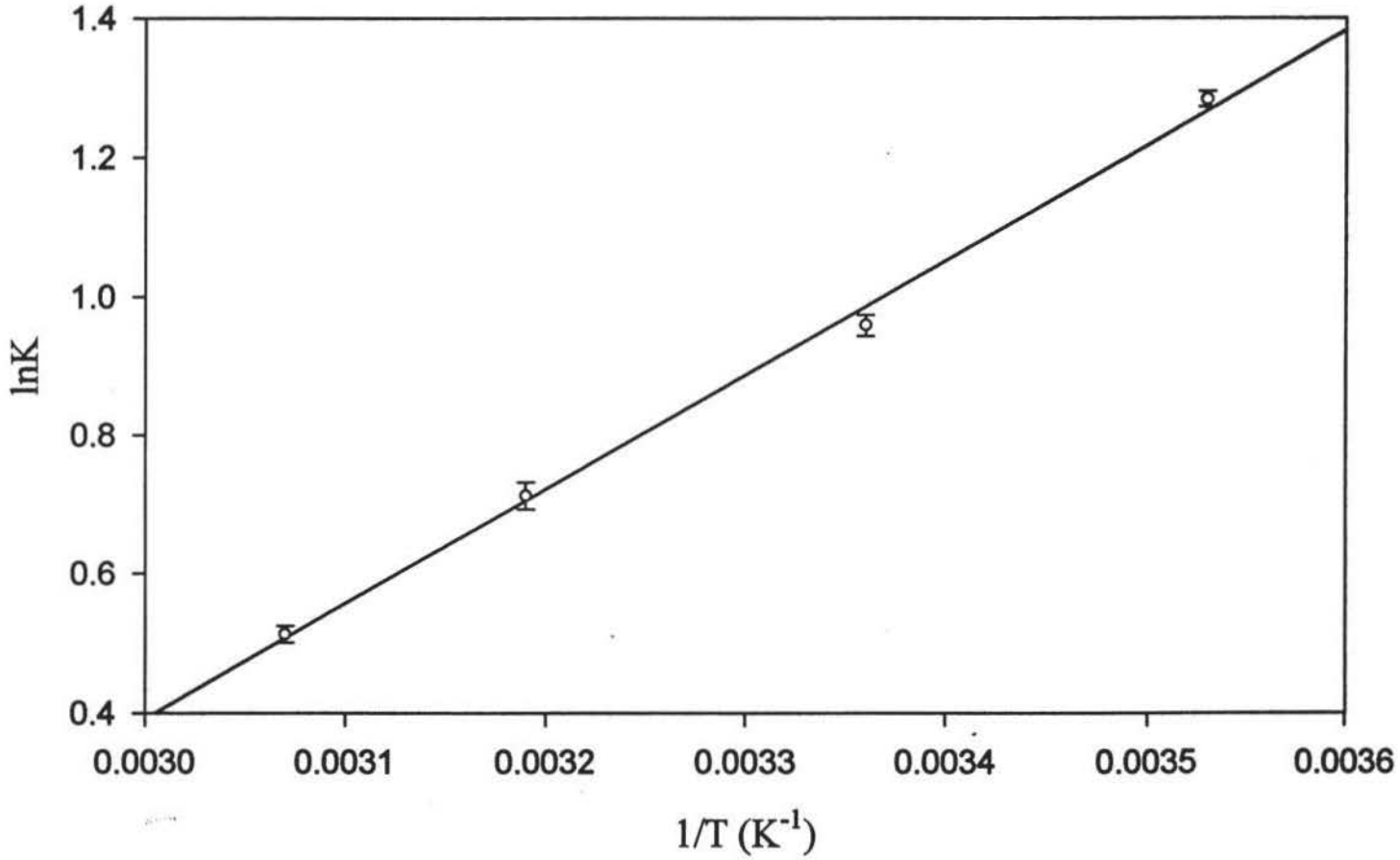

Figure 16. Plot of lnK vs. 1/T for isomerization of Cr complexes in $CDCl_3$. K is the equilibrium constant of the reaction.

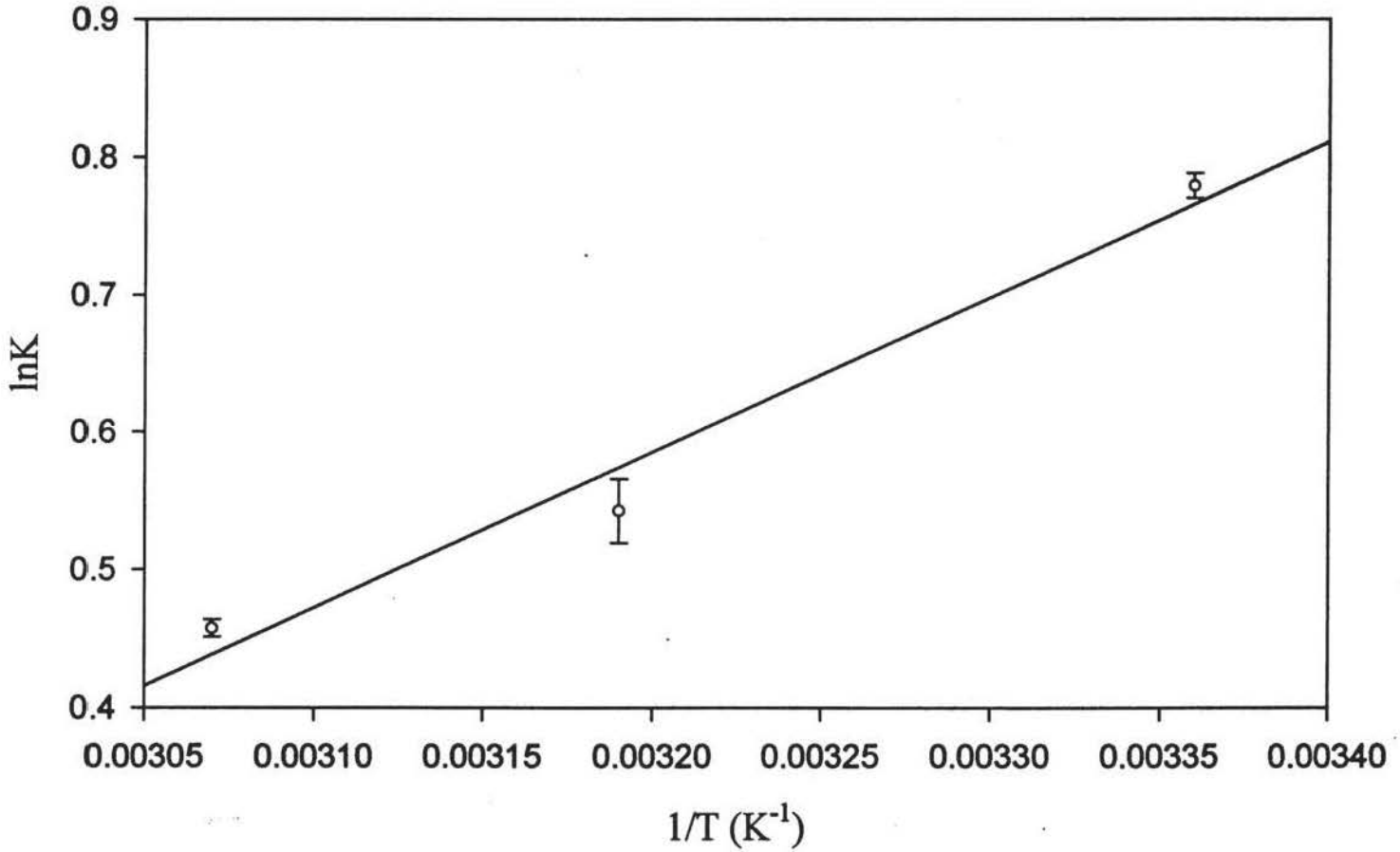

Figure 17. Plot of lnK vs. 1/T for isomerization of Cr complexes in toluene-d_8 solution. K is the equilibrium constant of the reaction.

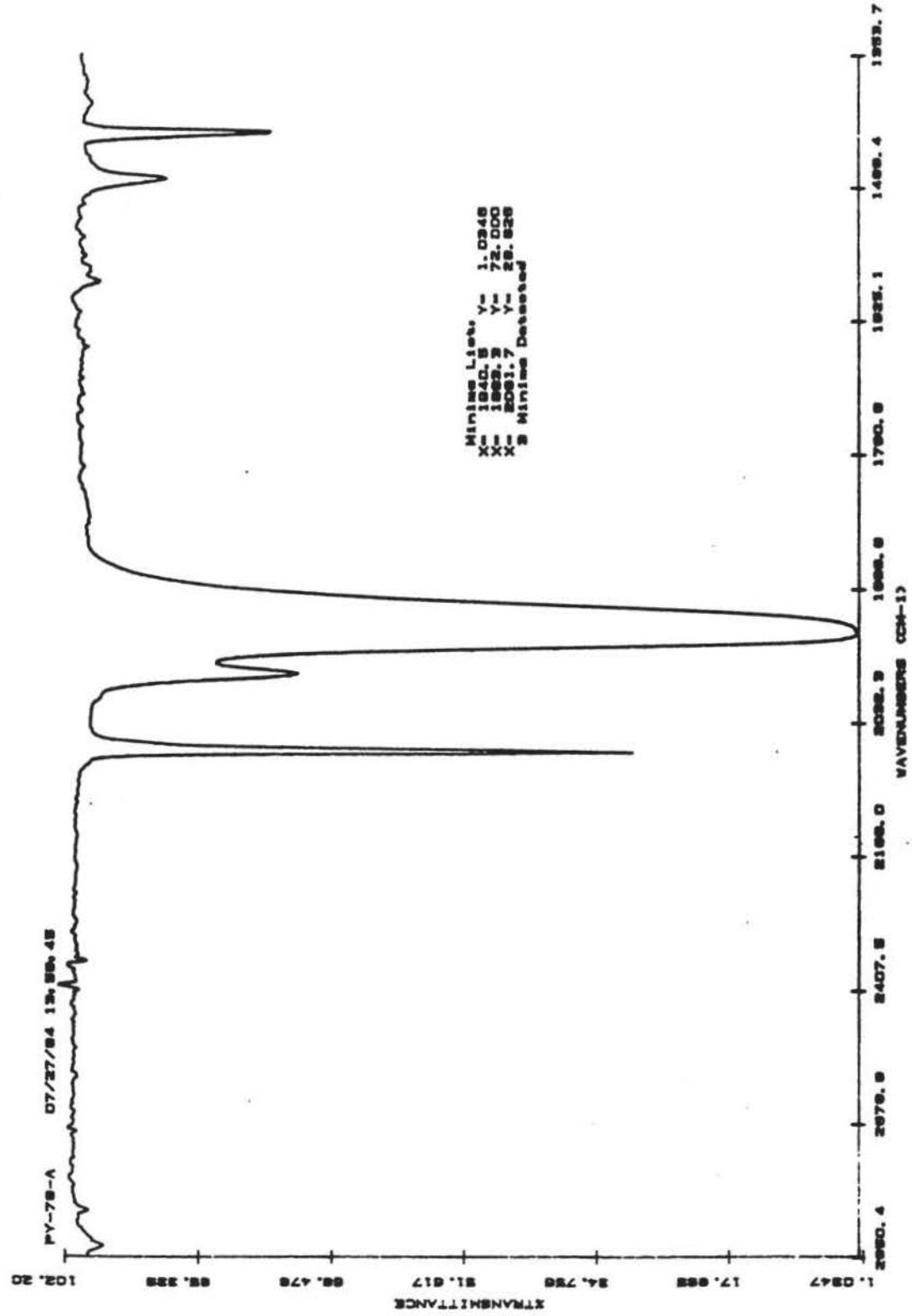

Figure 18. The IR spectrum of 6 and 7 in carbonyl region in $CHCl_3$

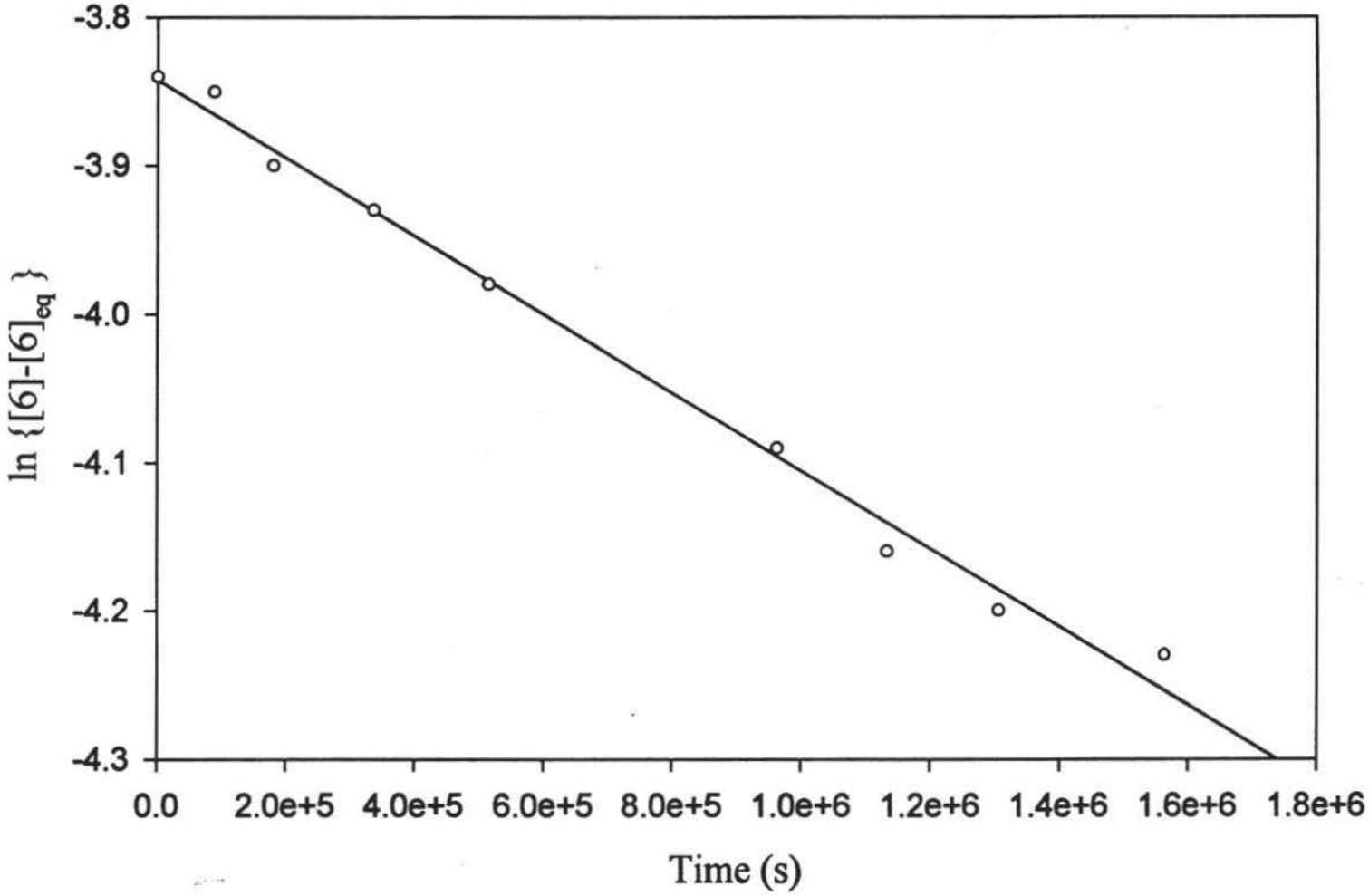

Figure 19. Plot of $\ln\{[6]-[6]_{eq}\}$ vs. time for isomerization of Cr complexes in $CDCl_3$, at $10^{o}C$. [6] is the concentration of $(OC)_5Cr[\eta^1\text{-}PPh_2CH_2CH(PPh_2)_2]$ at a certain time, $[6]_{eq}$ is the concentration of $(OC)_5Cr[\eta^1\text{-}PPh_2CH_2CH(PPh_2)_2]$ at equilibrium.

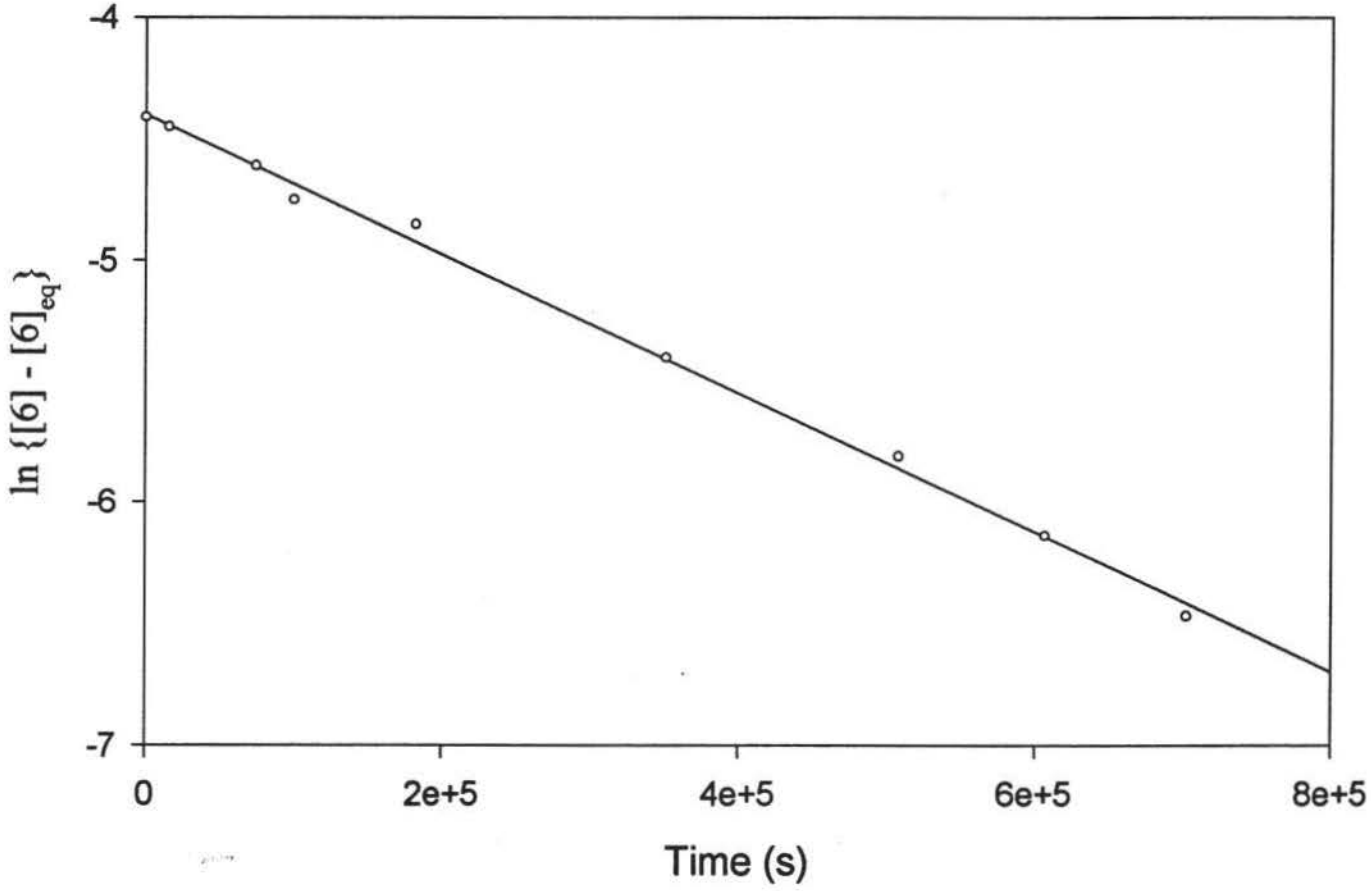

Figure 20. Plot of $\ln\{[6] - [6]_{eq}\}$ vs. time for isomerization of Cr complexes in $CDCl_3$, at 25°C. [6] is the concentration of $(OC)_5Cr[\eta^1\text{-}PPh_2CH_2CH(PPh_2)_2]$ at a certain time, $[6]_{eq}$ is the concentration of $(OC)_5Cr[\eta^1\text{-}PPh_2CH_2CH(PPh_2)_2]$ at equilibrium.

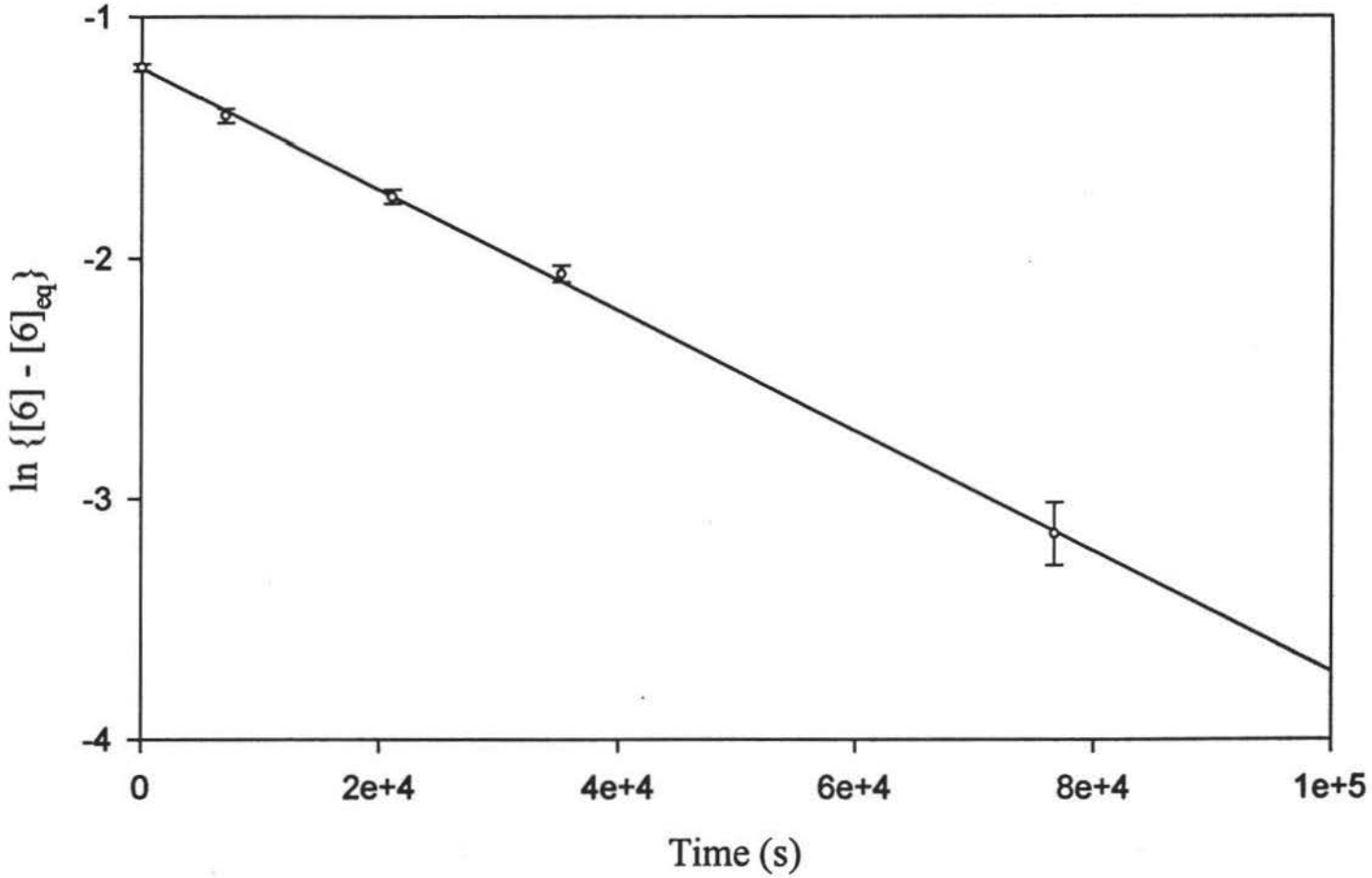

Figure 21. Plot of ln $\{[6] - [6]_{eq}\}$ vs. time for isomerization of Cr complexes in $CDCl_3$, at 40°C. [6] is the concentration of $(OC)_5Cr[\eta^1\text{-}PPh_2CH_2CH(PPh_2)_2]$ at a certain time, $[6]_{eq}$ is the concentration of $(OC)_5Cr[\eta^1\text{-}PPh_2CH_2CH(PPh_2)_2]$ at equilibrium.

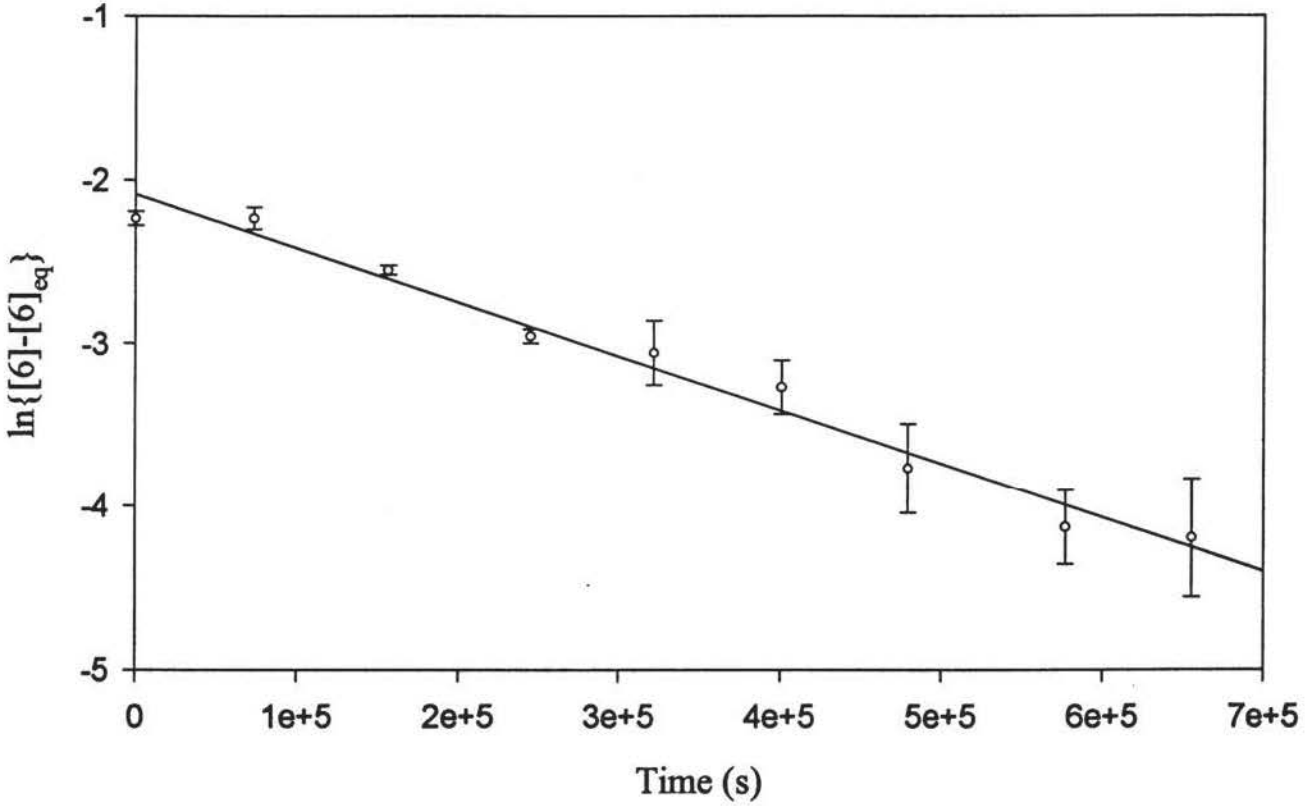

Figure 22. Plot of $\ln\{[6] - [6]_{eq}\}$ vs. time for isomerization of Cr complexes in toluene-d_8, at 25°C. [6] is the concentration of $(OC)_5Cr[\eta^1\text{-}PPh_2CH_2CH(PPh_2)_2]$ at a certain time, while $[6]_{eq}$ is the concentration of $(OC)_5Cr[\eta^1\text{-}PPh_2CH_2CH(PPh_2)_2]$ at equilibrium.

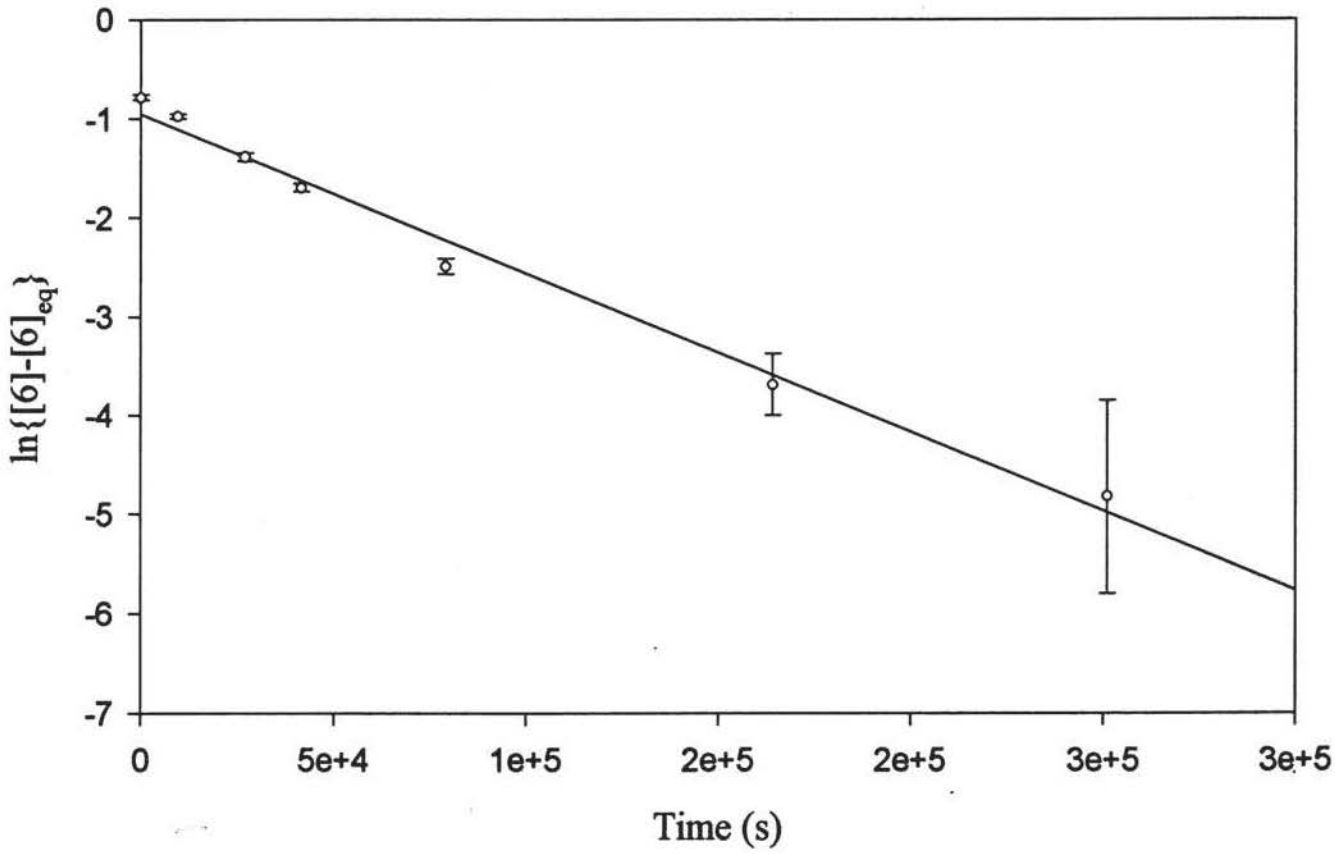

Figure 23. Plot of $\ln\{[6] - [6]_{eq}\}$ vs. time for isomerization of Cr complexes in toluene-d_8, at 40°C. [6] is the concentration of $(OC)_5Cr[\eta^1\text{-}PPh_2CH_2CH(PPh_2)_2]$ at a certain time, while $[6]_{eq}$ is the equilibrium constant of the reaction.

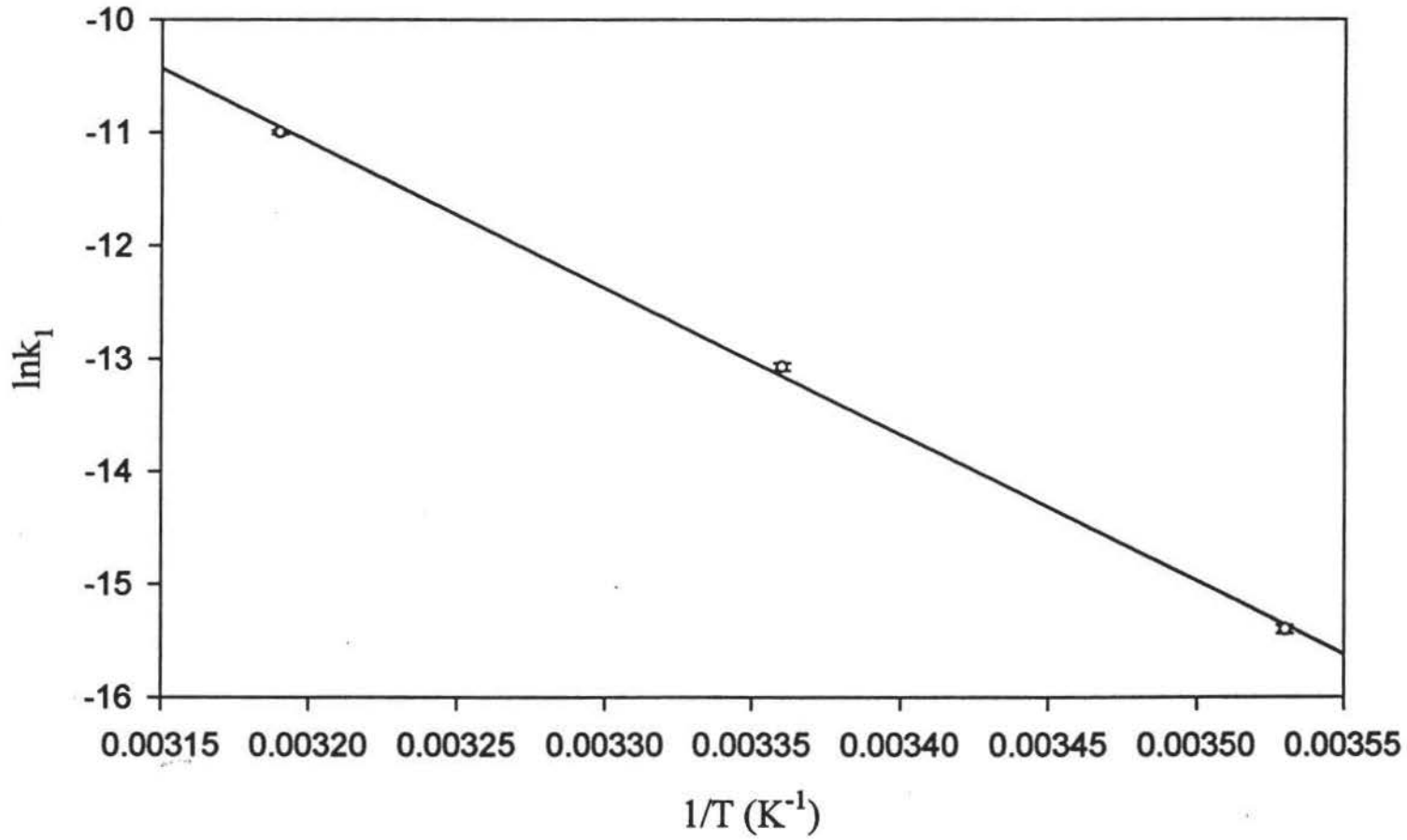

Figure 24. Plot of $\ln k_1$ vs. 1/T for isomerization of Cr complexes in $CDCl_3$ solution. k_1 is the rate constant of forward reaction.

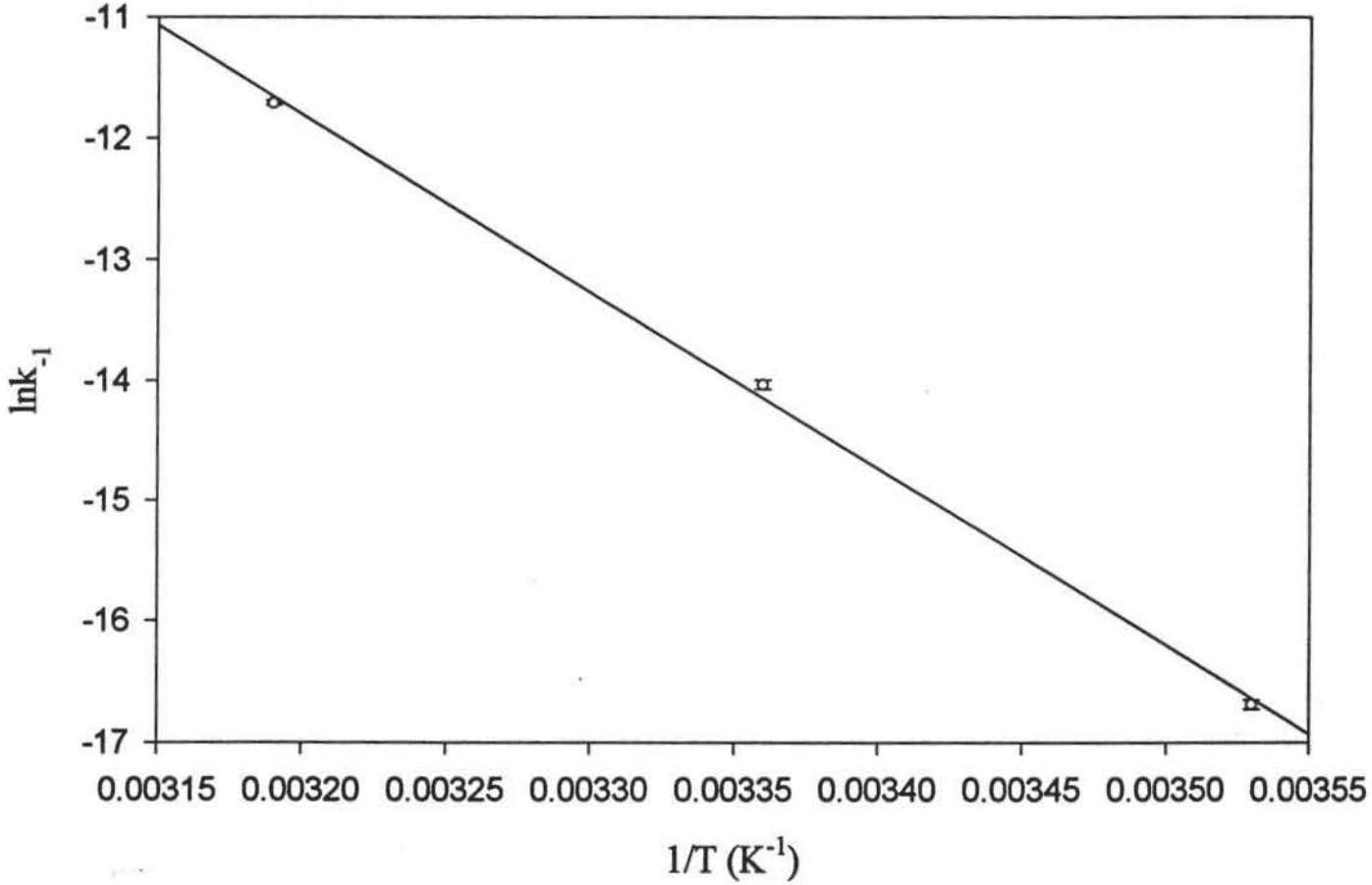

Figure 25. Plot of $\ln k_{-1}$ vs. 1/T for isomerization of Cr complexes in $CDCl_3$ solution. k_{-1} is the rate constant of backward reaction.

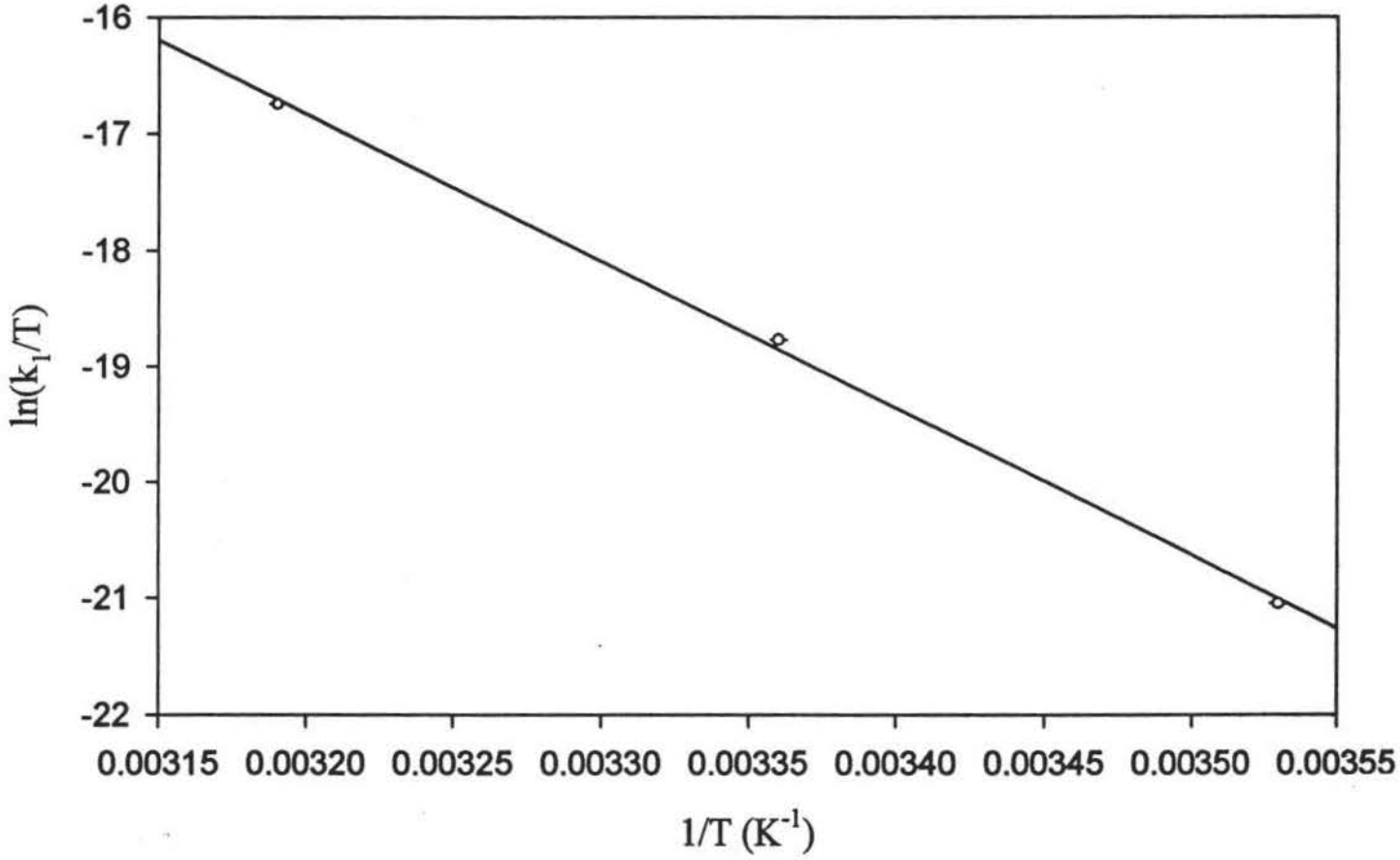

Figure 26. Plot of $\ln(k_1/T)$ vs. 1/T for isomerization of Cr complexes in $CDCl_3$. k_1 is the rate constant of forward reaction.

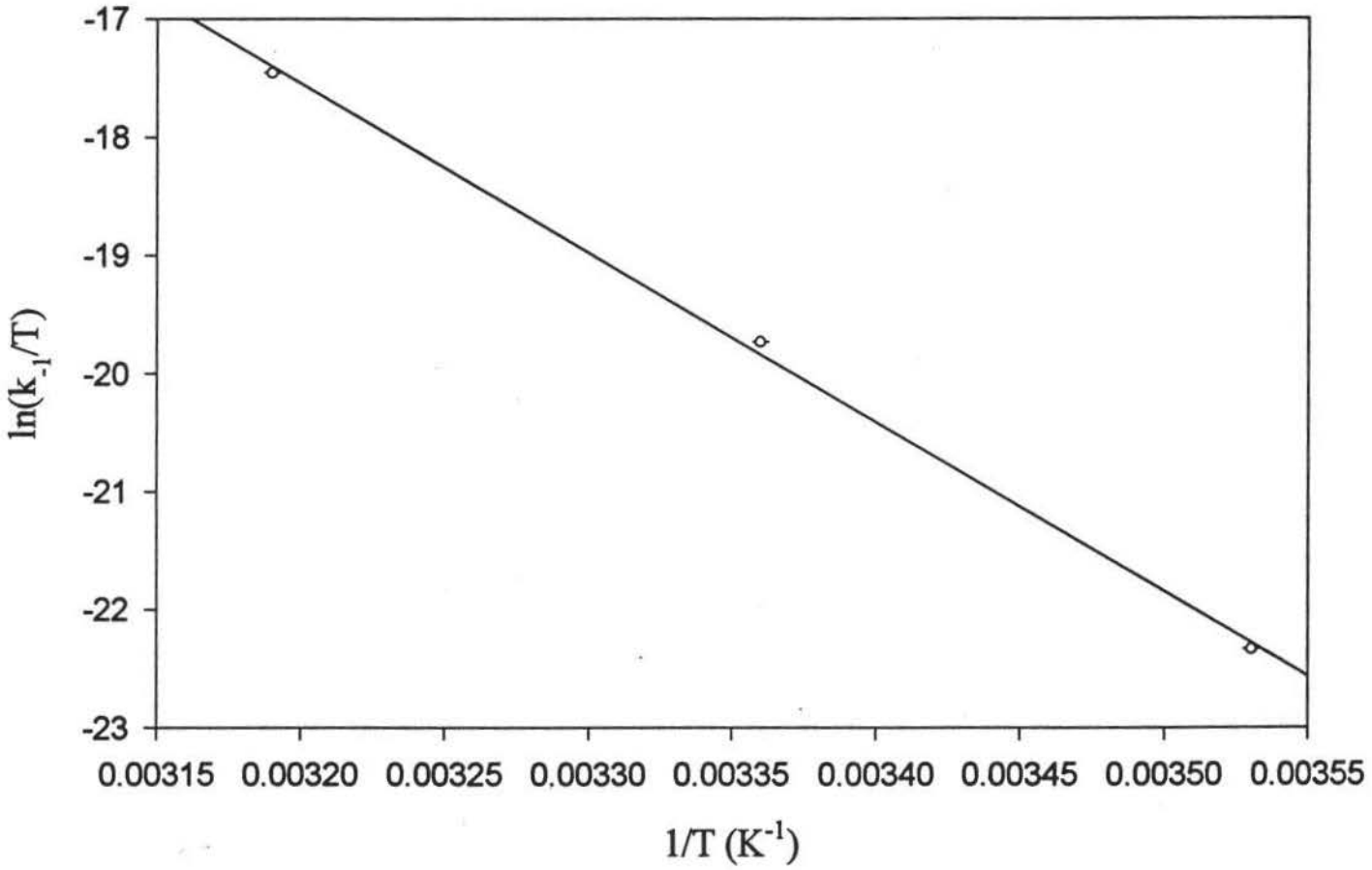

Figure 27. Plot of $\ln(k_{-1}/T)$ vs. 1/T for isomerization of Cr complexes in $CDCl_3$ solution. k_{-1} is the rate constant of backward reaction.

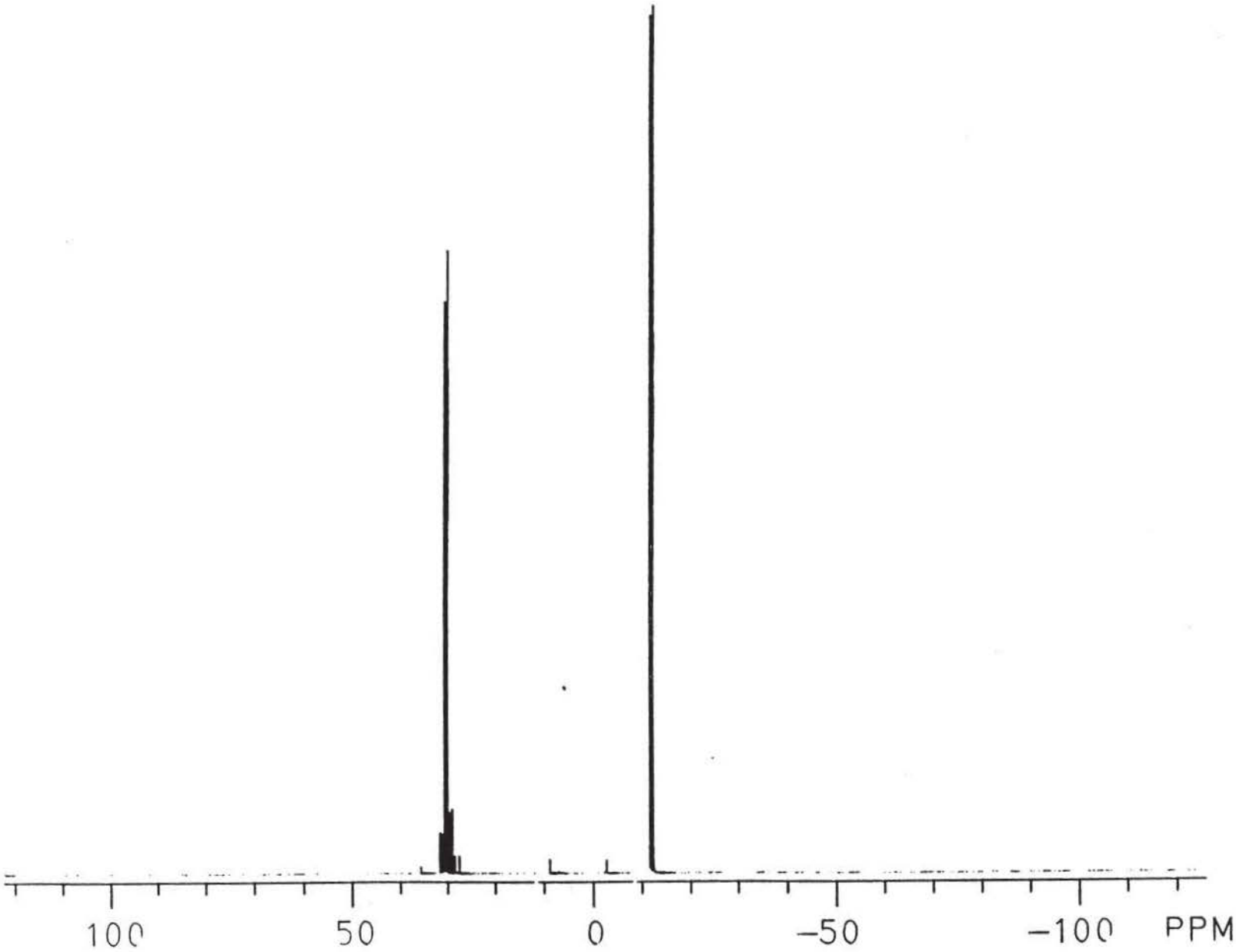

Figure 28. The $^{31}P\{^{1}H\}$ NMR spectrum of $(OC)_5WPPh_2C(PPh_2)=CH_2$ in $CDCl_3$

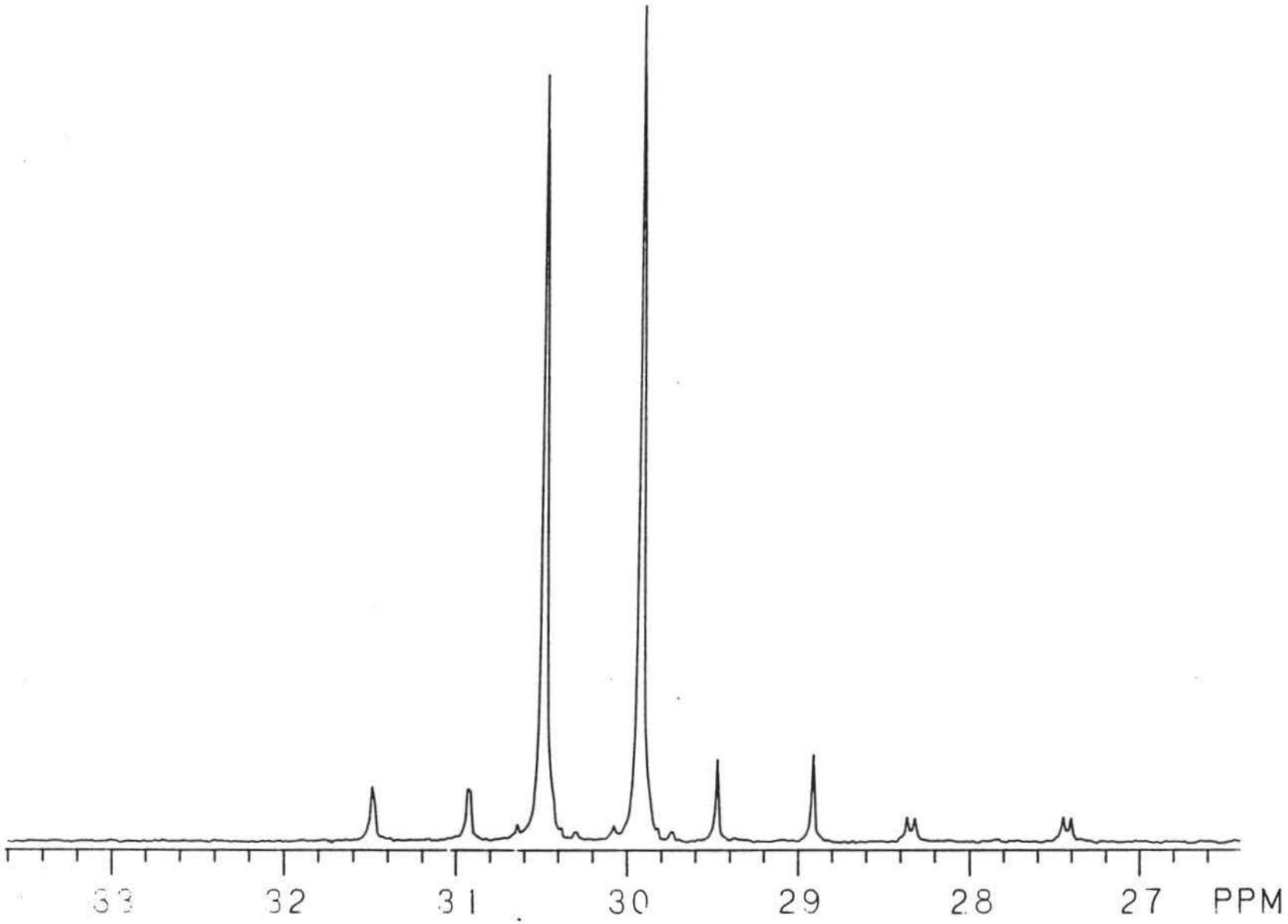

Figure 28a. The expansion of figure 28

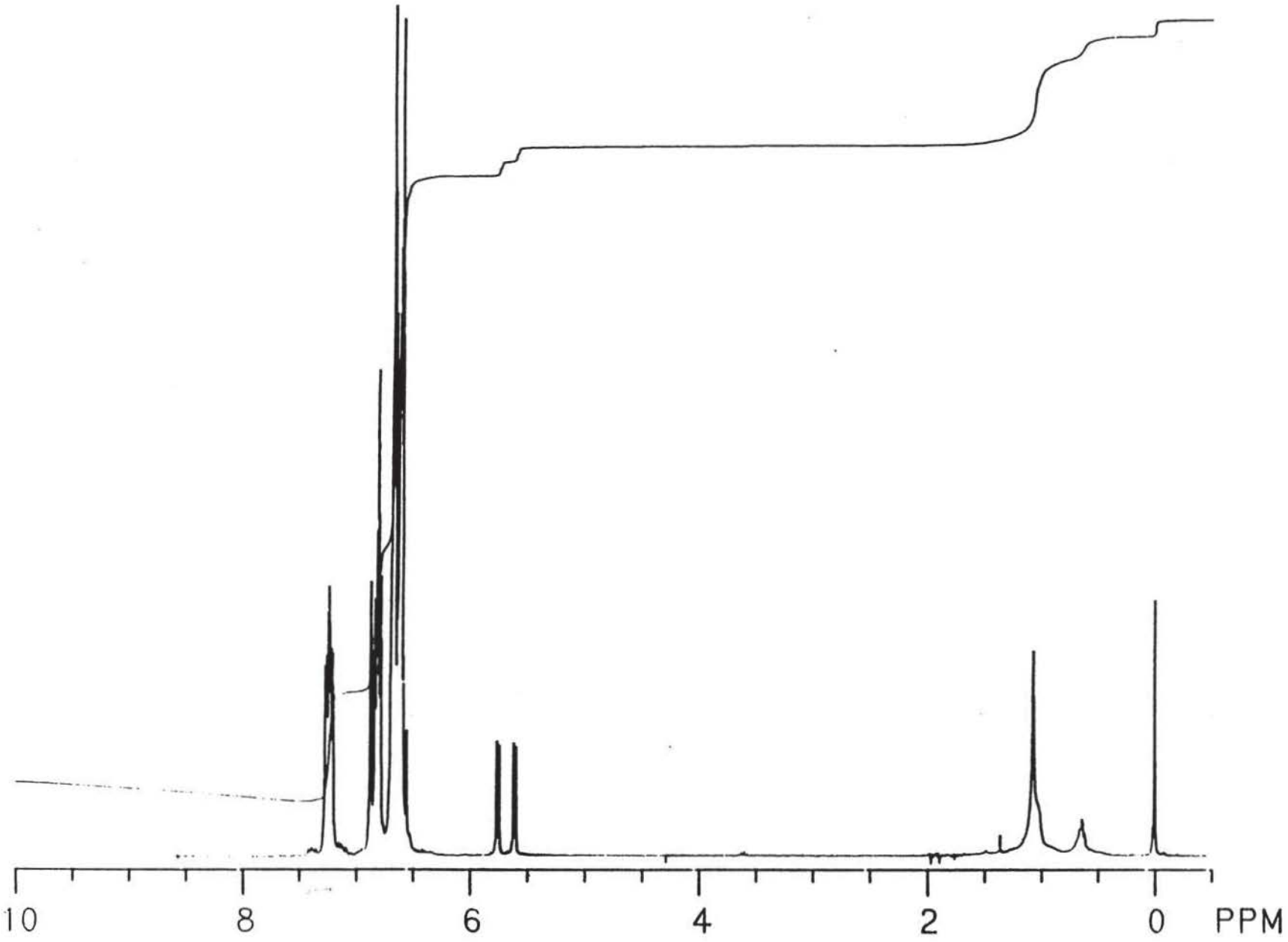

Figure 29. The ^{1}H NMR spectrum of $(OC)_5WPPh_2C(PPh_2)=CH_2$ in $CDCl_3$

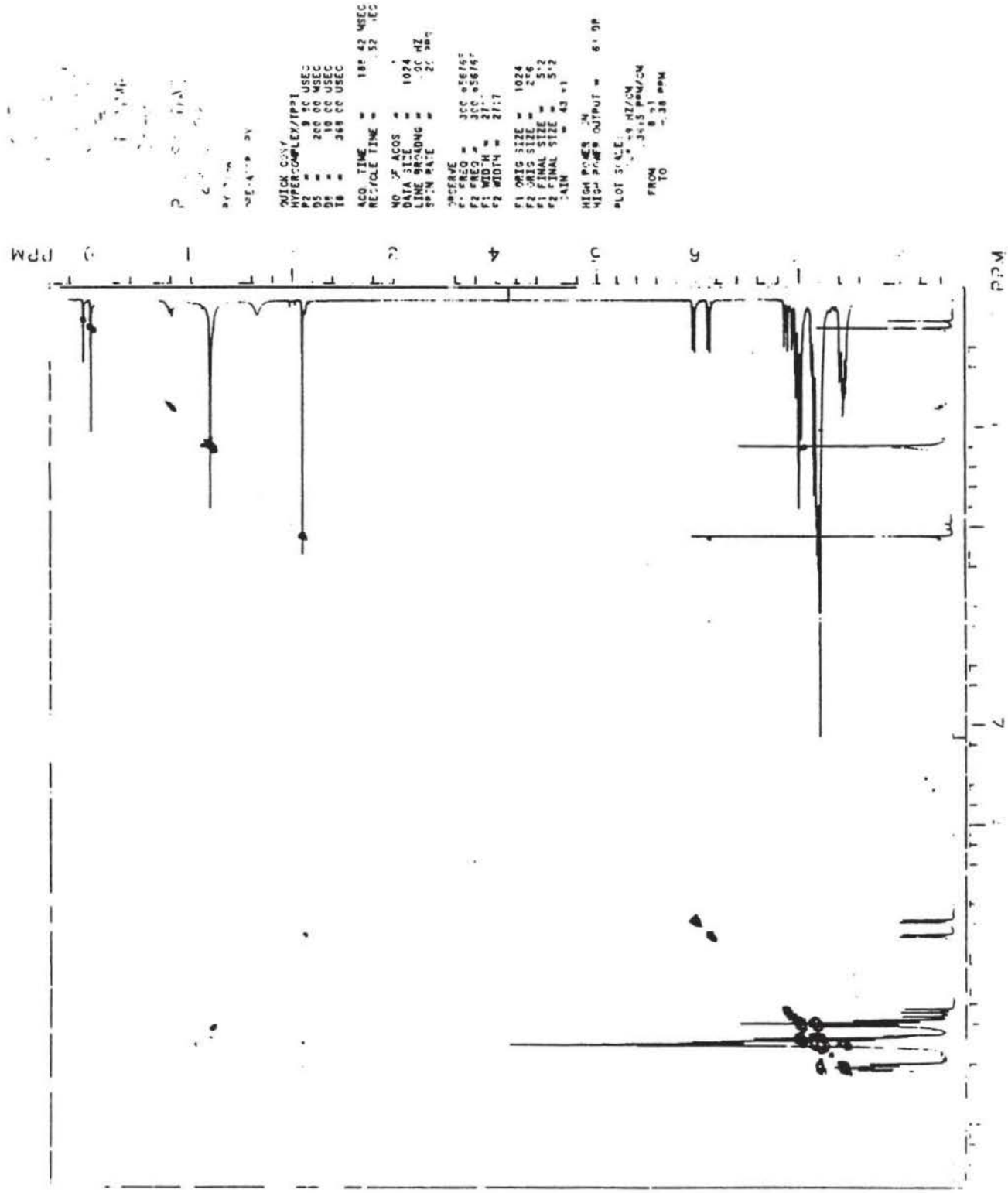

Figure 30. The COSY spectrum of $(OC)_5WPPh_2C(PPh_2)=CH_2$ in $CDCl_3$

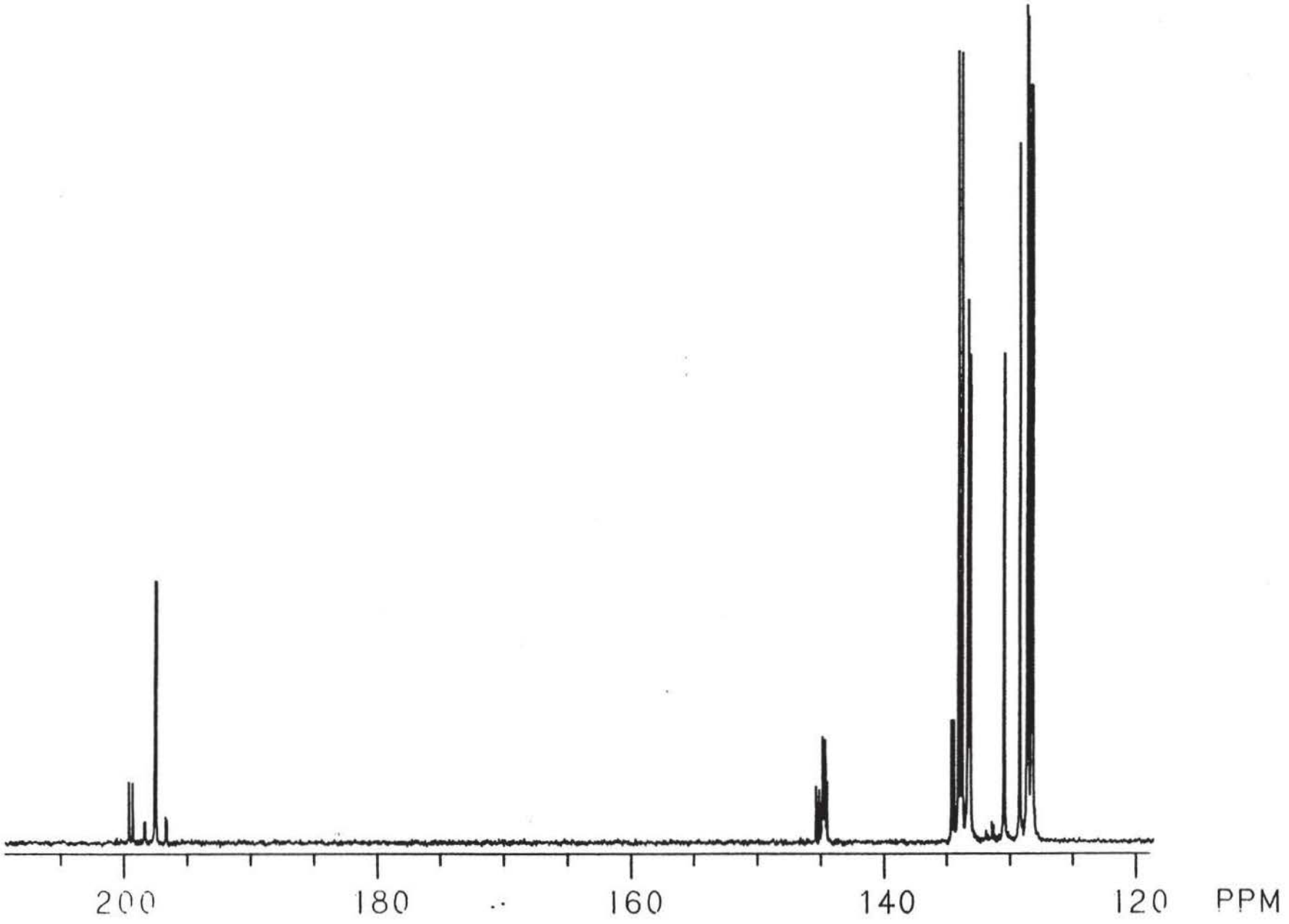

Figure 31. The $^{13}C\{^{1}H\}$ NMR spectrum of $(OC)_5WPPh_2C(PPh_2)=CH_2$ in $CDCl_3$

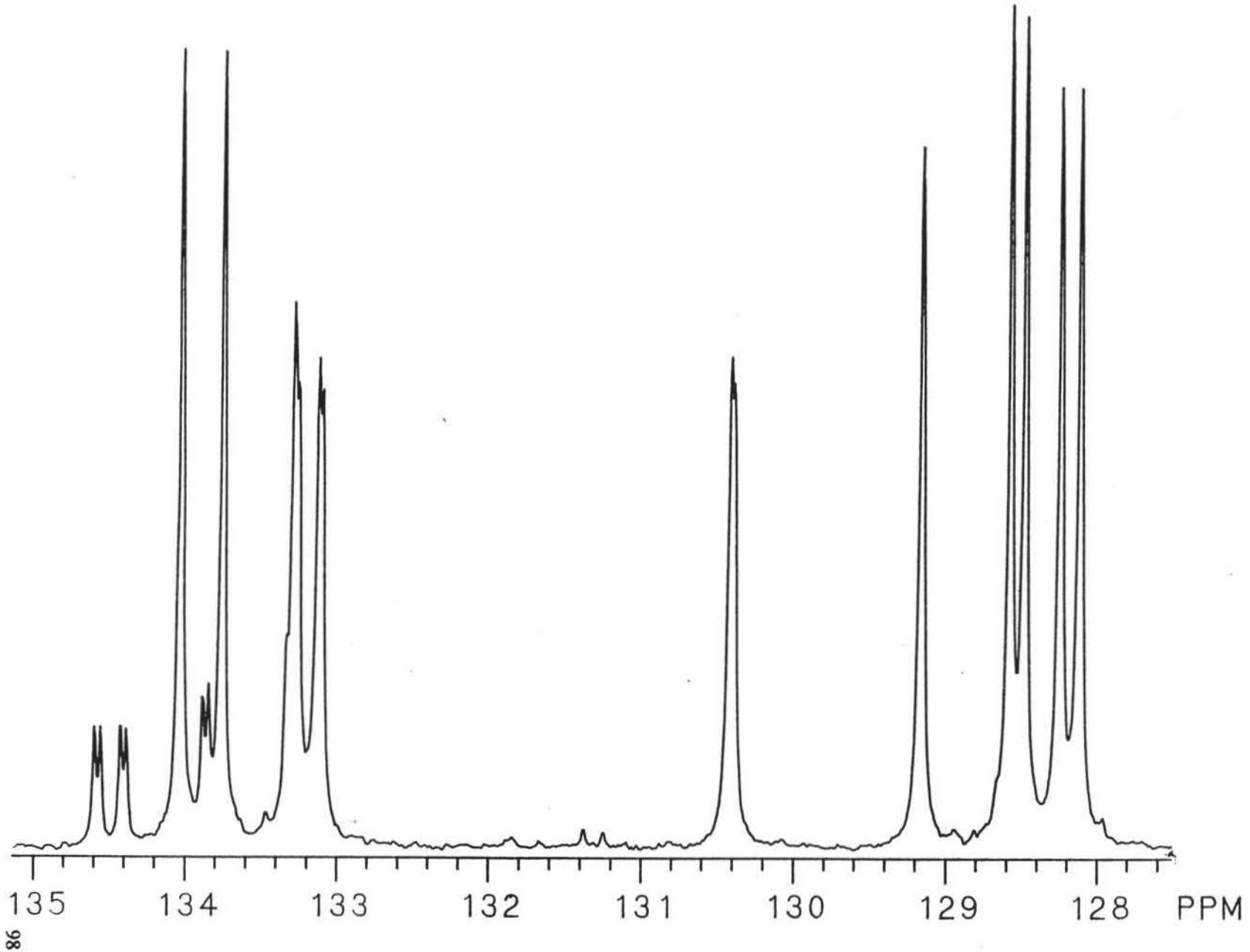

Figure 31a. The expansion of phenyl region

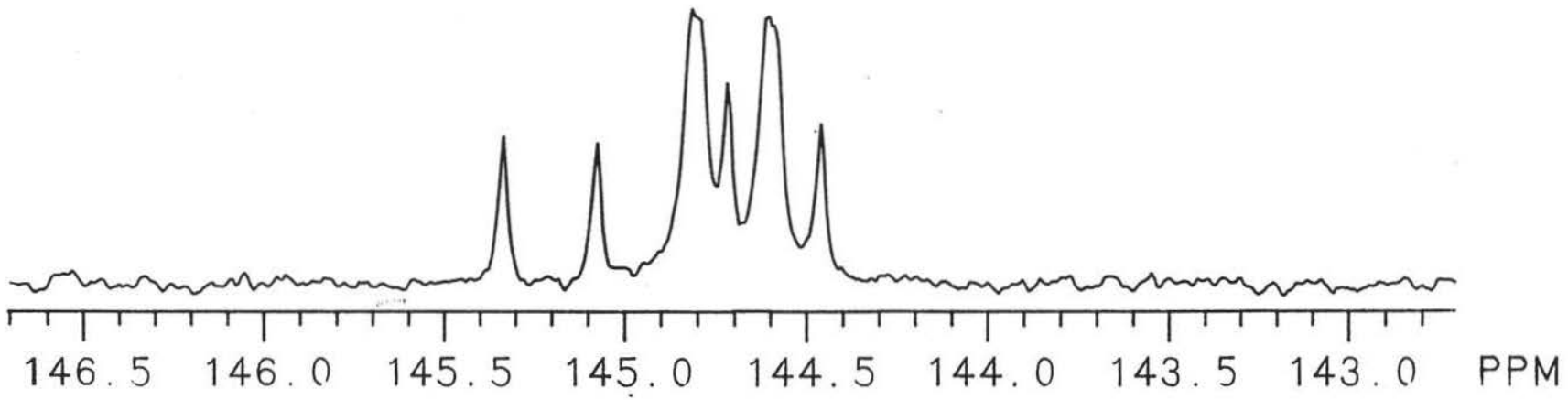

Figure 31b. The expansion of vinyl region

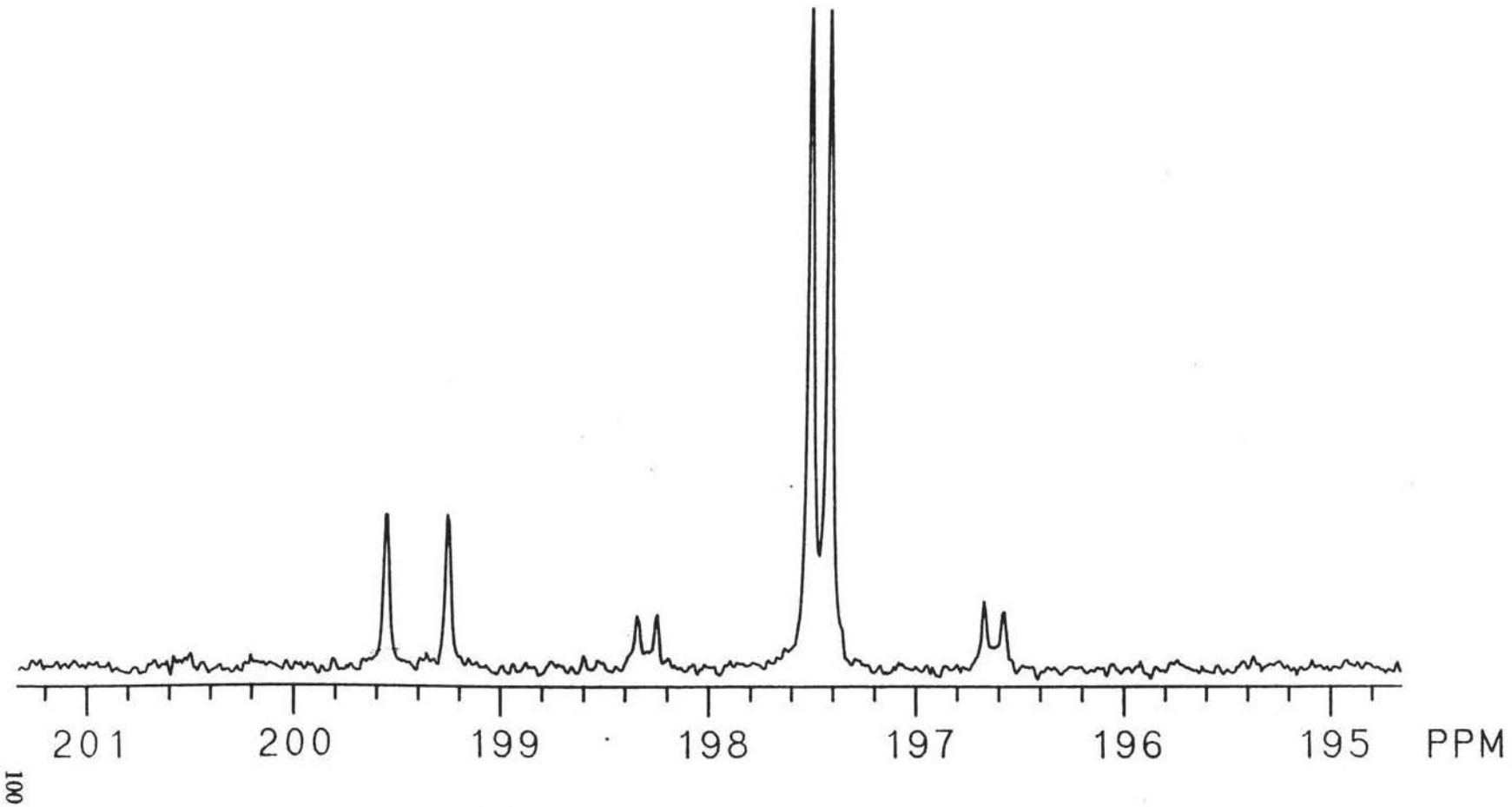

Figure 31c. The expansion of carbonyl region

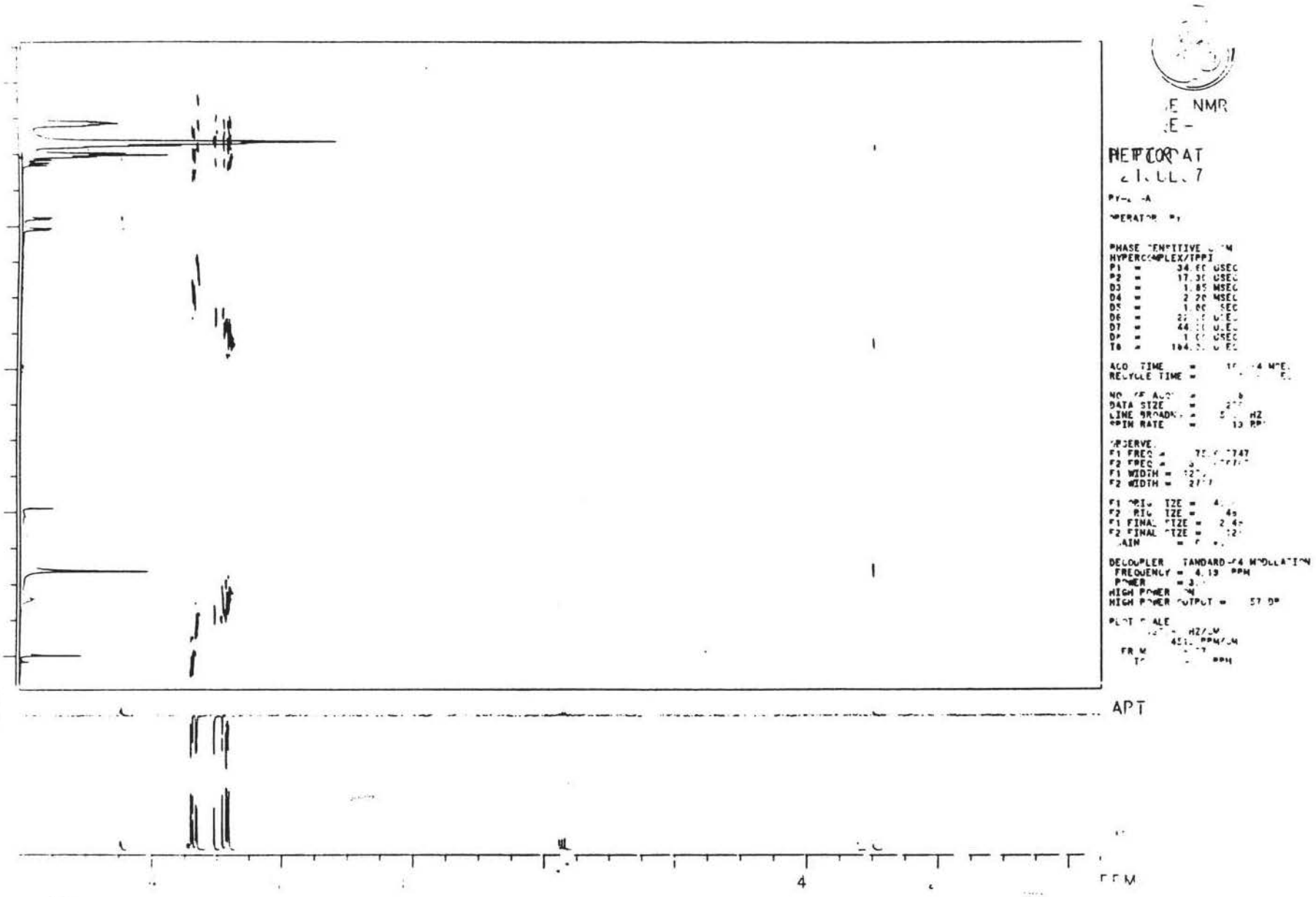

Figure 32. The HETCOR spectrum of $(OC)_5WPPh_2C(PPh_2)=CH_2$ in $CDCl_3$

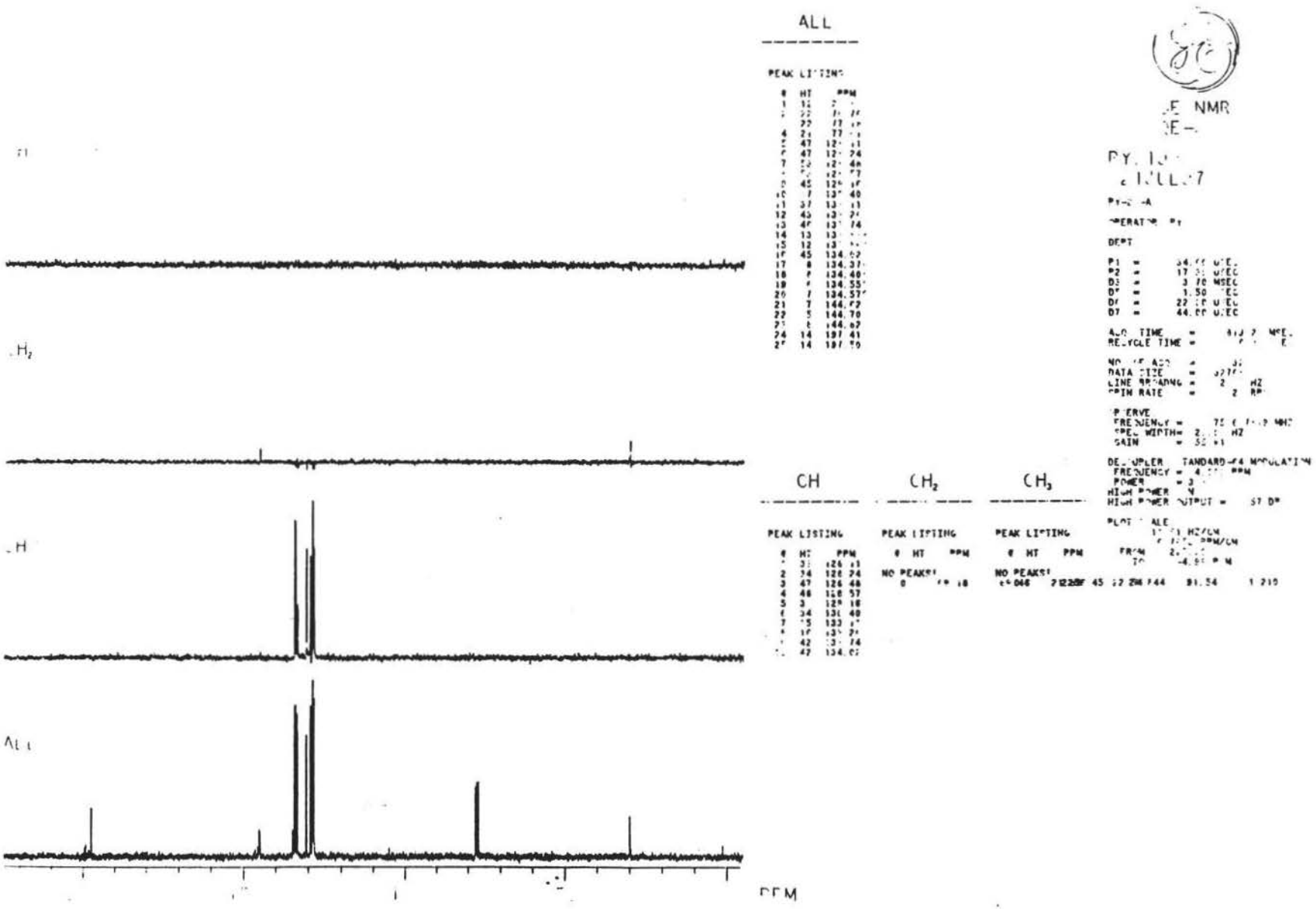

Figure 33. The DEPT spectrum of $(OC)_5WPPh_2C(PPh_2)=CH_2$ in $CDCl_3$

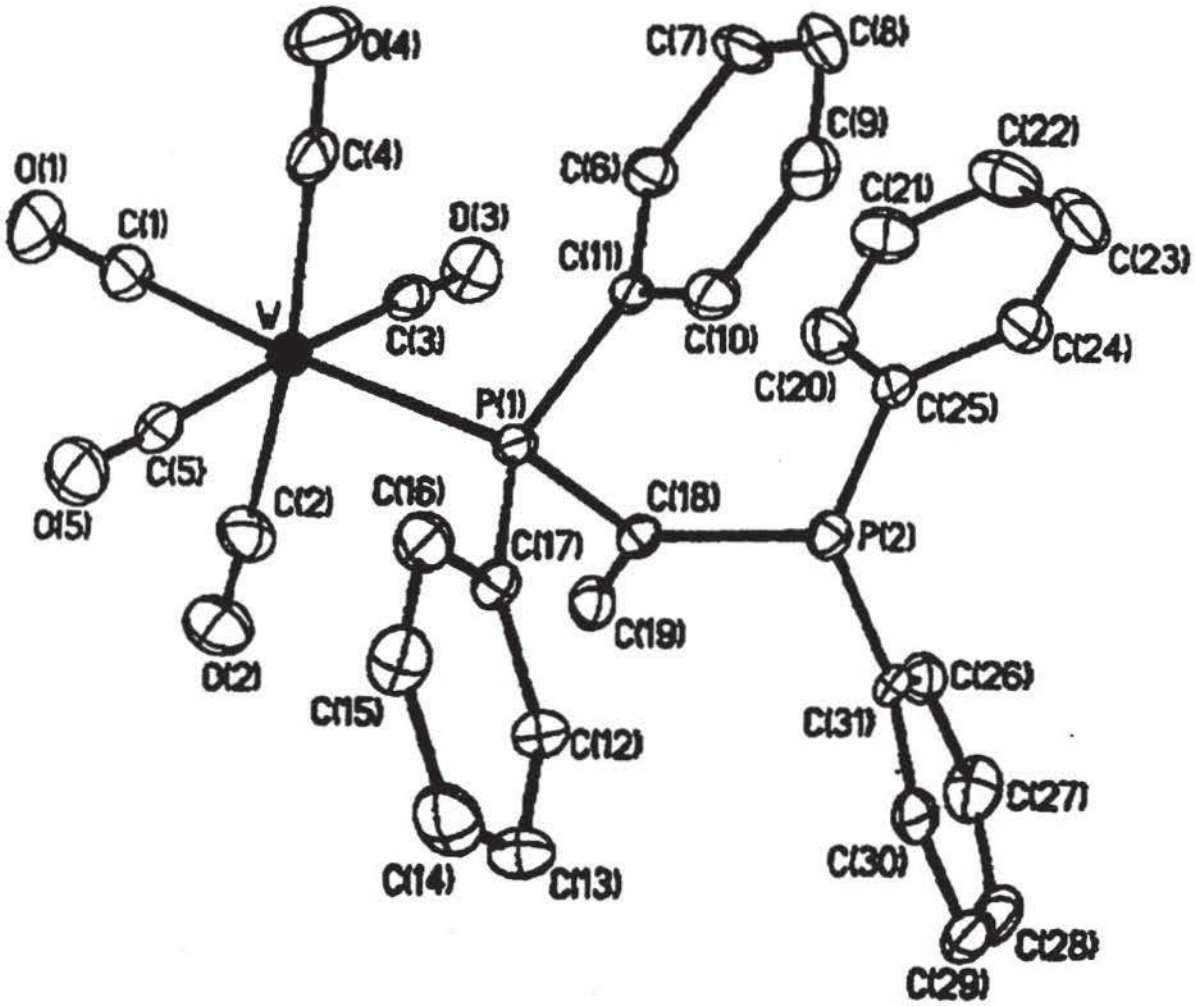

Figure 34. The molecular structure of $(OC)_5WPPh_2C(PPh_2)=CH_2$

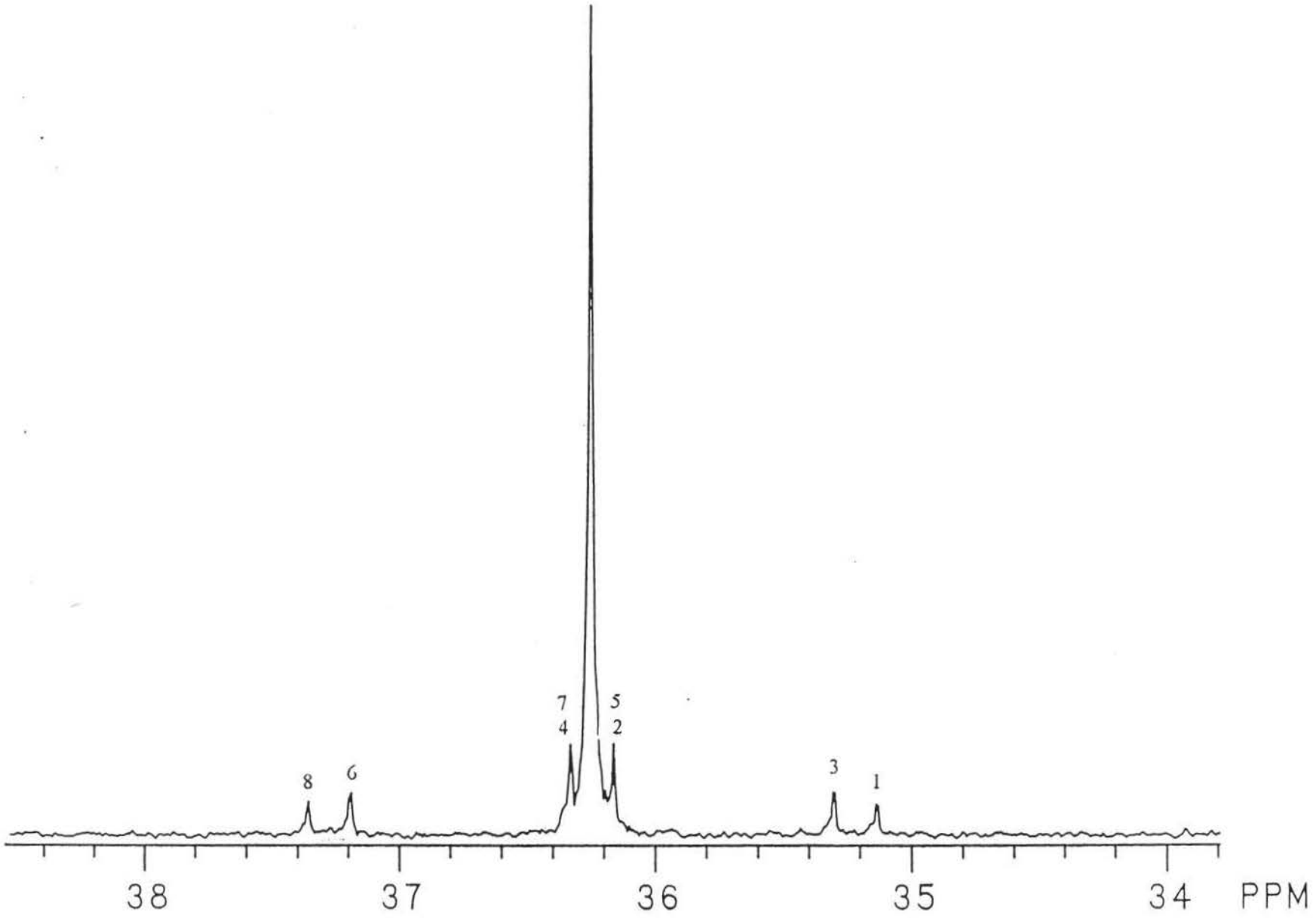

Figure 35. The $^{31}P\{^{1}H\}$ NMR spectrum of $[(OC)_5WPPh_2]_2C{=}CH_2$ in $CDCl_3$

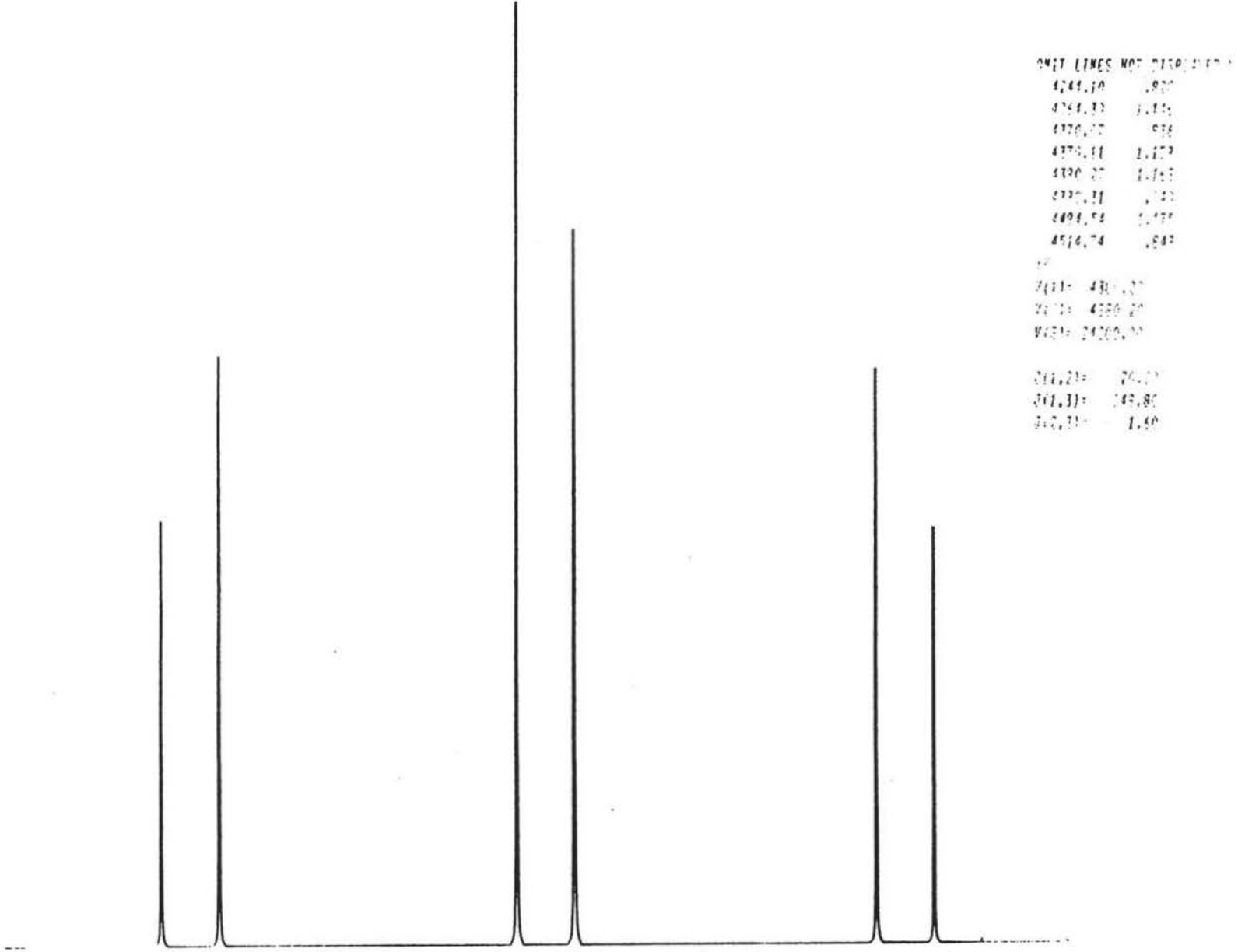

Figure 36. The simulation of ABX pattern in $^{31}P\{^{1}H\}$ NMR spectrum of $[(OC)_5WPPh_2]_2C{=}CH_2$

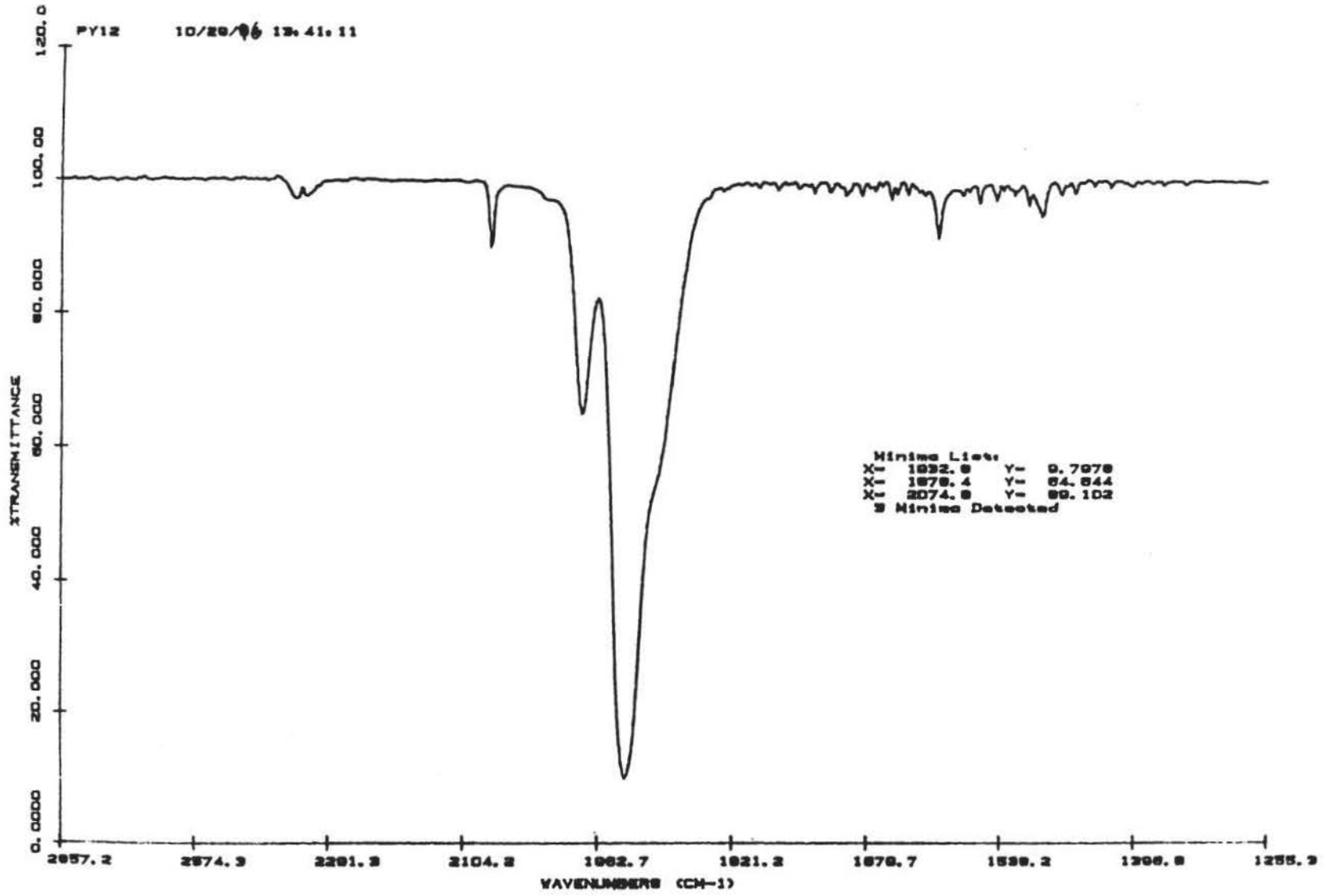

Figure 37. The IR spectrum of $W(CO)_5NH_2Ph$ of carbonyl region in $CHCl_3$

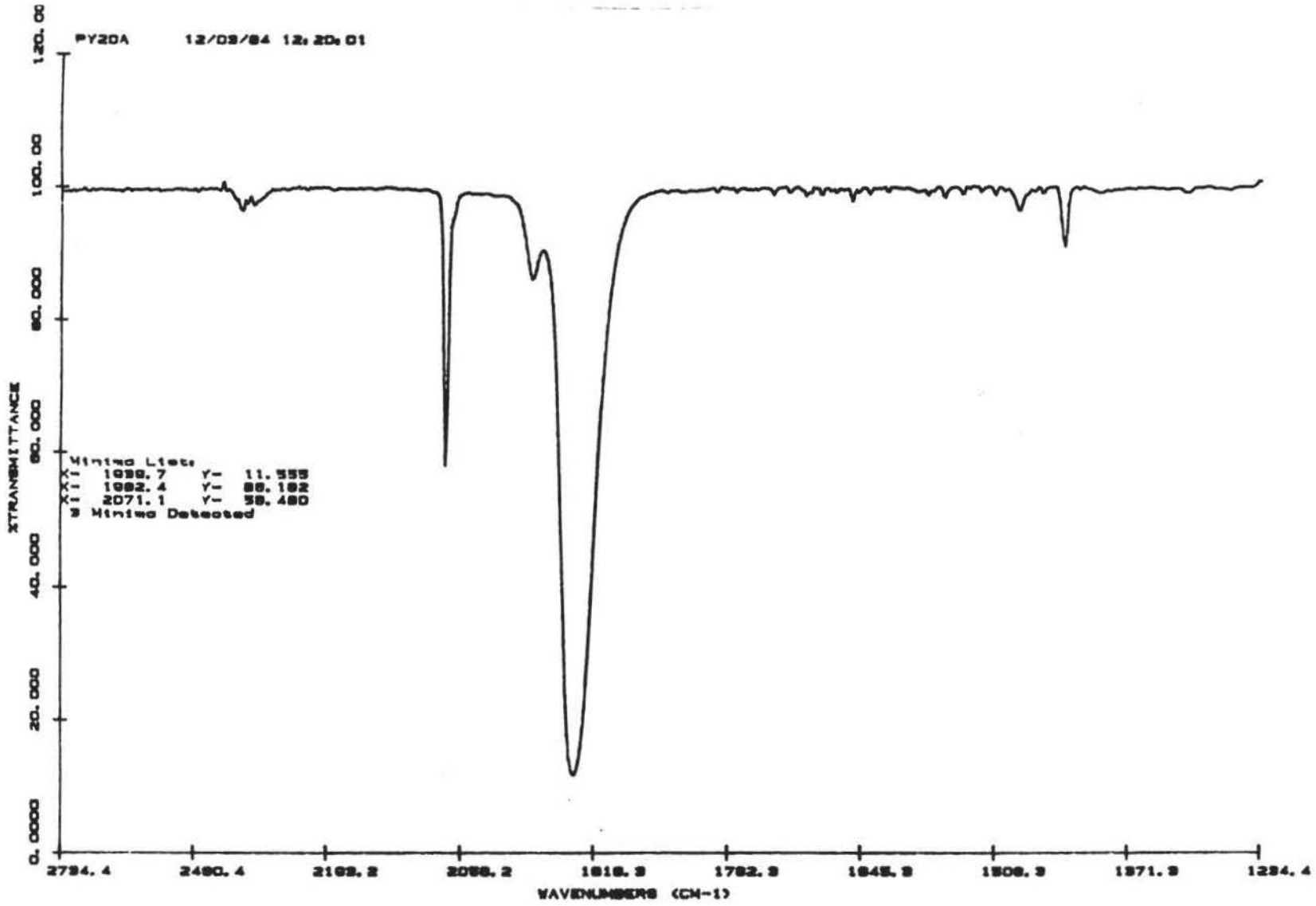

Figure 38. The IR spectrum of $W(CO)_5PPh_2C(PPh_2)=CH_2$ of carbonyl region in $CHCl_3$

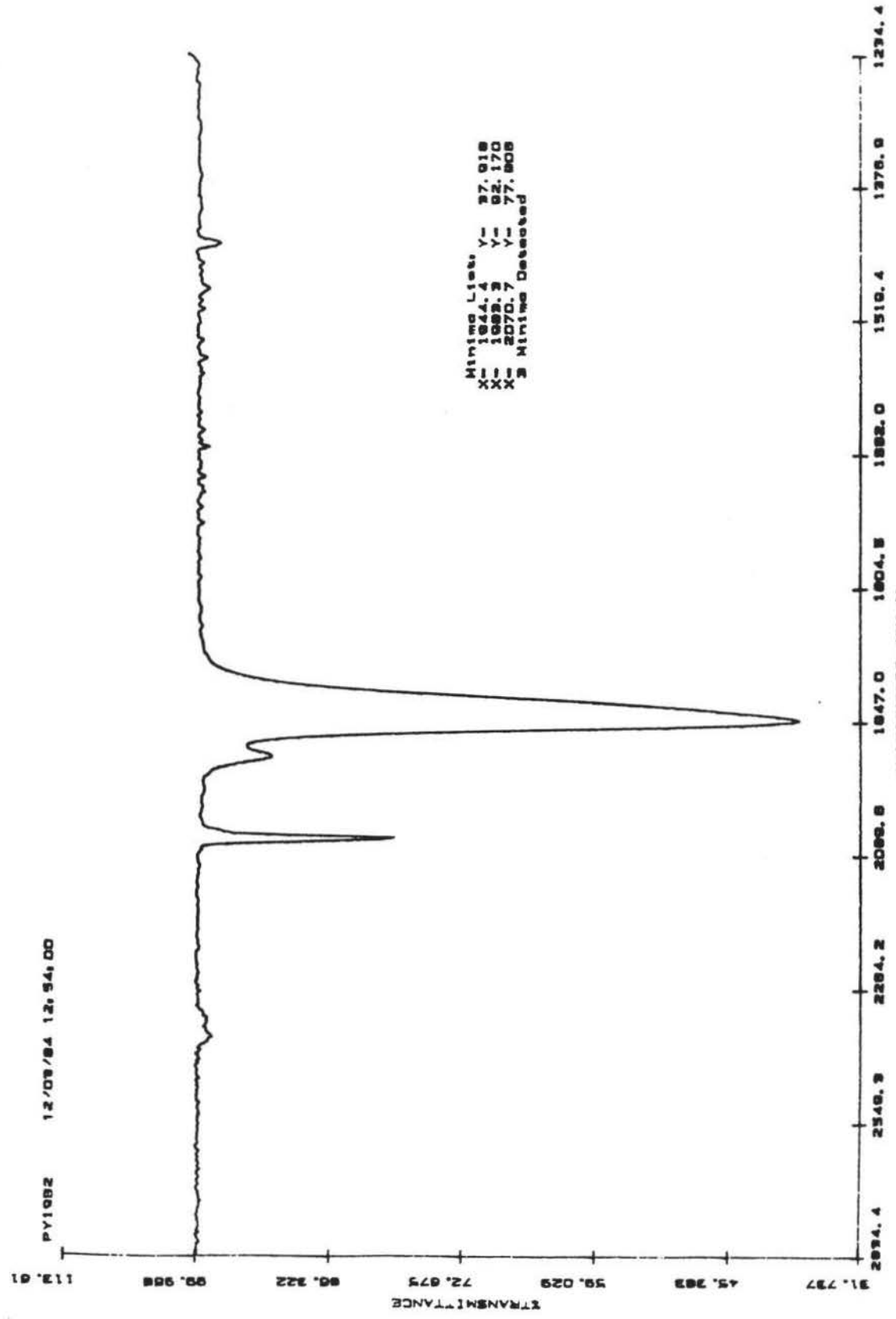

Figure 39. The IR spectrum of $[(OC)_5WPPh_2]_2C{=}CH_2$ of carbonyl region in $CHCl_3$

References:

1. Hegedus, L.S.; Norton, J.R.; Finke, R.G. *Principles and Applications of Organotransition Metal Chemistry*. University Science Books: Mill Valley, CA, **1987**.
2. Pignolet, L.H. *Homogeneous Catalysis with Metal Phosphine Complexes*. Plenum Press: New York, **1983**.
3. Kirtley, S.W. *Comprehensive Organometallic Chemistry*. Wilkinson,G.; Stone, F.G.A.; Abel, E.W., Eds; Perganon: Oxford, U.K., **1982**, Vol 3.
4. (a) Darenbourg, D.F. *Adv. Organomet. Chem.* **1982**, *21*, 113. (b) Howell, J.A.S.; Burkinshaw, P.M. *Chem. Rev.* **1983**, *83*, 227. (c) Graham, J.R.; Angelici, R. *J. Inorg. Chem.* **1967**, *6*, 2082.
5. Chatt, J.; Hart, F.A. *J. Chem. Soc.* **1960**, 1378.
6. Levason, W. *The Chemistry of Organophosphorus Compounds*; Hartley, F.R., Ed.; John Wiley, New York, **1990**.
7. (a) Puddephatt, R.F. *Chem. Soc. Rev.* **1983**, *12*, 99. (b) Chandret, B.; Delavanx, B.; Poilblanc. R. *Coord. Chem. Rev.* **1988**, *86*, 191.
8. (a) Werner, H.; Prinz, R.; Bundschuh, E.; Deckelmann, K. *Angew. Chem.* **1966**, 5, 606. (b) Hor, T.S.A.; Chan, H.S.O. *Inorg. Chem. Acta.* **1989**, *160*, 53. (c) Hor. T.S.A. *J. Organomet. Chem.* **1988**, *340*, 51.
9. Mawby, R.J.; Morris, D.; Thorsteinson, E.M.; Basolo, F. *Inorg. Chem.* **1996**, *5*, 27.
10. King, R.B.; Etraty, A. *Inorg. Chem.* **1969**, *8*, 2374.
11. Rigo, P.; Longato, B.; Fevero, G. *Inorg. Chem.* **1972**, *11*, 300.

12. Brown, M.L.; Dramer, J.L.; Ferguson, J.A.; Meyer, T.J.; Winterton, N. *J. Am. Chem. Soc.* **1972**, *94*, 8707.

13. King, R.B.; Saran, M.S. *J. Am. Chem. Soc.* **1973**, *95*, 1817.

14. (a) Keiter, R.L.; Shah, D.P. *Inorg. Chem.* **1972**, *11*, 191. (b) Keiter, R.L.; Cary, L.W. *J.Am. Chem. Soc.* **1972**, *94*, 9232.

15. (a) Connor, J.A.; Jones, E.M. McEwen A.K. *J.Organomet. Chem.* **1972**, *43*, 357. (b) Conner J.A.; Day, J.P.; Jones, E.M.; McEwen, G.K. *J. Chem. Soc.* **1973**, 347.

16. Keiter, R.L.; Borger, R.D.; Hamerski, J.J.; Garbis, S.J.; Leotsakos, G.S. *J. Am. Chem. Soc.* **1977**, *99*, 5224.

17. Iggo, J.A.; Shaw, B.L. *J. Chem. Soc., Dalton Trans.* **1985**, 1009-1013.

18. Rahn, J.A.; DeCian, A.; Nelson, J.H. *Inorg. Chem.* **1989**. *28*. 215-217

19. Keiter, R.L.; Arnold, R.L.; Hamerski, J.J.; Charles, C.K. *Organometallics* **1983**, *2*, 1635 - 1635.

20. Siefert, E.E.; Angelici, R.J. *Organomet. Chem.* **1967**, *8*, 374.

21. Modi, S.P.; Atwood, J.D. *Inorg. Chem.* **1983**,*22* 26-28.

22. Keiter, R.L.; Bradack, W.J.; Borger, R.D.; Cary, L.W. *Inorg. Chem.* **1982**, *21*, 1256.

23. Keiter, R.L.; Sun, Y.Y.; Brodack, J.W.; Cary, L.W. *J. Am. Chem. Soc.* **1979**. *101*, 2638.

24. Özer, Z.; Özkar, S.; Pamuk, H.Ö. *Z. Naturforsch.*,48b, **1993**, 37.

25. Benson, J.W.; Keiter, E.A.; Keiter, R.L. *J. Organomet. Chem.* **1995**, *495*, 77.

26. Bruce, M.I. *J. Organomet. Chem.* **1985,** *283*, 339.

27. Bruce, M.I. *J. Organomet. Chem.* **1983.** *242*, 147.

28. Soriaga, M.P. *Chem. Rev.* **1990**, *90*, 771.

29. Gonzalez, R.D. *Appl. Surf. Sci.* **1984**, *19*, 181.

30. He, Z.; Jugan, N.; Neibecker, E.; Mathieu, R.; Bunnet, J.J. *J. Organomet. Chem.* **1992**, *426*. 247.

31. Delavaux, B.; Chaudret, B.; Devillers, J.; Dahan, F.; Commenges, G.; Poilblanc, R. *J. Am. Chem. Soc.* **1986**, *108*, 3703.

32. Orth, S.D.; Terry, M.R.; Abboud, K.A.; Dodson, B.; McElwee-White, L. *Inorg. Chem.* **1996**, *35*, 916.

33. County, G.R.; Dickson, R.S.; Jenkins, S.M.; Johnson, J.; Paravagna, O. *J. Organomet. Chem.* **1997**, *530*, 49.

34. Colquhoun, I.J.; McFarlane, W. *J. Chem. Soc. Dalton Trans.* **1982**, 1915.

35. Weber, L.; Wewers, D. *Chem. Ber.* **1985**, *118*, 3560.

36. Carr, S.W.; Fontaine, X.L.R.; Shaw, B.L. *J. Chem. Soc. Dalton Trans.* **1991**, 1025.

37. Muetterties, E.L.; Alegranti, C.W. *J. Am. Chem. Soc.* **1972**, *94*, 6386.

38. Hassan, F.S.M.; Shaw, B.L.; Thornton-Pett, M. *J. Chem. Soc. Dalton Trans.* **1988**, 89.

39. Herring, A.M.; Koskimes, S.M.K.; Shaw, B.L. *J. Organomet. Chem.* **1988**, *338*, 13.

40. Fontaine, X.L.R.; Hassan, F.S.M.; Higgins, S.J.; Jacobsen, G.B.; Shaw, B.L.; Thornton-Pett, M. *J. Chem. Soc., Chem. Commum.*, **1985**, 1635.

41. Hassan, f.S.M.; Higgins, S.J.; Jacobsen, G.B.; Shaw, B.L.; Thornton-Pett, M. *J. Chem. Soc. Dalton Trans.* **1988**, 3011.

42. Higgins, S.J.; Shaw, B.L. *J. Chem. Soc. Dalton Trans.* **1989**, 1527.

43. Bookham, J.L.; McFarlane, W. *J. Chem. Soc. Dalton Trans.* **1988**, 503.

44. Kubas, G.J. *Inorg. Chem.* **1983**, *22*, 692.

45. Cooper, G.R.; Hassan, F.; Shaw, B.L.; Thornton-Pett, M. *J. Chem. Soc., Chem. Commun.*, **1985**, 614.

46. Keiter, R.L.; Keiter, E.A.; Olson, D.M.; Bush, J.R.; Lin, W.; Benson, J.W. *Organometallics*, **1994**, 13.

47. Chatt, J.; Hart, F.A. *J. Chem. Soc.* **1960**, 1378.

48. (a) Smith, J.G.; Tompson, D.T. *J. Chem. Soc.* (A) **1967**, 1694. (b) Nelson, J.H. private communication.

49. Huheey, J.E.; Keiter, E.A.; Keiter, R.L. *Inorganic Chemistry*. HarperCollins College Publishers: New York, **1993.**

50. Drago, R.S. *Physical Methods in Chemistry*. W.B. Saunders Company. **1977**, 510.

51. Keiter, R.L.; Benson, W.J.; Keiter, A.E.; Lin, W.; Jia, Z.; Olson, M.D.; Brandt, E.D.; Wheeler, J. unpublished.

52. (a) Bodner, M.G.; May, P.M.; McKinney, E.L. *Inorg. Chem.* **1980**, *19*, 1951. (b) Bodner, M.G. *Inorg. Chem.* **1975**, *14*, 2694. (c) Bancroft, M.G.; Dignard-Bailey, L.; Puddephatt, R.J. *Inorg. Chem.* **1986**, *25*, 3675.

53. (a) Wilkins, R.G. *Kinetics and Mechanism of Reactions of Transition Metal Complexes*, 2nd ed.; VCH: New York, **1991**. (b) Atwood, J.D. *Inorganic*

and Organometallic Reaction Mechanisms; Brooks/Cole: Monterey, **1985**.

(c) Basolo, F.; Pearson, R.G. *Mechanisms of Inorganic Reactions*. 2nd ed.; John Wiley: New York, **1967**.

54. Lin, W. Master's degree thesis in the chemistry department of Eastern Illinois University. **1995**.

55. (a) Atwood, J.D.; Brown, T.L. *J. Am. Chem. Soc.* **1976**, *98*, 3160. (b) Wovkulich, M.J.; Atwood, J.D. *J. Organomet. Chem.* **1980**, *184*, 77.

(c) Jia, Z. Master's degree thesis in the chemistry department of Eastern Illinois University. **1995**.

56. Wieland, S.; van Eldik, R. Organometallics **1991**, *10*, 3110.

57. Amis, E.S. *Solvent Effects on Reaction Rates and Mechanisms*. Academic Press: New York and London, **1966**.

58. Rottink, M.K.; Angelici, R.J. *Inorg. Chem.* **1993**, *32*, 2421.

59. Albers, M.O.; Liles, D.C.; Robinson, D.J.; Singleton, E. *J. Organomet. Chem.* **1987**, *323*, C39.

60. (a) Alyea, E.C.; Ferguson, G.; Fisher, K.J.; Gossage, R.A.; Jennings, M.C. *Polyhedron* **1990**, *9*, 2393. (b) Grim, S.O.; Barth, R.C.; Mitchell, J.D.; Del Gaudio, J. *Inorg. Chem.* **1977**, *16*, 1776. (c) Juh, L.S.; Eke, U.B.; Liu, L.K. *Organometallics* **1995**, *14*, 440.

61. Benson, J.W.; Keiter, R.L.; Keiter, E.A. unpublished.

62. Colquhoun, I.J.; McFarlane, H.C.E.; McFarlane, W.; Nash, J.A.; Keat, R.; Rycroft, D.S.; Thompson, D.G. *Org. Magn. Reson.* **1979**, *12*, 473.

63. Bovey, F.A. *Nuclear Magnetic Resonance*, 2nd edn, Academic Press, San Diego, **1987**.

64. (a) Grim, S.O.; Wheatland, D.A.; McFarlane, W. *J. Am. Chem. Soc.* **1967**, *89*, 5573. (b) Keiter, R.L.; Verkade, J.G. *Inorg. Chem.* **1969**, *8*, 2115. (c) Fischer, E.O.; Knauss, L.; Keiter, R.L.; Verkade, J.G.; *J. Organomet. Chem.* **1972**, *37*, C7. (d) Verkade, J.G.; Mosbo, J.A. *Phosphorus-31 NMR spectroscopy in stereochemical Analysis*, VCH, Deerfield Beach, **1987**.

Appendix

1. The kinetic data of isomerization of **6** and **7** in $CDCl_3$

Plot I (ln{[6]-[6]eq} vs. time, 10 °C) (from Lin's thesis[54])

Time (s)	ln{[6]-[6]eq}
0	-3.84
88620	-3.85
180300	-3.9
336480	-3.93
515100	-3.98
962520	-4.09
1133160	-4.16
1305840	-4.2
1563720	-4.23

Slope = $(-2.6 \pm 0.1) \times 10^{-7}$; Intercept = -3.8419 ± 0.0079

Plot II (ln{[6]-[6]eq} vs. time, 25 °C) (from Lin's thesis[54])

Time (s)	ln{[6]-[6]eq}
0	-4.41
15300	-4.45
73680	-4.61
99180	-4.75
181980	-4.85
350760	-5.4
508260	-5.81
606840	-6.14
701760	-6.47

Slope = $(-2.9 \pm 0.1) \times 10^{-6}$; Intercept = -4.39945 ± 0.02324

Plot III (ln{[6]-[6]eq} vs. time, 40 °C)

Time (s)	ln{[6]-[6]eq}	Δln{[6]-[6]eq}
0	-1.211	0.0150
6910	-1.411	0.0296
21025	-1.743	0.0286
35165	-2.064	0.0352
76695	-3.147	0.1316

Slope = $(-2.5 \pm 0.04) \times 10^{-5}$; Intercept = -1.21517 ± 0.01515

Plot IV ($\ln k_f$ vs. 1/T)

$1/T(K^{-1})$	$\ln k_f$	$\Delta \ln k_f$
0.00353	-15.4071	0.0385
0.00336	-13.0752	0.0347
0.00319	-10.9955	0.0169

Slope = $-13{,}027.22 \pm 51.56$; Intercept = 30.63 ± 0.17

Plot V [$\ln(k_f/T)$ vs. 1/T]

$1/T(K^{-1})$	$\ln(k_f/T)$	$\Delta \ln(k_f/T)$
0.00353	-21.05255	0.00014
0.00336	-18.77225	0.00012
0.00319	-16.74175	0.00005

Slope = $-12{,}729.85 \pm 55.88$; Intercept = 23.93 ± 0.19

Plot VI ($\ln k_b$ vs. 1/T)

$1/T(K^{-1})$	$\ln k_b$	$\Delta \ln k_b$
0.00353	-16.6908	0.0394
0.00336	-14.0345	0.0362
0.00319	-11.7085	0.0204

Slope = -14,714.90 ± 135.41; Intercept = 35.32 ± 0.46

Plot VII [$\ln(k_b/T)$ vs. 1/T]

$1/T(K^{-1})$	$\ln(k_b/T)$	$\Delta \ln(k_b/T)$
0.00353	-22.33626	0.00014
0.00336	-19.73160	0.00012
0.00319	-17.45470	0.00007

Slope = -14.417.53 ± 139.73; Intercept = 28.62 ± 0.47

2. Kinetic data of isomerization of **6** and **7** in toluene-d_8

Plot I ($\ln\{[6]-[6]eq\}$ vs. time, 25 °C)

Time (s)	$\ln\{[6]-[6]eq\}$	$\Delta \ln\{[6]-[6]eq\}$
0	-2.23493	0.0418
73140	-2.23493	0.0680
156360	-2.55105	0.0287
244800	-2.95651	0.0430
321780	-3.05761	0.1962
400920	-3.27017	0.1664
479580	-3.77226	0.2750
576900	-4.13517	0.2253
655140	-4.19971	0.3590

Slope = $(-3.3 \pm 0.2) \times 10^{-6}$; Intercept = -2.09 ± 0.07

Plot II (ln{[6]-[6]eq} vs. time, 40 °C)

Time (s)	ln{[6]-[6]eq}	Δln{[6]-[6]eq}
0	-0.78307	0.0264
9645	-0.97551	0.0228
26975	-1.38629	0.0412
41495	-1.69282	0.0424
79255	-2.48891	0.0771
164285	-3.68888	0.3124
251165	-4.82831	0.9763

Slope = $(-1.61 \pm 0.08) \times 10^{-5}$; Intercept = -0.95 ± 0.09

Plot III ($\ln k_f$ vs. 1/T)

1/T (K^{-1})	$\ln k_f$	$\Delta \ln k_f$
0.00336	-12.9991	0.0607
0.00319	-11.4950	0.0504

Slope = -9353.18; Intercept = 18.39

Plot IV [$\ln(k_f/T)$ vs. 1/T]

1/T(K^{-1})	$\ln(k_f/T)$	$\Delta \ln(k_f/T)$
0.00336	-18.69624	0.00020
0.00319	-17.24120	0.00016

Slope = -90473.80; Intercept = 11.66

Plot V ($\ln k_b$ vs. 1/T)

$1/T\ (K^{-1})$	$\ln k_b$	$\Delta \ln k_b$
0.00336	-13.7785	0.0609
0.00319	-12.0373	0.0518

Slope = -10826.91; Intercept = 22.55

Plot VI [$\ln(k_b/T)$ vs. 1/T]

$1/T(K^{-1})$	$\ln(k_b/T)$	$\Delta \ln(k_b/T)$
0.00336	-19.47556	0.00020
0.00319	-17.78353	0.00017

Slope = -10521.53; Intercept = 15.83